Dear Dr. Zhang:

Please find below our itemized responses to the reviewer's comments. We have addressed the comments raised by both reviewers, and incorporated their comments / suggestions in the revised manuscript. In addition, we have added two new co-authors (Dr. Y. X. Sun and Prof. J. Ren) in the paper, both of them made substantial contribution to the revision of manuscript as well as the monitoring study (we forgot to include them as co-authors in the ACPD paper).

Thank you very much for your consideration.

Sincerely,

Xuejun Liu and Wen Xu

On behalf of all co-authors

Anonymous Referee #1

General comments

The manuscript 'Quantifying atmospheric nitrogen deposition through a nationwide monitoring network across China' presents the results from 5 years of reactive nitrogen atmospheric concentrations and bulk deposition monitoring combined with modeled dry nitrogen deposition across China. This is an important contribution to the field of reactive nitrogen monitoring in a rapidly developing hotspot of air pollution. However, some general aspects may need to be improved so that results can be interpreted correctly.

Response: The authors are grateful to the referee for the valuable and insightful suggestions. We believe that addressing the issues raised by the referee will considerably improve the quality of manuscript. Please see our response to each comment below.

Specific comments

1. The description of the results is based on ranking Chinese regions according to their levels of reactive nitrogen pollution and nitrogen deposition levels. However, the monitoring sites since some regions include more urban sites, with higher pollution levels, than others or a higher proportion of background sites, away from pollution sources. Thus, the mean value obtained in each region may not be informative of the pollution levels of the whole region. Alternatively, the comparisons between regions can be based on the analysis across urban sites, rural and background sites. For instance, the regional ranking based on mean dry deposition levels can change depending on whether all sites are considered (as it is now in the manuscript), only background sites or only rural sites. The same may be true for wet and total deposition. The comparisons across regions would be fairer this way.

Response: We agree with the reviewer that the monitoring sites included within

each region are not homogenously distributed but they reflected the real situation in China: more research has been done in eastern and mid eastern regions and less work been conducted in western (including Tibetan Plateau) and northwestern regions. To our best knowledge, there is no systematic and comprehensive measurement study focused on comparisons of wet and dry N deposition fluxes between different land use types across China. Thus, according to the reviewer's suggestion we have reanalyzed the data on N_r concentrations as well as N deposition (dry, wet/bulk and total) fluxes based on the three land use types (urban, rural and background sites) within each region, among six regions, and across the country in the revised paper.

2. In the same line with the previous comment, Table 2 presents a comparison between NNDMN results and other monitoring networks. This comparison is biased by the fact that CASTNET monitoring sites, unlike NNDMN, are located in rural and protected areas, with no sites in urban environments. EMEP data considered here is produced from modelled data representing large scale areas within each grid cell that make comparisons with point measurements difficult. EMEP also has a monitoring network of background sites across Europe with data downloadable from the internet that maybe more useful for comparisons in Table 2. Also, of the 10 EANET sites presented by Endo et al. (2011), 8 were classified as remote stations, one rural and only one urban. The latter two stations showed higher nitrogen deposition fluxes than remote sites. It was recognized in this study that concentrations in Japan were generally lower compared to other EANET sites in East Asia because most locations were categorized as remote sites. Thus, comparisons in Table 2 with CASNET, EMEP and EANET Japan should be based only on rural and/or background sites of the NNDMN.

Response: We agree to this comment. We have improved Table 2 (now being Table 1 in the revision) as suggested by the reviewer, i.e. removed the urban sites in NNDMN and then made comparisons with other 3 networks. But the revised Table 2 is still not perfect because of the following two reasons: 1) the data on concentrations and deposition fluxes of N_r species for the three land use types (i.e. remote, rural and urban) presented by Endo et al. (2011) cannot be extracted separately; 2) to our knowledge the observation data of EMEP was not available, though the gridded data can be downloaded via the website of EMEP. Since the current study is a Chinese survey, the aim here is to give a general summary of how the range of nitrogen deposition values which we have measured in China compares with other regions of the world and demonstrate that China is a global hot spot for N deposition. During the literature review, we find the most appropriate way of comparison is to use the conclusion from the WMO/GAW assessment work (Vet et al, 2014). So, we have revised the text at the end of Section 4.2 to make a more comprehensive and scientific comparison, instead of comparison from EANET and EMEP.

"On the basis of 2001 ensemble-mean modeling results from 21 global chemical transport models (Vet et al., 2014), three regions of the globe where total

deposition is very high: western Europe (with levels from 20.0 to 28.1 kg N ha^{-1} yr^{-1}); South Asia (Pakistan, India and Bangladesh) from 20.0 to 30.6 kg N ha^{-1} yr^{-1} and East Asia from 20 to 38.6 kg N ha^{-1} yr^{-1} in eastern China (the global maximum). Extensive areas of high deposition from 10 to 20 kg N ha^{-1} yr^{-1} appear in the eastern U.S. and southeastern Canada as well as most of central Europe. Small areas with total deposition of N from 10 to 20 kg N ha^{-1} yr^{-1} are present, and very large areas of the continents have deposition from 2 to 10 kg N ha^{-1} yr^{-1}. In contrast, the present study shows much higher total deposition flux (39.9 kg N ha^{-1} yr^{-1}) at a national scale. In China, the consumption rates of chemical fertilizer and fossil fuel have increased 2.0-and 3.2-fold, respectively, between the 1980s and the 2000s (Liu et al., 2013). As a result, the estimated total emission of NH_3 reached 9.8 Tg in 2006, contributing approximately 15% and 35% to the global and Asian NH_3 emissions (Huang et al., 2012), and NO_x emissions from fossil fuel combustion increased from 1.1 Tg N in 1980 to about 6.0 Tg N in 2010 (Liu et al., 2013). The increasing NO_x and NH_3 emissions in China led to higher atmospheric N deposition than those observed in other regions. In addition, emissions of nitrogen compounds in other parts of the world are declining. In the US, for example, NO_x emissions from the power sector and mobile sources were reduced by half from 1990 to 2010 (Xing et al., 2013), which explained the declined N deposition fluxes during period of 1990-2009 observed at 34 paired dry and wet monitoring sites in the eastern US (Sickles II et al., 2015). In Europe, the total NO_x and NH_3 emissions decreased by 31% and 29% from 1990 to 2009 (Torseth et al., 2012). N deposition has decreased or stabilized in the United States and Europe since the late 1980s or early 1990s with the implementation of stricter legislation to reduce emissions (Goulding et al., 1998; Holland et al., 2005). However, wet deposition of ammonium, due to no regulation on NH_3 emission, has increased over recent decades in the US (Du et al., 2014).”

Table 1 Comparison of dry, wet (wet/bulk), and total deposition fluxes of N_r compounds between NNDMN in China and 3 networks in other countries.

Network		Japan EANET network[a]			CASTNET[b]			EMEP[c]			NADMM[d]		
Number of sites or grids		10 sites			130 sites			2447 girds (0.5° × 0.5°)			33 sites		
Observation period		Apr. 2003-Mar. 2008			Apr. 2006-Dec. 2013			Jan. 2003-Dec. 2007			Aug. 2006-Sep. 2014		
N deposition ($kg\ N\ ha^{-1}\ yr^{-1}$)		Dry	Wet	Total	Dry	Wet	Total	Dry	Wet	Total	Dry	Wet/bulk	Total
	Average	3.9	6.6	10.6	3.1	1.3	4.4	3.9	4.8	8.7	18.7	18.2	36.9
	Median	4.1	5.9	11.2	3.0	0.7	4.1	3.7	4.7	8.5	18.7	21.3	36.5
	Max	7.0	15.8	18.2	9.7	10.3	19.6	15.8	16.9	28.0	43.1	32.4	70.9
	Min	1.0	2.1	3.0	0.03	0.1	0.3	0.1	0.6	0.7	1.1	1.5	2.9

[a]The Japan EANET data are sourced from Endo et al. (2011). Gaseous NO_2 was not included in estimates of dry N deposition.

[b] The CASNET data are available online (http://www.epa.gov/castnet/). Gaseous NH_3 was not included in estimates of dry N deposition.

[c]The EMEP data are sourced from Endo et al. (2011), in which the dry and wet deposition amounts at each grid covering 27 EMEP countries were estimated by the unified EMEP models (Simpson et al., 2003).

[d] Only including the rural and background sites in NNDMN

References:

Du, E. Z., Vries, W. D., Galloway, J. N., Hu, X. Y., and Fang, J. Y.: Changes in wet nitrogen deposition in the United States between 1985 and 2012, Environ. Res. Lett.,9, 095004, doi:10.1088/1748-9326/9/9/095004, 2014.

Endo, T., Yagoh, H., Sato, K., Matsuda, K., Hayashi, K., Noguchi, I., and Sawada, K.: Regional characteristics of dry deposition of

sulfur and nitrogen compounds at EANET sites in Japan from 2003 to 2008, Atmos. Environ., 45, 1259–1267,doi:10.1016/j.atmosenv.2010.12.003, 2010.

Goulding, K. W. T., Bailey, N. J., Bradbury, N. J., Hargreaves, P., Howe, M., Murphy, D. V., Poulton, P. R., and Willison, T. W.: Nitrogen deposition and its contribution to nitrogen cycling and associated soil processes, New Phytol., 139, 49–58, 1998.

Holland, E. A., Braswell, B. H., Sulzman, J., and Lamarque, J. F.: Nitrogen deposition onto the United States and Western Europe: synthesis of observations and models, Ecol. Appl., 15, 38–57, 2005.

Huang, X., Song, Y., Li, M. M., Li, J. F., Huo, Q., Cai, X. H., Zhu, T., Hu, M., and Zhang, H. S.: A high-resolution ammonia emission inventory in China, Global Biogeochem. Cy., 26, GB1030, doi:10.1029/2011GB004161, 2012.

Liu, X. J., Zhang, Y., Han, W. X., Tang, A., Shen, J. L., Cui, Z. L., Vitousek, P., Erisman, J. W., Goulding, K., Christie, P., Fangmeier, A., and Zhang, F. S.: Enhanced nitrogen deposition over China, Nature,494, 459–462, doi:10.1038/nature11917, 2013.

Sickles, J. E. and Shadwick, D. S.: Air quality and atmospheric deposition in the eastern US:20 years of change, Atmos. Chem. Phys., 15, 173–197, doi: 10.5194/acp-15-173-2015, 2015.

Simpson, D., Fagerli, H., Jonson, J.E., Tsyro, S., Wind, P., and Tuovinen, J. P.: Trans-boundary Acidification and Eutrophication and Ground Level Ozone in Europe: Unified EMEP Model Description, EMEP Status Report 1/2003 Part I, EMEP/MSC-W Report, The Norwegian Meteorological Institute, Oslo, Norway, 2003.

Torseth, K., Aas, W., Breivik, K., Fjaeraa, A. M., Fiebig, M., Hjellbrekke, A. G., Myhre, C. L., Solberg, S., Yttri, K. E.: Introduction to the European Monitoring and Evaluation Programme (EMEP) and observed atmospheric composition change during 1972–2009, Atmos. Chem. Phys., 12, 5447–5481, doi: 10.5194/acp-12-5447-2012, 2012.

Vet, R., Artz, R. S., Carou, S., Shaw, M., Ro, C-U., Aas, W., Baker, A., and 14 authors: A global assessment of precipitation chemistry and deposition of sulfur, nitrogen, sea salt, base cations, organic acids, acidity and pH, and phosphorus, Atmos. Environ., 93, 3–100, doi:10.1016/j.atmosenv.2013.10.060.

Xing, J., Pleim, J., Mathur, R., Pouliot, G., Hogrefe, C., Gan, C. M., Wei, C.: Historical gaseous and primary aerosol emissions in the United States from 1990 to 2010, Atmos. Chem. Phys., 13, 7531–7549, doi: 10.5194/acp-13-7531-2013, 2013.

3. Another general comment is related with the terminology. Throughout the manuscript it is said that wet deposition was measured with precipitation gauges. However, in the discussion it is acknowledged that dry deposition in precipitation gauges can account for 20 to 40% of the deposition measured in precipitation. Thus, bulk deposition was in fact monitored and the terminology should be clarified in the manuscript.

Response: Thank you for pointing this out. We have clarified the difference between bulk and wet-only deposition in the revision. Indeed, the wet deposition fluxes determined with precipitation gauges were commonly regarded as bulk deposition fluxes which contain wet plus unquantifiable dry deposition (including both gases and particles) and therefore it should be higher than wet deposition (Liu et al., 2015). Throughout the revised manuscript we have changed "wet deposition" to "wet/bulk deposition".

Reference:

Liu, X. J., Xu, W., Pan, Y. P., and Du, E. Z.: Liu et al. suspect that Zhu et al. (2015) may have underestimated dissolved organic nitrogen (N) but overestimated total particulate N in wet deposition in China, Sci. Total Environ., 520, 300–301, doi.org/10.1016/j.scitotenv.2015.03.004, 2015

4. The analysis of uncertainties in section 4.4 does not mention the uncertainties associated with the location and spatial coverage of the network. From Figure 1 it is evident that large areas of the country or islands lack of sampling points may be missing hotspots of nitrogen deposition and/or pristine sites. Some recommendations about this issue could probably be suggested.

Response: We agree that some hotspots of nitrogen deposition and/or pristine sites may be missing due to incomplete coverage of the network. We have added some recommendations about this issue in the uncertainty section 4.4 as follows:
"Although the NNDMN is the only long-term national deposition network to monitor both N wet/bulk and dry deposition in China till now, large areas of the country or islands lack of sampling points may be missing hotspots or pristine sites of N deposition. The implementation of an adequate monitoring program is also difficult at present in some regions (e.g., northwest China and Tibetan Plateau). To address this issue, more new monitoring sites, covering regions with both extremely low and high N_r emissions, should be set up in the NNDMN in future work."

5. P18368, L18: Include some measure of variability in the averaged nitrogen deposition fluxes in China to show that important reactive nitrogen deposition gradients exist in the country.

Response: Thank you for this suggestion. We have changed the sentence to "(…) Average dry and wet/bulk N deposition fluxes were 20.6 ± 11.2 (mean ± standard deviation) and 19.3 ± 9.2 kg N ha^{-1} yr^{-1} across China, with reduced N deposition dominating both dry and wet/bulk deposition."

6. P18374, L20 and S5: Which land use map was used to model the deposition velocities across China and how was the land use selected in each sampling point?

Response: We now state in the Section 2.5: "The model uses the land map of the Global Land Cover Characteristics Data Base Version 2.0 (http://edc2.usgs.gov/glcc/globdoc2_0.php), which defines the land types (e.g., urban, forest, etc.) at the native 1 km × 1 km resolution and is then binned to the model resolution as fraction of the grid cell covered by each land type. The model 1/2° resolution may coarsely represent the local land characteristics at the monitoring sites. Future work using a single-point dry deposition model as for CASTNET (Clarke et al., 1997) would further improve the dry deposition flux estimates, but that requires concurrent *in-situ* measurements of meteorological variables which are not available at present."

Added reference:

Clarke, J. F., Edgerton, E. S., and Martin, B. E.: Dry deposition calculations for the Clean Air Status and Trends Network, Atmos. Environ., 31, 3667-3678, 1997.

7. P18376, L2: The comparison presented here is also true for other regions apart from NC, SE and SW?

Response: Not the same but the fact is that NH_3 concentrations were higher at urban and rural sites than at background sites in almost all regions. We have revised the sentence as follows:

"(…) In NC, SE and SW, the NH_3 concentrations at the urban sites (average for the three regions, 9.5 ± 2.1 μg N m^{-3}) were about 1/3 higher than at the rural sites (6.2 ± 2.3 μg N m^{-3}) and were almost twice of those at the background sites (4.8 ± 1.4 μg N m^{-3}), whereas in NE and NW NH_3 concentrations at the urban sites were lower (average two regions, 5.5 ± 3.2 μg N m^{-3}) than at the rural sites (8.8 ± 0.3 μg N m^{-3}) but 4.6-times greater than at the background sites (1.2 ± 0.5 μg N m^{-3})."

8. P18376, L4: What about NH_3 levels in urban and background sites?

Response: We have added the following sentence here "Comparing land use types by region, annual NH_3 concentrations at the rural sites in northern regions (NC, NE and NW) were approximately equal, which on average were 1.8-times greater than the average of southern rural sites. In contrast, annual NH_3 concentrations at urban and background sites ranked in the order: SW > NC > NW > SE > TP > NE, and SW > NC > SE > NW > TP > NE, respectively (Fig. 3a)."

9. P18376, L9: The comparison of urban and rural areas for NO_2 also holds for other regions of China?

Response: Yes, we have revised this sentence to read: "In the six regions, the NO_2 concentrations at urban sites were 1.4-4.5 times higher than those at rural sites, and were even 2.0-16.6 times higher than the background sites (except for

SW).”

10. P18379, L5: Were there any differences in reduced/oxidized nitrogen ratios depending on the site type (urban, rural or background)?

Response: Yes, we noticed some differences in reduced/oxidized N ratios based on site types: urban (1.2 ± 0.4) < rural (1.3 ± 0.5) < background (1.6 ± 0.4). However, such changes were not significantly different (p>0.05). We add the following sentence in the revision: “In our network, the NH_x (i.e. wet/bulk NH_4^+-N deposition plus dry deposition of NH_3 and particulate NH_4^+)/NO_y (wet/bulk NO_3^--N deposition plus dry deposition of NO_2, HNO_3 and particulate NO_3^-) ratio at urban sites (from 0.8 to 1.8, averaging 1.2) was not significantly different (p>0.05) from rural (from 0.5 to 2.7, averaging 1.3) and background (from 1.0 to 2.5, averaging 1.6) sites.”

11. P18379, L13: It is interesting that, despite reactive nitrogen concentrations in rural sites are consistently lower than in urban sites, total annual mean deposition fluxes are quite similar. Have the authors any hypothesis to explain this result?

Response: The reason for this result should be mainly due to lower V_d for N_r species (esp. V_d of NO_2 and HNO_3) at urban sites than at rural sites. We assume that urban areas act as greater N_r pollution sources (more N_r emission than deposition) compared with rural areas (based on per unit land area). On average, annual N_r concentrations of NH_3, NO_2, HNO_3, and particulate NH_4^+ and NO_3^- at rural sites were 14.8, 39.1, 32.1 19.3 and 30.3% lower than those at urban sites. Correspondingly, annual dry deposition fluxes of NH_3, NO_2, HNO_3, and particulate NH_4^+ and NO_3^- at rural sites were 17.3, 11.2, 22.7, 11.9 and 28.8% lower than those at urban sites. Therefore, it is quite clear that comparable total dry deposition flux between urban sites (averaged 26.9 kg N ha^{-1} yr^{-1}) and rural sites (averaging 23.0 kg N ha^{-1} yr^{-1}) probably resulted from similar dry deposition fluxes of NO_2 and HNO_3 between rural (averaging 3.6 and 5.6 kg N ha^{-1} yr^{-1}, respectively) sites and urban sites (averaging 4.0 and 7.2 kg N ha^{-1} yr^{-1}, respectively), which can be attributed to somewhat higher deposition velocities of NO_2 and HNO_3 at rural sites (averaging 0.17 and 1.49 cm s^{-1}, respectively), compared with those at urban sites (averaging 0.12 and 1.22 cm s^{-1}, respectively).

12. P18379, L14: grassland sites-> background sites

Response: Changed as suggested.

13. P18380, L23: I believe the authors refer here to Figure S2 d and e

Response: Yes, and we have included a reference here to Figure S2 d and e in the revision.

14. P18381, L10: The discussion here would have benefited from an analysis of differences between regions across land use types. Are all the rural sites in China homogeneously affected by reactive nitrogen pollution?

Response: This is a good suggestion. All the rural sites in China were not homogeneously affected by reactive N pollution. We have revised the sentence to be as following: "Rural sites in this study also had relatively high concentrations of all measured N_r species in air, altogether ranking in the order of NC > NE > NW > SE > SW (Fig. 3f). The higher concentrations in northern China are mainly due to the combined effect of high NH_3 emissions from N fertilized farmland (Zhang et al., 2008a) and urban air pollution (e.g. NO_2, HNO_3, pNH_4^+ and pNO_3^-) transported from population centers to the surrounding rural areas (Luo et al., 2013)."

References:

Luo, X. S., Liu, P., Tang, A. H., Liu, J. Y., Zong, X. Y., Zhang, Q., Kou, C. L., Zhang, L. J., Fowler, D., Fangmeier, A., Christie, P., Zhang, F. S., and Liu, X. J.: An evaluation of atmospheric N_r pollution and deposition in North China after the Beijing Olympics, Atmos. Environ., 74, 209–216, doi:10.1016/j.atmosenv.2013.03.054, 2013.

Zhang, F. S., Wang, J. Q., Zhang, W. F., Cui, Z. L., Ma, W. Q., Chen, X. P., and Jiang, R. F.: Nutrient use efficiency of major cereal crops in China and measures for improvement. Acta Pedologia Sinica, 45, 915–924, 2008a (in Chinese with English abstract).

15. P18383, L4: Does this hypothesis work in the monitoring sites in China? In other words, was the NHx/NOy ratio in urban sites different from rural or background sites in this network?

Response: Yes, the NH_4^+-N/NO_3^--N ratio in wet/bulk deposition still works for indicating the relative contribution of N_r from agricultural and industrial activities to N deposition at monitoring sites in China. We found that NH_4^+-N/NO_3^--N ratios in wet/bulk deposition followed the sequence of urban sites < rural sites < background sites across our monitoring network.

16. P18384, L19: There is no mention in this section of the discussion to differences in modelled deposition velocities for China compared with other estimates, as presented in table S4. This is also applicable in P18387, L8.

Response: We now state in the section 4.4 "The dry deposition fluxes were estimated by combining measured concentrations with modeled V_d. As summarized in Table S4, our estimates of dry deposition velocities for different N_r species are generally consistent with the estimates in previous studies (e.g., Flechard et al., 2011; Pan et al., 2012). Some uncertainties may still exist in the inputs for dry deposition modeling."

We also have revised the sentence (P18387, L8) to read: "In previous work, dry deposition flux was inferred from atmospheric N_r concentrations and a literature-based annual mean deposition velocity (Shen et al., 2009), or reported by Luo et al. (2013) who did not consider the different dry deposition velocities of various N_r species among different land use types. Clearly, in this study we have greatly improved the estimation of dry deposition, but further work is still

required to increase the reliability and accuracy of N dry deposition values."

References:

Endo, T., Yagoh, H., Sato, K., Matsuda, K., Hayashi, K., Noguchi, I., and Sawada, K.: Regional characteristics of dry deposition of sulfur and nitrogen compounds at EANET sites in Japan from 2003 to 2008, Atmos. Environ., 45, 1259–1267,doi:10.1016/j.atmosenv.2010.12.003, 2010.

Luo, X. S., Liu, P., Tang, A. H., Liu, J. Y., Zong, X. Y., Zhang, Q., Kou, C. L., Zhang, L. J., Fowler, D., Fangmeier, A., Christie, P., Zhang, F. S., and Liu, X. J.: An evaluation of atmospheric N_r pollution and deposition in North China after the Beijing Olympics, Atmos. Environ., 74, 209–216, doi:10.1016/j.atmosenv.2013.03.054, 2013.

Shen, J. L., Tang, A. H., Liu, X. J., Fangmeier, A., Goulding, K. T. W., and Zhang, F. S.: High concentrations and dry deposition of reactive nitrogen species at two sites in the North China Plain, Environ. Pollut., 157, 3106–3113, doi:10.1016/j.envpol.2009.05.016, 2009.

17. Figures 2 and 4: Vertical lines could be included to separate regions or even land use categories within regions in order to ease comparisons.

Response: Thanks for the suggestion. In the revision, Figure 4 was changed to Figure 5. We have added vertical lines in Figures 2 and 5 to separate regions and land use categories within regions. Please see the revised Figures 2 and 5 as below.

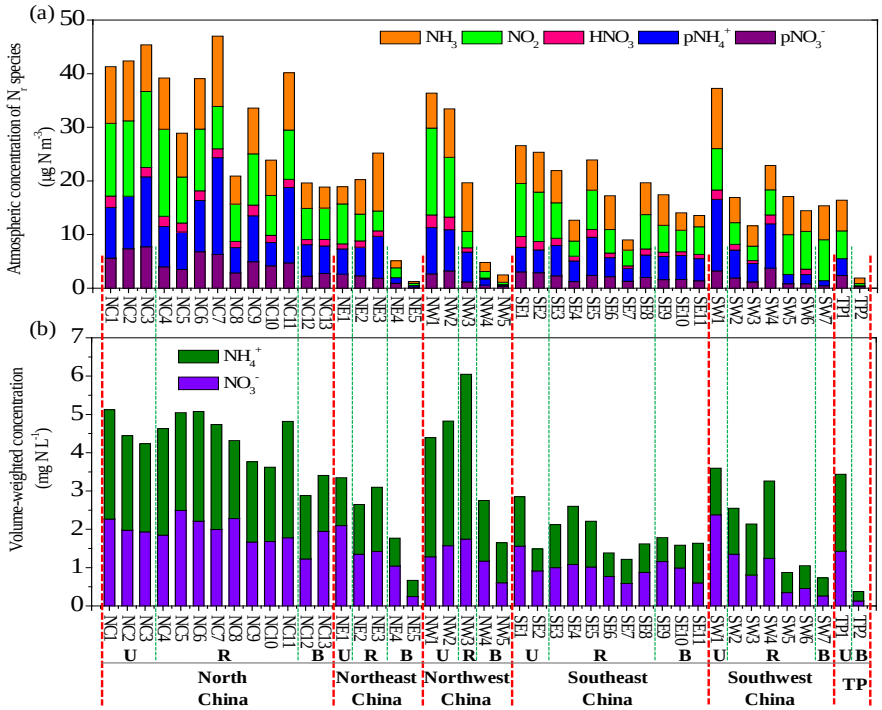

Figure 2. Annual mean concentrations of N_r compounds in air (a) and volume-weighted concentrations of inorganic nitrogen species in precipitation (b) at all monitoring sites. U, R, and B denote urban, rural, and background sites, respectively. TP denotes the Tibetan

Plateau.

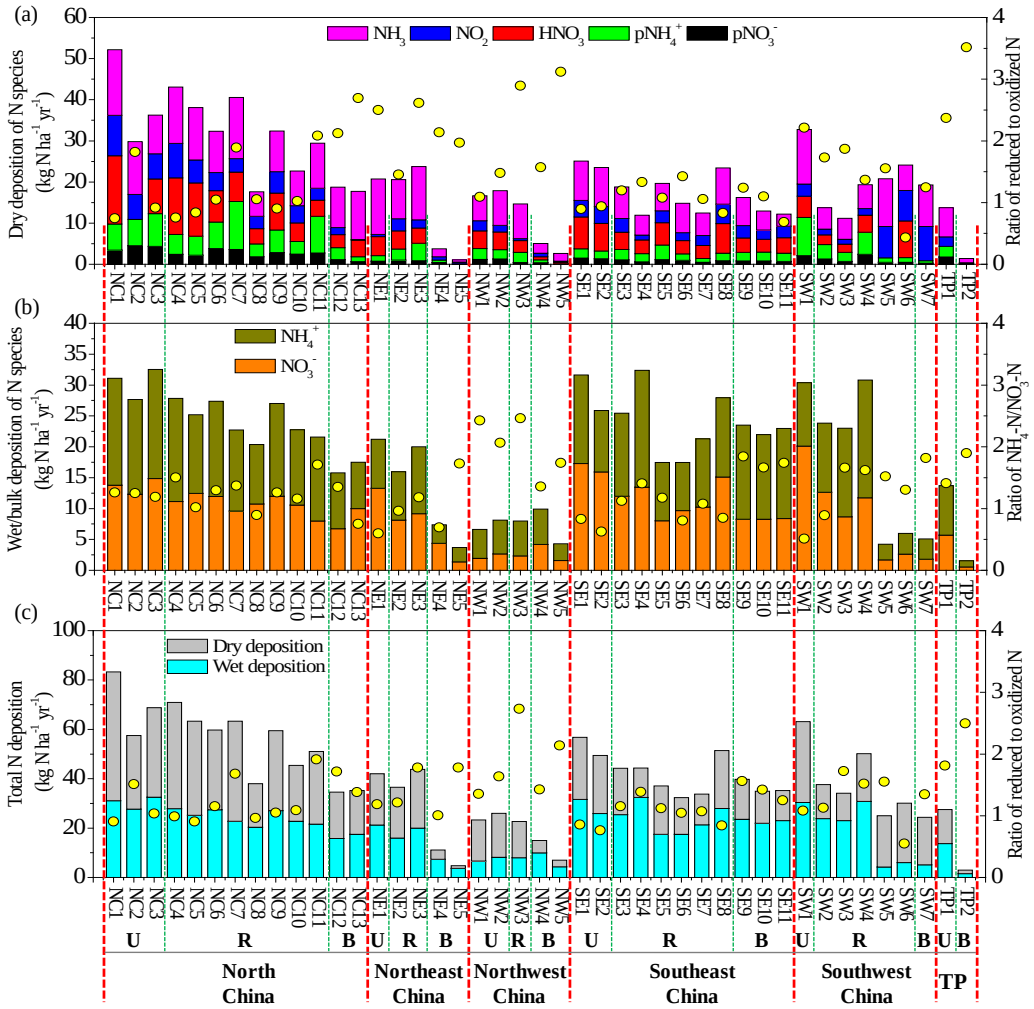

Figure 5. Annual deposition flux of various N_r species at the forty-three selected sites in China: (a) dry deposition flux; (b) wet/bulk deposition flux; (c) total deposition flux. Yellow dots denote ratios of reduced N to oxidized N in dry deposition (a), NH_4^+-N to NO_3^--N in wet/bulk deposition (b) and/or reduced N to oxidized N in total deposition (c) at all sampling sites.

18. Supplement S2: Renumber subsections as 2. X.

Response: We have renumbered subsections as suggested: S2.1 Sampling sites in north China (NC), S2.2 Sampling sites in northeast China (NE), S2.3 Sampling sites in northwest China (NW), S2.4 Sampling sites in southeast China (SE), S2.5 Sampling sites in southwest China (SW), S2.6 Sampling sites in the Tibetan plateau (TP).

19. Supplement S2.1: Thirty -> Thirteen

Response: Changed as suggested.

20. Supplement S2.5: 2 rural sites -> 5 rural sites

Response: Changed as suggested.

21. Supplement S5: The tables referenced here should be S3 and S4

Response: Yes, we have referenced the tables S3 and S4 in Supplement S5. The text is revised to be:"the monthly V_d at each site was averaged based on the hourly dataset for further estimation of dry deposition flux of each N_r species during the observation, which was statistically summarized according to land use type and is presented in Table S3. Annual mean dry deposition velocities of N_r species for three land use types in this study, averaged from monthly mean values, fit well into range of annual values calculated and used for similar land use types in other studies (Table S4 of Supplement)."

Anonymous Referee #2

General comments:

This paper is a useful contribution to the issue of atmospheric nitrogen (N) deposition in China. It presents a 5-year monitoring data of dry and wet N deposition at 43sites across China. However, the methods to obtain deposition fluxes are questionable which can result in large uncertainties to the conclusions made in this study. Some of the uncertainties are not necessary and could be constrained. I explained this in detail below.

Response: The authors appreciate the reviewer for the valuable comments and suggestions that greatly help us improve our work. To reduce uncertainties to the conclusion made in this study, we have optimized the methods for computing dry deposition flux, and have made more clarification on the method of wet/bulk deposition measurement and discussion for wet/bulk deposition fluxes. Detailed responses to the comments are given below.

Specific comments

1. Site locations:

Different from the air quality monitoring networks which focus on the protection of human health, the deposition networks are used to assess the pollutant impacts on sensitive ecosystem and vegetation. Therefore, many networks, for example, CASTNET/NADP in US, CAPMoN in Canada, and IMPACTS in China, locate their sites in rural or protected areas in order to minimize effects from local pollution sources. In this paper, 10 out of the total 43 sites are located in urban areas, which are not homogeneously distributed in China. The comparison of regional averages including results from urban sites may not reveal the real spatial differences. For example, southeast China has two of the largest industrial centres and megacity clusters (the Pearl River Delta region and the Yangtze River Delta region) in China. Severe air pollution has been reported in this region (e.g., Chan and Yao, 2008). But this study shows the mean concentrations of reactive N species in southeast China were 15-25% lower than the national averages (Table 1). I suggest to remove all the

urban results in the analysis.

Response: Thank you for your suggestion on site locations. We agree many deposition networks worldwide mainly located in rural or protected areas. But the main objective of our study focuses on a systematic evaluation of dry plus wet deposition along different anthropogenic impacts (with differing reactive N emission intensities) across China. That's why we include ten urban sites in our network. We admit the current monitoring network is not complete and some more sites should be added in the future studies (please see our reply to reviewer #1's comment No. 4). We have noticed that atmospheric reactive N concentrations in southeast China (covering the Pearl River Delta and Yangtze River Delta regions) even lower than the national averages. Two reasons may explain this: 1) reactive N pollutants removed by frequent and high precipitation; 2) only three of total ten monitoring sites located in Pearl River Delta and Yangtze River Delta regions. In addition, our monitoring sites were mainly located at rural areas in southeast China and this could also lead to lower atmospheric N_r concentration and deposition. To avoid misunderstanding, we have deleted Table 1 and related comparison in the revision.

2. The method to derive the dry deposition flux: This paper estimated the dry deposition flux by the inferential method where the modeled dry deposition velocity (Vd) is paired with the measured concentration. Vd results were extracted from the 1-year productions by a global CTM model (GEOS-Chem),which has a horizontal resolution of 1/2 x 2/3 degree. This resolution is in fact too coarse for this study. Many sites (for example, NC1-NC2, NC4-NC5, NE2-NE3, SE9-SE10, SW5-SW6-SW7) are too close from each other and located within the same grid. It means the same Vd values are used for different sites although they may have different surface characteristics. What is the height where the Vds were calculated?70 m AGL? Vd for HNO3 is very sensitive to the calculation of Ra and the values computed at 70 m AGL should be much smaller than that at 2 m AGL. This also applies to the other species at some extend. The Vd calculations highly rely on the landuse types. Did you confirm the landuse map used in the simulation with the actual landuse types of the monitoring sites? They may not be consistent. In this paper, only 1-year simulation (2012) was used to derive Vds for the 5-year (2010-2014) period. This ignored the year-to-year variations in Vd. Several approaches can be taken to improve this. For example, you can run the GEOS-Chem model from 2010 to May 2013 and fill the gap in the period when GEOS meteorological data is unavailable using the means calculated from all the available simulations. Or you may try a single-point dry deposition model which can use the meteorological driving forces from various sources (e.g., field measurements if available, MM5/WRF simulation).

Response: We have re-modelled dry deposition velocities (V_ds) of N_r species at 2 m AGL. Indeed, the V_ds of N_r species computed at 2 m AGL show various degrees of increases compared to those at 70 m AGL. Meanwhile, we have run the GEOS-Chem model from January 2010 to May 2013 for all the 43 sites and fill the gap for the period when GEOS meteorological data is unavailable using

the mean values calculated from all the available simulations, as suggested by the reviewer. This approach of dry deposition estimate provides large improvements compared to previous work on nitrogen deposition over China as described below in addressing the Comment No. 6.

We now state in the text: "For a detailed description of the V_d calculation as well as the estimation of N dry deposition, the reader is referred to the Supplement (Sect. S5), with monthly and annual dry deposition velocities of N_r for different land use types presented in Tables S3 and S4 therein. The model uses the land map of the Global Land Cover Characteristics Data Base Version 2.0 (http://edc2.usgs.gov/glcc/globdoc2_0.php), which defines the land types (e.g., urban, forest, etc.) at the native 1 km × 1 km resolution and is then binned to the model resolution as fraction of the grid cell covered by each land type. The model 1/2° resolution may coarsely represent the local land characteristics at the monitoring sites. Future work using a single-point dry deposition model as for CASTNET (Clarke et al., 1997) would further improve the dry deposition flux estimates, but that requires concurrent *in-situ* measurements of meteorological variables which are not available at present. "

Added reference:

Clarke, J. F., Edgerton, E. S., and Martin, B. E.: Dry deposition calculations for the Clean Air Status and Trends Network, Atmos. Environ., 31, 3667-3678, 1997.

Table S3 has been corrected to show the improved dry deposition velocities over the different land types.

Table S3. Statistics of monthly mean dry deposition velocities of N_r species for three land use types, basing on the modeled hourly values at the forty-three sites during January 2010 and May 2013[a].

Land use type		Monthly mean deposition velocities (cm s^{-1})				
		NH_3	NO_2	HNO_3	pNH_4^+	pNO_3^-
Urban	N	410	410	410	410	410
	Min	0.30	0.01	0.12	0.06	0.06
	Max	1.63	0.44	5.78	0.35	0.35
	Mean	0.45	0.12	1.22	0.17	0.17
	Median	0.34	0.10	1.15	0.17	0.17
	SD	0.29	0.10	1.00	0.07	0.07
Rural	N	902	902	902	902	902
	Min	0.09	0.01	0.05	0.07	0.07
	Max	1.10	0.46	5.78	0.37	0.37
	Mean	0.40	0.17	1.49	0.18	0.18
	Median	0.35	0.16	1.49	0.18	0.18
	SD	0.16	0.12	1.10	0.06	0.06
Background	N	451	451	451	451	451
	Min	0.20	0.01	0.06	0.05	0.05
	Max	1.48	0.57	8.88	0.31	0.31
	Mean	0.47	0.17	1.78	0.16	0.16
	Median	0.43	0.13	1.48	0.16	0.16

SD	0.22	0.15	1.66	0.06	0.06

[a]The forty-three sites consist of 10 urban, 22 rural and 11 background sites. Among the forty-three monitoring sites, 20 farmland, 5 coastal, 6 forest and 2 grassland sites were included in the rural and background sites.

3. The sampling method of wet deposition: This study utilized a bulk sampler instead of a wet-only sampler to collect the wet depositions. A well-known problem about the bulk sampler is that the wet deposition samples can be contaminated by the dry deposition. This is even worse in the north region of China where precipitation is not frequent and dry deposition may dominate the total deposition. As mentioned in the manuscript, the bulk deposition flux of N can be 20-39% higher than the wet-only deposition. This needs to be emphasized in the conclusion and abstract of the manuscript to remind the readers be careful when comparing your results with previous studies.

Response: We have answered this question in the Reviewer [#]1's similar comment (Response to Reviewer [#]1's Comment No. 3). Briefly we have replaced "wet deposition" by "wet/bulk deposition" in the revision, and have emphasized the difference between bulk and wet-only deposition.

4. P18372: The description of sampling methods is not clear. At the sites without power, how HNO3 was sampled? Was NO2 sampled using Gradko diffusion tubes at all sites? If yes, there is no need to mention this twice in the same section.

Response: Thanks for pointing it out. At the seven sites (i.e., NC2, NE4, NE5, SW5, SW7, TP1 and TP2) without power supply, ambient HNO_3 concentrations were not measured due to lack of passive samplers for HNO_3. Thus, there were no data on HNO_3 concentrations and dry deposition fluxes shown for those seven sites in corresponding Figures (e.g. Figs 2, 3 and 5, Fig. S2c). As for total dry deposition fluxes at the seven sites, gaseous HNO_3 was not taken into consideration. At all sites in the network, gaseous NO_2 was sampled using Gradko diffusion tubes.

As suggested we have made more clarification on above issues in the revised Sect. 2.2.

5. P18378L23: annual precipitation -> annual precipitation amount?

Response: Yes, we have changed "annual precipitation" to "annual precipitation amount"

6. P18387L8: According to the references given, I think it means this study made improvements compared with previous work in China. It is better to clarify this.

Response: Thank you for this suggestion. We have revised the corresponding sentences in the Section 4.4 to clarify this.

"In previous work, dry deposition flux was inferred from atmospheric N_r concentrations and a literature-based annual mean deposition velocity (Shen et al., 2009), or reported by Luo et al. (2013) which did not consider the different

dry deposition velocities of various N_r species among different land use types. Clearly, in this study we have greatly improved the estimation of dry deposition, but further work is still needed to increase the reliability and accuracy of N dry deposition values."

References:

Luo, X. S., Liu, P., Tang, A. H., Liu, J. Y., Zong, X. Y., Zhang, Q., Kou, C. L., Zhang, L. J., Fowler, D., Fangmeier, A., Christie, P., Zhang, F. S., and Liu, X. J.: An evaluation of atmospheric N_r pollution and deposition in North China after the Beijing Olympics, Atmos. Environ., 74, 209–216, doi:10.1016/j.atmosenv.2013.03.054, 2013.

Shen, J. L., Tang, A. H., Liu, X. J., Fangmeier, A., Goulding, K. T. W., and Zhang, F. S.: High concentrations and dry deposition of reactive nitrogen species at two sites in the North China Plain, Environ. Pollut., 157, 3106–3113,doi:10.1016/j.envpol.2009.05.016, 2009.

7. P18387L20-25: The organic N species have been found as important contributors to the N dry deposition. For example, Turnipseed et al. (2006) reported that PAN accounted for 20% of the daytime NOy flux at a forest site. This should be included in the uncertainty discussion (section 4.4).

Response: Thank you for this valuable suggestion. We have added the following sentences to discuss this issue in the revised Section 4.4.

"On the other hand, the total dry deposition flux in this study may be underestimated due to omission of the dry-deposited organic N species in our network and missing HNO_3 data at very few sites as noted earlier (Sect. 2.2). The organic N species have been found as important contributors to the N dry deposition. For example, PAN accounted for 20% of the daytime, summer time NO_y ($NO + NO_2 + HNO_3 + NO_3^- + PAN$) dry deposition at a coniferous forest site (Turnipseed et al., 2006). However, the contribution of PAN and other known atmospheric organic nitrates to total N_r inputs must be minor on the annual time scale, as reported by Flechard et al. (2012)."

References:

Flechard, C. R., Nemitz, E., Smith, R. I., Fowler, D., Vermeulen, A.T., Bleeker, A., Erisman, J. W., Simpson, D., Zhang, L., Tang, Y. S., and Sutton, M. A.: Dry deposition of reactive nitrogen to European ecosystems: a comparison of inferential models across the NitroEurope network, Atmos. Chem. Phys., 11, 2703–2728,doi:10.5194/acp-11-2703-2011, 2011.

Turnipseed, A. A., Huey, L. G., Nemitz, E., Stickel, R., Higgs, J., Tanner, D. J., Slusher, D. L., Sparks, J. P., Flocke, F., and Guenther, A.: Eddy covariance fluxes of peroxyacetyl nitrates (PANs) and NOy to a coniferous forest, J. Geophys. Res., 111,D09304, doi:10.1029/2005JD006631, 2006.

8. Supplement section S5: As stated in the manual of GEOS-Chem(http://wiki.seas.harvard.edu/geos-chem/index.php/Dry_deposition), the dry deposition for particles followed Zhang et al.(2001) scheme, instead of Wesely

(1989),which is a dry deposition scheme for gases.

Response: Yes, we now state in both the Section 2.5 and Section S5 "The model calculation of dry deposition of N_r species follows a standard big-leaf resistance-in-series model as described by Wesely (1989) for gases and Zhang et al. (2001) for aerosols."

Added Reference:

Zhang, L. M., Gong, S. L., Padro, J., and Barrie, L.: A size-segregated particle dry deposition scheme for an atmospheric aerosol module, Atmos. Environ., 35 (3), 549-560, doi:10.1016/s1352-2310(00)00326-5, 2001.

Technical corrections:

9. P18372L3: Sutton et al. (2001) -> Sutton et al. (2001))

Response: Revised as suggested.

10. P18372L11: delete "produced by"

Response: Deleted as suggested.

11. Supplement section S1: South China (SC) -> Southeast China (SE)

Response: Revised as suggested (changed "South China (SC)" to "Southeast China (SE)".

acp-2015-445

Quantifying atmospheric nitrogen deposition through a nationwide monitoring network across China

W. Xu[1], X. S. Luo[1,2], Y. P. Pan[3], L. Zhang[4], A. H. Tang[1], J. L. Shen[5], Y. Zhang[6], K. H. Li[7], Q. H. Wu[1], D. W. Yang[1], Y. Y. Zhang[1], J. Xue[1], W. Q. Li[8], Q. Q. Li[1,9], L. Tang[9], S. H. Lu[10], T. Liang[11], Y. A. Tong[11], P. Liu[12], Q. Zhang[12], Z. Q. Xiong[13], X. J. Shi[14], L. H. Wu[15], W. Q. Shi[16], K. Tian[17], X. H. Zhong[17], K. Shi[18], Q. Y. Tang[19], L. J. Zhang[20], J. L. Huang[21], C. E. He[22], F. H. Kuang[23], B. Zhu[23], H. Liu[24], X. Jin[25], Y. J. Xin[25], X. K Shi[26], E. Z. Du[27], A. J. Dore[28], S. Tang[28], J. L. Jr. Collett[29], K. Goulding[30], Y. X. Sun[31], J. Ren[32], F. S. Zhang[1], X. J. Liu[1,*]

[1]College of Resources and Environmental Sciences, China Agricultural University, Beijing 100193, China

[2]Institute of Plant Nutrition, Resources and Environmental Sciences, Henan Academy of Agricultural Sciences, Zhengzhou 450002, China

[3]State Key Laboratory of Atmospheric Boundary Layer Physics and Atmospheric Chemistry (LAPC), Institute of Atmospheric Physics, Chinese Academy of Sciences, Beijing 100029, China

[4]Laboratory for Climate and Ocean-Atmosphere Studies, Department of Atmospheric and Oceanic Sciences, School of Physics, Peking University, Beijing 100871, China

[5]Institute of Subtropical Agriculture, Chinese Academy of Sciences, Changsha 4410125, China

[6]College of Nature Conservation, Beijing Forestry University, Beijing 100083, China

[7]Xinjiang Institute of Ecology and Geography, Chinese Academy of Sciences, Urumqi 830011, China

[8]Fujian Institute of Tobacco Agricultural Sciences, Fuzhou 350003, China

[9]College of Resources and Environmental Sciences, Yunnan Agricultural University, Kunming 650224, China

[10]Soil and Fertilizer Institute, Sichuan Academy of Agricultural Sciences, Chengdu 610066, China

[11]Nature Resource and Environment College, Northwest A&F University, Yangling 712100, China

[12]Institute of Agricultural Environment and Resource, Shanxi Academy of Agricultural Sciences, Taiyuan 030031, China

[13]College of Resources and Environmental Sciences, Nanjing Agricultural University, Nanjing 210009, China

[14]College of Resources and Environment, Southwest University, Chongqing 400716, China

[15]College of Environmental and Resource Sciences, Zhejiang University, Hangzhou 310029, China

[16]South Subtropical Crops Research Institute, Chinese Academy of Tropical Agricultural Science, Zhanjiang 524091, China

[17]Rice Research Institute, Guangdong Academy of Agricultural Sciences, Guangzhou 510640,

China
[18]College of Environmental and Chemical Engineering, Dalian Jiaotong University, Dalian 116028, China
[19]College of Agriculture, Hunan Agricultural University, Changsha 410128, China
[20]College of Resources and Environment, Agricultural University of Hebei, Baoding 071001, China
[21]College of Plant Science and Technology, Huazhong Agricultural University, Wuhan, China
[22]Institute of Geographic Sciences and Natural Resources, Chinese Academy of Sciences, Bei jing 100101, China
[23]Institute of Mountain, Hazards and Environment, Chinese Academy of Sciences, Chengdu 610041, China
[24]Research Institute of Soil & Fertilizer and Agricultural Water Conservation, Xinjiang Academy of Agricultural Sciences, Urumqi 830091, China
[25]The Bureau of Qinghai Meteorology, Xining 810001, China
[26]Agriculture, Forestry and Water Department of Changdao County, Changdao 265800, China
[27]State Key Laboratory of Earth Surface Processes and Resource Ecology, and College of Resources Science & Technology, Beijing Normal University, Beijing 100875, China
[28]Centre for Ecology & Hydrology Edinburgh, Bush Estate, Penicuik, Midlothian EH26 0QB, UK
[29]Department of Atmospheric Science, Colorado State University, Fort Collins, CO 80523, USA
[30]The Sustainable Soils and Grassland Systems Department, Rothamsted Research, Harpenden AL5 2JQ, UK
[31]Institute of Soil and Fertilizer, Anhui Academy of Agricultural Sciences, Hefei 230031, China
[32]Institute of Soil and Fertilizer, Jilin Academy of Agricultural Sciences, Changchun 130124, China
Corresponding author: liu310@cau.edu.cn (X. J. Liu).

Abstract: Global reactive nitrogen (N_r) deposition to terrestrial ecosystems has increased dramatically since the industrial revolution. This is especially true in recent decades in China due to continuous economic growth. However, there are no comprehensive reports of both measured dry and wet/bulk N_r deposition across China. We therefore conducted a multiple-year study during the period mainly from 2010 to 2014 to monitor atmospheric concentrations of five major N_r species of gaseous NH_3, NO_2 and HNO_3, and inorganic nitrogen (NH_4^+ and NO_3^-) in both particles and precipitation, based on a Nationwide Nitrogen Deposition Monitoring Network (NNDMN, covering 43 sites) in China. Wet/bulk deposition fluxes of N_r species were collected by precipitation gauge method and measured by continuous flow analyzer; dry deposition fluxes were estimated using airborne concentration measurements and

删除的内容: measured directly

inferential models. Our observations reveal large spatial variations of atmospheric N_r concentrations and dry and wet/bulk N_r deposition. On a national basis, the annual average concentrations (1.3-47.0 μg N m^{-3}) and dry plus wet/bulk deposition fluxes (2.9-83.3 kg N ha^{-1} yr^{-1}) of inorganic N_r species ranked by land use as urban > rural > background sites, reflecting the impact of anthropogenic N_r emission. Average dry and wet/bulk N deposition fluxes were 20.6 ± 11.2 (mean ± standard deviation) and 19.3 ± 9.2 kg N ha^{-1} yr^{-1} across China, with reduced N deposition dominating both dry and wet/bulk deposition. Our results suggest atmospheric dry N deposition is equally important to wet/bulk N deposition at the national scale. Therefore both deposition forms should be included when considering the impacts of N deposition on environment and ecosystem health.

Keywords: air pollution; reactive nitrogen; dry deposition; wet deposition; ecosystem; China

1. Introduction

Humans continue to accelerate the global nitrogen (N) cycle at a record pace as rates of anthropogenic reactive nitrogen (N_r) fixation have increased 20-fold over the last century (Galloway et al., 2008). New N_r from anthropogenic fixation is formed primarily through cultivation of N-fixing legumes, the Haber-Bosch process and combustion of fossil-fuel (Galloway et al., 2013). As more N_r have been created, emissions of N_r (NO_x=NO+NO_2, and NH_3) to the atmosphere have increased from approximately 34 Tg N yr^{-1} in 1860 to 109 Tg N yr^{-1} in 2010 (Fowler et al., 2013; Galloway et al., 2004); most of this emitted N_r is deposited back to land and water bodies. As an essential nutrient, N supplied by atmospheric deposition is useful for all life forms in the biosphere and may stimulate primary production in an ecosystem if it does not exceed the ecosystem-dependent critical load (Liu et al., 2010, 2011). However, long-term high levels of atmospheric N_r and its deposition can reduce biological diversity (Clark et al., 2008), degrade human health (Richter et al., 2005), alter soil and water chemistry (Vitousek et al., 1997) and influence the greenhouse gas balance (Matson et al., 2002).

Nitrogen deposition occurs via dry and wet processes. Neglecting dry deposition can lead to substantial underestimation of total flux as dry deposition can contribute up to 2/3 of total N deposition (Flechard et al., 2011; Vet et al., 2014). For quantification of atmospheric deposition at the national scale, long-term monitoring networks such as CAPMoN (Canada), IDAF (Africa), CASTNET/NADP (the United States), EMEP

删除的内容: The

删除的内容: 75.2

删除的内容: by region as North China > Southeast China > Southwest China > Northeast China > Northwest China > the Tibetan Plateau or

删除的内容: 18.5

删除的内容: , respectively,

删除的内容: and

(Europe) and EANET (East Asia) have been established; such networks are essential for quantification of both wet and dry deposition and revealing long-term trends and spatial patterns under major environmental and climate change (Skeffington and Hill, 2012). Wet deposition, by means of rain or snow, is relatively easily measured in existing networks. In contrast, dry deposition of gases and particulate matter is much more difficult to measure, and strongly influenced by factors such as surface roughness, surface wetness, and climate and environmental factors (Erisman et al., 2005). Direct methods (e.g., eddy correlation, chambers) and indirect methods (e.g., inferential, gradient analysis) can determine dry deposition fluxes (Seinfeld and Pandis, 2006). The inferential method is widely used in many monitoring networks (e.g. CASTNET and EANET), where dry deposition rates are derived from measured ambient concentrations of N_r species and computed deposition velocities (Endo et al., 2011; Holland et al., 2005; Pan et al., 2012). Additionally, atmospheric modeling has been used as an operational tool to upscale results from sites to regions where no measurements are available (Flechard et al., 2011; Zhao et al., 2015).

According to long-term trends observed by the above monitoring networks, N deposition has decreased over the last two decades in Europe (EEA, 2011). Measurements of wet deposition in the US show a strong decrease in NO_3-N deposition over most of the country (Du et al., 2014), but NH_4-N deposition increased in agricultural regions. China, as one of the most rapidly developing countries in East Asia, has witnessed serious atmospheric N_r pollution since the late 1970s (Hu et al., 2010; Liu et al., 2011). Accurate quantification of N deposition is key to assessing its ecological impacts on terrestrial ecosystems (Liu et al., 2011). Previous modeling studies (e.g., Dentener et al., 2006; Galloway et al., 2008; Vet et al., 2014) suggested that central-east China was a global hotspot for N deposition. More recently, based on meta-analyses of historic literature, both Liu et al. (2013) and Jia et al. (2014) reported a significant increase in N wet/bulk deposition in China since the 1980s or 1990s. However, most measurements in China only reported wet/bulk deposition (e.g., Chen et al., 2007; Zhang et al., 2012a; Huang et al., 2013; Zhu et al., 2015) and/or dry deposition (Luo et al., 2013; Shen et al., 2009; Pan et al., 2012) at a local or regional scale. Although national N deposition has been investigated by Lü and Tian (2007, 2014), the deposition fluxes were largely underestimated due to the inclusion only of gaseous NO_2 in dry deposition and not NH_3, HNO_3 and particulate ammonium and nitrate etc. Therefore, the magnitude and spatial patterns of *in situ* measured N wet

删除的内容: globally

删除的内容:, EMEP

/bulk and dry deposition across China are still not clear.

Against such a background, we have established a Nationwide Nitrogen Deposition Monitoring Network (NNDMN) in China in 2010, measuring both wet/bulk and dry deposition. The NNDMN consists of forty-three *in-situ* monitoring sites, covering urban, rural (cropland) and background (coastal, forest and grassland) areas across China. The focus of the network is to conduct high-quality measurements of atmospheric N_r in gases, particles and precipitation. These data provide a unique and valuable quantitative description of N_r deposition in China, but have never been published as a whole. The objectives of this study were therefore to: (1) obtain the first quantitative information on atmospheric N_r concentrations and pollution status across China; and (2) analyze overall fluxes and spatial variations of N wet/bulk and dry deposition in relation to anthropogenic N_r emissions in different regions.

2. Materials and Methods

2.1 Sampling sites

The distribution of the forty-three monitoring sites in the NNDMN is shown in **Fig. 1**. Although sampling periods varied between sites, most of our monitoring started from 2010 to 2014 (see Supporting Materials for details). The NNDMN comprise 10 urban sites, 22 rural sites and 11 background sites (**Table S1** of the online Supplement). To better analyze atmospheric N deposition results among the sites, we divided the forty-three sites into six regions: north China (NC, 13 sites), northeast China (NE, 5 sites); northwest China (NW, 6 sites), southeast China (SE, 11 sites), southwest China (SW, 6 sites), and Tibetan Plateau (TP, 2 sites), representing China's various social-economical and geo-climatic regions (for details, see **Sect. A1** of the online Supplement). The sites in the six regions are described using region codes (i.e., NC, NE, NW, SE, SW, TP) plus site numbers such as NC1, NC2, NC3, ..., NE1, NE2, etc. The longitudes and latitudes of all 43-sites ranged from 83.71 to 129.25 ºE, and from 21.26 to 50.78 ºN, respectively. Annual mean rainfall ranged from 170 to 1748 mm and the annual mean air temperature ranged from -6.2 to 23.2 °C. Site names, land use types and population densities are summarized in **Table S1** of the Supplement. More detailed information on the monitoring sites, such as specific locations, surrounding environment and possible emission sources are provided in **Sect. A2** of the Supplement.

2.2 Collection of gaseous and particulate N_r samples

In this study ambient N_r concentrations of gaseous NH_3, NO_2 and HNO_3, and

particulate NH_4^+ (pNH_4^+) and NO_3^- (pNO_3^-) were measured monthly at the 43 sites using continuous active and passive samplers. DELTA active sampling systems (DEnuder for Long-Term Atmospheric sampling, described in detail in Flechard et al. (2011) and Sutton et al. (2001)), were used to collect NH_3, HNO_3, pNH_4^+ and pNO_3^-; NO_2 samples were collected using Gradko diffusion tubes (Gradko International Limited, UK) at all sampling sites. The air intakes of the DELTA system and the NO_2 tubes were set at a height of 2 m above the ground (at least 0.5 m higher than the canopy height) at most sites. At a few sites, the DELTA systems could not be used due to power constraints. Therefore, NH_3 samples were collected using ALPHA passive samplers (Adapted Low-cost High Absorption, designed by the Center for Ecology and Hydrology, Edinburgh, UK), while the pNH_4^+ and pNO_3^- in PM_{10} were collected using particulate samplers (TSH-16 or TH-150III, Wuhan Tianhong Corp., Wuhan, China). However, HNO_3 measurements were not performed due to lack of corresponding passive samplers. Briefly, all the measurements of N_r concentration were based on monthly sampling (one sample per month for each N_r species) except at the very few sites without DELTA systems, where pNH_4^+ and pNO_3^- samples were calculated from daily sampling transformed to monthly averaged data. Detailed information on measuring methods, sample replication and collection are given in **Sect. A3** of the Supplement with sampling periods listed in **Table S2** of the Supplement. Comparisons between the ALPHA samplers and the DELTA systems at six network sites for gaseous NH_3 measurements indicated that the two methods provided comparable NH_3 concentrations (values between the two methods were not significantly different) (cf. **Sect. A4** in the Supplement and **Fig. S1** therein).

删除的内容: and NO_2

删除的内容: and Gradko diffusion tubes, respectively

删除的内容: produced by

2.3 Collection of precipitation

At all monitoring sites precipitation (here we define it as wet/bulk deposition which contains wet and part dry deposition) samples were collected using precipitation gauges (SDM6, Tianjin Weather Equipment Inc., China) located beside the DELTA systems (c. 2 m). The collector, consisting of a stainless steel funnel and glass bottle (vol. 2000-2500 ml), collects precipitation (rainwater, snow) without a power supply. Precipitation amount was measured using a graduated cylinder (scale range: 0-10 mm; division: 0.1 mm) coupled with the gauge. After each daily (8:00 am-8:00 am next day) event, the collected samples were thoroughly mixed and then immediately stored in clean polyethylene bottles (50 mL). All collected samples (including melted snow) samples were frozen at −18 °C at each site until delivery to the laboratory at China

Agricultural University (CAU) for analysis of inorganic N (NH_4^+ and NO_3^-). The gauges were cleaned with high-purity water after each collection and once every week in order to avoid cross contamination.

2.4 Analytical procedures

In CAU's analytical laboratory, the exposed sampling trains of the DELTA systems and passive samples were stored at 4 °C and analyzed at one-month intervals. The HNO_3 denuders and alkaline-coated filters were extracted with 10 mL 0.05 % H_2O_2 in aqueous solution. The NH_3 denuders and acid-coated filters, and ALPHA samplers were extracted with 10 mL high-purity water. The loaded PM_{10} filters were extracted with 50 mL high-purity water by ultrasonication for 30-60 min and then filtered through a syringe filter (0.45 μm, Tengda Inc., Tianjin, China). Ammonium (NH_4^+) and nitrate (NO_3^-) in the extracted and filtered solutions were measured with an AA3 continuous-flow analyzer (Bran+Luebbe GmbH, Norderstedt, Germany). The detection limits were 0.01 mg N L^{-1} for NH_4^+ and NO_3^-. It should be noted that NO_3^- was converted to NO_2^- during the chemical analysis. So, NO_2^- here was included in the analysis, and NO_3^- equals to the sum of NO_2^- and NO_3^-. The disks from the Gradko samplers were extracted with a solution containing sulphanilamide, H_3PO_4 and N-1-Naphthylethylene-diamine, and the NO_2^- content in the extract determined using a colorimetric method by absorption at a wavelength of 542 nm. The detection limit for NO_2^- was 0.01 mg N L^{-1}. Three laboratory and three field blank samples were extracted and analyzed using the same methods as the exposed samples. After correcting for the corresponding blanks, the results were used for the calculation of ambient concentrations of gaseous and particulate N_r. Each collected precipitation sample was filtered with a 0.45 μm syringe filter, and 15 mL filtrates frozen and stored in polypropylene bottles until chemical analysis within one month. The NH_4^+ and NO_3^- concentrations of the filtrates were determined using an AA3 continuous-flow analyzer as described above.

2.5 Deposition flux estimation

The inferential technique, which combines the measured concentration and a modeled dry deposition velocity (V_d), was used to estimate the dry deposition fluxes of N_r species (Schwede et al., 2011; Pan et al., 2012). The concentrations of gases (HNO_3, NO_2 and NH_3) and aerosols (NH_4^+ and NO_3^-) were measured as described in Section 2.2. The monthly average V_d over China was calculated by the GEOS-Chem chemical transport model (CTM) (Bey et al., 2001; http://geos-chem.org). The GEOS-Chem

删除的内容: l

删除的内容: l

删除的内容: l

删除的内容: absorbance

删除的内容: ml

CTM is driven by GEOS-5 (Goddard Earth Observing System) assimilated meteorological data from the NASA Global Modeling and Assimilation Office (GMAO) with a horizontal resolution of 1/2° latitude × 2/3° longitude and 6-h temporal resolution (3-h for surface variables and mixing depths). We used a nested-grid version of GEOS-Chem for Asia that has the native 1/2°×2/3° resolution over East Asia (70°E-150°E, 11°S-55°N) (Chen et al., 2009). The nested model has been applied to examine atmospheric nitrogen deposition to the northwestern Pacific (Zhao et al., 2015), and a similar nested model for North America has been used to analyze nitrogen deposition over the United States (Zhang et al., 2012b; Ellis et al., 2013). The model calculation of dry deposition of N_r species follows a standard big-leaf resistance-in-series model as described by Wesely (1989) for gases and Zhang et al. (2001) for aerosol. For a detailed description of the V_d calculation as well as the estimation of N dry deposition, the reader is referred to the Supplement (**Sect. A5**), with monthly and annual dry deposition velocities of N_r for different land use types presented in **Tables S3 and S4** therein. The model uses the land map of the Global Land Cover Characteristics Data Base Version 2.0 (http://edc2.usgs.gov/glcc/globdoc2_0.php), which defines the land types (e.g., urban, forest, etc.) at the native 1 km × 1 km resolution and is then binned to the model resolution as fraction of the grid cell covered by each land type. The model 1/2° resolution may coarsely represent the local land characteristics at the monitoring sites. Future work using a single-point dry deposition model as for CASTNET (Clarke et al., 1997) would further improve the dry deposition flux estimates, but that requires concurrent *in-situ* measurements of meteorological variables which are not available at present.

Wet/bulk N deposition flux was calculated as the product of the precipitation amount and the concentration of N_r species in precipitation, using the following equations (1) and (2):

$$C_w = \sum_{i=1}^{n}(C_i P_i) / \sum_{i=1}^{n} P_i \quad (1)$$

where C_w is the volume-weighted mean (VWM) concentration (mg N L^{-1}) calculated from the n precipitation samples within a month or a year, and the individual sample concentration C_i is weighted by the rainfall amount P_i for each sample.

$$D_w = P_t C_w / 100 \quad (2)$$

where D_w is the wet/bulk deposition flux (kg N ha^{-1}), P_t is the total amount of all

删除的内容: 2012a

删除的内容: (Wesely, 1989)

删除的内容: -

precipitation events (mm), and 100 is a unit conversion factor.

2.6 Statistics

A one-way analysis of variance (ANOVA) and nonparametric t-tests were conducted to examine the differences in the investigated variables between sites (urban, rural and background) and between the six regions. Linear regression analysis was used to analyze the relationships among annual wet N deposition flux, annual precipitation amount and annual VWM concentration of inorganic N in precipitation. All analyses were performed using SPSS 11.5 (SPSS Inc., Chicago, IL, USA). Statistically significant differences were set at P values < 0.05.

3. Results

3.1 Concentrations of N_r species in air

Monthly mean concentrations of NH_3, NO_2, HNO_3, pNH_4^+ and pNO_3^- were 0.08-34.8, 0.13-33.4, 0.02-4.90, 0.02-55.0 and 0.02-32.1 μg N m^{-3}, respectively (**Fig. S2a-e**, Supplement). The annual mean concentrations of gaseous and particulate N_r were calculated for each site from the monthly N_r concentrations (**Fig. 2a**), and further were averaged for land use types in the six regions (**Fig. 3a-e**) and the whole nation (**Fig. 4a**) according to geographical location and the classification of each site. Annual mean NH_3 concentrations ranged from 0.3 to 13.1 μg N m^{-3}, with an overall average value of 6.1 μg N m^{-3}. In NC, SE and SW, the NH_3 concentrations at the urban sites (average for the three regions, 9.5 ± 2.1 μg N m^{-3}) were about 1/3 higher than at the rural sites (6.2 ± 2.3 μg N m^{-3}) and were almost twice of those at the background sites (4.8 ± 1.4 μg N m^{-3}), whereas in NE and NW NH_3 concentrations were lower at the urban sites (average two regions, 5.5 ± 3.2 μg N m^{-3}) than at the rural sites (8.8 ± 0.3 μg N m^{-3}) but 4.6-times greater than at the background sites (1.2 ± 0.5 μg N m^{-3}). Comparing land use types by region, annual NH_3 concentrations at the rural sites in northern regions (NC, NE and NW) were approximately equal, which on average were 1.8-times greater than the average of southern rural sites. In contrast, annual NH_3 concentrations at urban and background sites ranked in the order: SW > NC > NW > SE > TP > NE, and SW > NC > SE > NW > TP > NE, respectively (**Fig. 3a**). Annual mean NO_2 concentrations showed similar spatial variations (0.4 to 16.2 μg N m^{-3}) to those of NH_3, and overall averaged 6.8 μg N m^{-3}. In the six regions, the NO_2 concentrations at urban sites were 1.4-4.5 times higher than those at rural sites, and were even 2.0-16.6 times higher than the background sites (except for SW). By

删除的内容: over region and

删除的内容: as listed in **Table 1**

删除的内容: Among the six regions, the gaseous NH_3 concentrations decreased in the order of NC > SW > NW > SE > NE > TP. In NC, SE and SW, the NH_3 concentrations at the urban sites (average three regions, 9.5 μg N m^{-3}) were slightly higher than at the rural sites (6.2 μg N m^{-3}). The annual mean NH_3 concentration across northern rural sites, on average, was 1.8-times greater than the average of southern rural sites

comparison among regions, annual mean NO_2 concentrations at rural sites in NC were about 2.6-times higher than in NE and NW, and overall averaged NO_2 concentrations in northern rural China (NC, NE and NW, 5.7 ± 3.5 μg N m^{-3}) were comparable to those at southern rural sites (average of SE and SW, 5.1± 0.1 μg N m^{-3}). As for urban and background sites, the annual mean NO_2 concentrations followed the order: NC > NW > SE > SW > NE > TP, and SW > NC > SE > NE > NW > TP, respectively (**Fig. 3b**). Annual mean HNO_3 concentrations were relatively low everywhere (from 0.1 to 2.9 μg N m^{-3}, averaging 1.3 μg N m^{-3}). In all regions except NE and TP, the HNO_3 concentrations were highest at the urban sites (averages: 1.7-2.4 μg N m^{-3}), followed by the rural sites (0.8-1.6 μg N m^{-3}), and were lowest at the background sites (0.2-1.1 μg N m^{-3}). The HNO_3 concentrations were comparable for the same land use types across northern and southern monitoring sites, on average, 1.8 vs. 1.8, 1.2 vs. 1.0, and 0.6 vs. 0.8 μg N m^{-3} at the urban, rural and background sites, respectively (**Fig. 3c**). The annual mean concentrations of pNH_4^+ and pNO_3^- were in the ranges of 0.2-18.0 μg N m^{-3} (average 5.7 μg N m^{-3}) and 0.2-7.7 μg N m^{-3} (average 2.7 μg N m^{-3}), respectively. Annual pNH_4^+ concentrations show a decreasing trend of urban > rural > background in all regions (except NE), where relatively higher concentrations were observed at the rural sites than the urban sites, and in SE, where no clear difference were observed among three land use types (**Fig. 3d**). In contrast, annual pNO_3^- concentrations showed a declining trend of urban > rural > background in all regions (**Fig. 3e**). Overall, annual mean concentrations of both pNH_4^+ and pNO_3^- at all land use types were both slightly higher in northern China (NC, NE and NW) than in southern China (SE, SW and TP).

In total, annual mean concentrations of gaseous and particulate N_r in air were 1.3-47.0 μg N m^{-3} among all sampling sites. The total annual concentrations of measured N_r generally decreased in the order of urban > rural > background in all regions except NE (**Fig. 3f**).

3.2 Concentrations of N_r species in precipitation

The monthly VWM concentrations of inorganic N_r species at the forty-three sampling sites during the study period ranged from 0.01 to 27.1 mg N L^{-1} for NH_4^+-N and from 0.02 to 27.9 mg N L^{-1} for NO_3^--N (**Fig. S3**, Supplement). The annual VWM concentrations of NH_4^+-N and NO_3^--N across all sites were in the ranges of 0.2-4.3 and 0.1-2.5 mg N L^{-1}, respectively, with averages of 1.6 and 1.3 mg N L^{-1} (**Fig. 2b**). The urban-rural-background distributions of annual VWM concentrations of NH_4^+-N

删除的内容: The highest NO_2 concentrations were found in NC, with an average value of 10.1 μg N m^{-3}, 1.5-3.6 times greater than the averages of the other five regions. Both the urban and rural sites in NC had relatively high NO_2 concentrations (on average, 13.9 vs. 9.7 μg N m^{-3})

删除的内容: and ranked by order of NC > NW ≈ SW > SE > NE

删除的内容: in

删除的内容: China

删除的内容: The regional variation of annual pNH_4^+ concentrations was consistent with that of NH_3, whereas annual pNO_3^- concentrations followed the order: NC > SE > SW > NE ≈ NW TP.

删除的内容: Annual

删除的内容: the

删除的内容: , compared with those in the other three regions

删除的内容: ; ranked in the order of NC > NW ≈ SW > SE > NE > TP

删除的内容: Comparing land use types, t

删除的内容: , as well as each N_r species,

删除的内容: S3, Supplement

删除的内容: S4

and NO_3^--N were, respectively, fairly coincided with corresponding reduced (i.e. NH_3 and pNH_4^+) and oxidized N_r (i.e. HNO_3 and pNO_3^-) in all regions except NH_4^+-N in SE and NO_3^--N in NW (**Figs. 3g and h**). Conversely, the regional variations in annual VWM concentrations of NH_4^+-N and NO_3^--N for the three land use types were not consistent with corresponding reduced and oxidized N_r, respectively. On a national basis, the VWM concentrations of NH_4^+-N and NO_3^--N were both decreased in the order urban ≥ rural > background (**Fig. 4b**). The annual total inorganic N (TIN) concentrations in precipitation across all sites were 0.4-6.0 mg N L^{-1}, decreasing from urban to background sites in all regions (except NE) as well as on a national basis (**Figs. 3i and 4b**).

3.3 Dry deposition of N_r species

The annual dry deposition fluxes of NH_3, NO_2, HNO_3, pNH_4^+ and pNO_3^- were in the ranges of 0.5-16.0, 0.2-9.8, 0.2-16.6, 0.1-11.7 and 0.1-4.5 kg N ha^{-1} yr^{-1}, and averaged 8.2, 3.2, 5.4, 3.2 and 1.5 kg N ha^{-1} yr^{-1}, respectively (**Fig. 5a**). The total dry N deposition across all sites ranged from 1.1 to 52.2 kg N ha^{-1} yr^{-1} (averaged 20.6 ± 11.2 kg N ha^{-1} yr^{-1}). Gaseous N species were the primary contributors to total dry-deposited N, ranging from 60% to 96%, despite of the missing HNO_3 data at a few sites. In general, NH_3 was predominant N_r species in total dry N deposition and accounted for 24-72%, compared with 1-43% from NO_2 and 9-37% from HNO_3. Comparing land use types in each region, spatial pattern of individual fluxes is fairly consistent with that of their respective concentrations except that of NH_3 for NC, that of NO_2 for SW, those of NO_2 and pNH_4^+ for NW and those of almost all measured N_r species for NE (**Figs. 3a-e and 6a-e**). Furthermore, a consistent picture is also seen for the total flux (sum of fluxes of five N_r species) at each land use type (**Figs. 5f and 6f**). Among the six regions, regional variations of individual fluxes at each land use type generally differed from those of their respective concentrations. Similarly, the inconsistent behavior appeared for the total fluxes at urban and rural sites but not at background site. On a national basis, there was no significant difference (p>0.05) in the total dry N deposition fluxes between urban (26.9 kg N ha^{-1} yr^{-1}) and rural (23.0 kg N ha^{-1} yr^{-1}) sites, both of which were significantly higher than background site (10.1 kg N ha^{-1} yr^{-1}). Also, a similar pattern was found for the dry deposition flux of each N_r species among different land use types (**Fig. 4c**).

3.4 Wet/bulk deposition of N_r species

删除的内容: The regional variations in NH_4^+-N and NO_3^--N were not totally consistent with ambient gaseous and particulate N_r (**Figs. S2** and **S4**, Supplement). For example, monthly mean concentrations of NH_3 and pNH_4^+ were significantly higher (both p<0.05) in NC than NW, whereas the opposite was observed for precipitation NH_4^+-N. In addition, monthly mean pNO_3^- concentrations were significantly lower (p<0.05) in NE than SE, but significantly higher precipitation NO_3^--N concentrations were found in NE. The annual VWM concentrations of NH_4^+-N and NO_3^--N across all sites were in the ranges of 0.2-4.3 and 0.1-2.5 mg N L^{-1}, respectively, with averages of 1.6 and 1.3 mg N L^{-1} (**Fig. 2b**) and showing no significant difference (p>0.05) between them. Among regions, annual VWM concentrations ranked in the order of NW > NC > NE ≈ SW ≈ TP > SE for NH_4^+-N, whereas the order was NC > NW > NE > SW > SE > TP for NO_3^--N (**Table 1**). Annual total inorganic N concentrations in precipitation averaged 4.3, 2.3, 3.9 and 2.0 mg N L^{-1} in NC, NE, NW and SW respectively, and 1.9 mg N L^{-1} in both SE and TP

删除的内容: 15

删除的内容: 2

删除的内容: 1

删除的内容: 2

删除的内容: 10

删除的内容: 0

删除的内容: 7.7

删除的内容: 1

删除的内容: 3.7

删除的内容: 4

删除的内容: **4a**

删除的内容: Comparing individual fluxes by region (**Table 1**), NC showed higher deposition levels for gaseous and particulate species. The deposition fluxes of gaseous species followed NC > SW > NE > SE > NW > TP for NH_3, NC > SW > SE > NE ≈ TP > NW for NO_2, and NC > SE > SW > NE > NW for NHO_3, while those of pNH_4^+ and pNO_3^- were NC > SW > SE > NE > NW > TP and NC > SW > SE ≈ TP > NW > NE, respectively. The total dry N deposition across all sites ranged from 1.0 to 44.1 kg N ha^{-1} yr^{-1} (averaged 18.5 kg N ha^{-1} yr^{-1}). Gaseous N species were the primary contributors to total dry-deposited ...

Annual wet/bulk N deposition fluxes at the forty-three sites ranged from 1.0 to 19.1 kg N ha^{-1} yr^{-1} for NH_4^+-N and from 0.5 to 20.1 kg N ha^{-1} yr^{-1} for NO_3^--N (**Fig. 5b**). The annual wet/bulk deposition fluxes of NH_4^+-N were, on average, 1.3 times those of NO_3^--N. The total annual wet/bulk N (NH_4^+-N+ NO_3^--N) deposition fluxes across all the sites were 1.5-32.5 kg N ha^{-1} yr^{-1} (average 19.3 kg N ha^{-1} yr^{-1}), with a large spatial variation. Region variation of annual wet N deposition followed the order of NC > SE > SW > NE > NW > TP for NH_4^+-N, and SE > NC > SW > NE > TP > NW for NO_3^--N, both of which differed from their orders of annual VWM concentration, reflecting differences in annual precipitation amount. Annual total wet/bulk N deposition fluxes averaged 24.6, 13.6, 7.4, 24.4, 17.6 and 7.6 kg N ha^{-1} yr^{-1}, respectively, in NC, NE, NW, SE, SW and TP (**Fig. 5b**). At national scale, annual wet/bulk deposition fluxes of total inorganic N and/or each N_r species at urban and rural sites were comparable but significantly higher (p<0.05) than those at background sites **(Fig. 4d)**.

3.5 Total annual dry and wet deposition of N_r species

The total (dry plus wet/bulk) annual N deposition at the 43 sites ranged from 2.9 to 83.3 kg N ha^{-1} yr^{-1} (average 39.9 kg N ha^{-1} yr^{-1}) for the period, with 23-83% dry-deposited (**Fig. 5c**). Separated by land use types, total annual mean N deposition fluxes were 49.7, 44.3 and 26.0 kg N ha^{-1} at the urban, rural and background sites, respectively, reflecting different anthropogenic impacts. In our network, the NH_x (i.e. wet/bulk NH_4^+-N deposition plus dry deposition of NH_3 and particulate NH_4^+)/NO_y (wet/bulk NO_3^--N deposition plus dry deposition of NO_2, HNO_3 and particulate NO_3^-) ratio at urban sites (from 0.8 to 1.8, averaging 1.2) was not significantly different (p>0.05) from rural (from 0.5 to 2.7, averaging 1.3) and background (from 1.0 to 2.5, averaging 1.6) sites. On a regional basis, the relative importance of dry vs. wet/bulk N deposition to the total deposition were different in the six regions, 57% vs. 43% in NC, 54% vs. 46% in NE, 61% vs. 39% in NW, 42% vs. 58% in SE, 55% vs. 45% in SW, and 50% vs. 50% in TP (**Fig. 7**).

4. Discussion

4.1 Concentration of N_r species in air and precipitation

China is facing serious atmospheric N_r pollution induced by anthropogenic N_r emissions (Liu et al., 2011, 2013). The present study shows that monthly N_r concentrations of species, through comparisons among regions, have a distinct spatial variability with values significantly higher (all p<0.05) in NC and significantly lower

删除的内容: 4b

删除的内容: 75.2

删除的内容: 37.8

删除的内容: 22-82

删除的内容: **S5**, Supplement

删除的内容: The contribution of reduced N deposition (NH_x, that is, wet NH_4^+-N deposition plus dry deposition of NH_3 and pNH_4^+) to the total N deposition (39-76%) was, on average, 1.4 times greater than that of oxidized N deposition (NO_y; wet NO_3^--N deposition plus dry deposition of NO_2, HNO_3 and pNO_3^-). On a regional basis, the total deposition fluxes across the six regions were in the range of 14.9-53.0 kg N ha^{-1} yr^{-1}, with 54-66% in the form of NH_x

删除的内容: The

删除的内容: 54

删除的内容: 46

删除的内容: 49

删除的内容: 51

删除的内容: 59

删除的内容: 41

删除的内容: 38

删除的内容: 62

删除的内容: 52

删除的内容: 48

删除的内容: 49

删除的内容: 51

删除的内容: **5**

删除的内容: Separated by land use types, total annual mean N deposition fluxes were 47.0, 42.0 and 24.7 kg N ha^{-1} yr^{-1} at the urban, rural and grassland sites, respectively, reflecting different anthropogenic impacts.

(all $p<0.05$) in TP. Annual mean NH_3 and NO_2 concentrations at most sampling sites are in good agreement with the emission inventory and satellite observations by Gu et al. (2012), who reported NH_3 hotspots in the North China Plain and South Central China such as Jiangsu and Guangdong provinces, while NO_x hotspots were mainly in more developed regions such as the Jing-Jin-Ji (Beijing-Tianjin-Hebei), the Yangtze River Delta and the Pearl River Delta. Our results confirm that NC, which consumes large quantities of fertilizers (for food production) and fossil fuel (for energy supply) (Zhang et al., 2010) experiences the most serious N_r pollution in China; TP is the least polluted region due to much less human activity. When considering different land use types, the average total annual N_r concentrations ranked urban > rural > background, with significant differences (all $p<0.05$) among them, despite site-to-site variability within regions. This reflects the dominant role of human activity on atmospheric N_r.

For individual N_r species, higher mean concentrations were observed at the urban sites than at rural and background sites (**Fig. 4a**). Higher NH_3 concentration in urban areas may be associated with NH_3 emissions from biological sources, such as human, sewage disposal systems and refuse containers (Reche et al., 2002). In addition, NH_3 can be produced by over-reduction of NO in automobile catalytic converters (Behera et al., 2013), increasing ambient NH_3 concentrations in urban areas with high traffic densities. Between 2006 and 2013, the number of civil vehicles increased from 2.39 to 5.17 million in Beijing and from 0.46 to 1.72 million in Zhengzhou (CSY, 2007-2014), which is likely to have resulted in elevated NH_3 emissions. Higher NO_2 concentrations are expected in urban areas due to NO_x emissions from the combustion of fossil fuels (Li and Lin, 2000), and also lead to higher HNO_3 concentrations in urban areas via NO_2 oxidation.

The higher pNH_4^+ and pNO_3^- concentrations observed at urban sites mainly resulted from the high concentrations at the northern urban sites (NC1~3, NW1 and NW2) (**Fig. 2a and Fig. S2d, e** in Supplement). This is probably due to the fact that cities in northern China, such as Beijing and Zhengzhou in NC and Urumqi in NW, are being surrounded by intensive agricultural production. Rapid developments along with urbanization in suburban areas shorten the transport distance between NH_3 emitted from agriculture and SO_2 and NO_x emitted from fossil fuel combustion (Gu et al., 2014). This allows the pollutants to react more readily and form aerosols (e.g. $PM_{2.5}$), leading to high concentrations of pNH_4^+ and pNO_3^- near or within cities. This explanation is supported by the recent MEPC (2013) report that the annual average

删除的内容: **S3**, Supplement

删除的内容: **1c**

删除的内容: **d**

$PM_{2.5}$ concentrations in the cities of Beijing, Zhengzhou and Urumqi were more than twice the Chinese annual mean $PM_{2.5}$ standard value of 35 μg m^{-3}, whereas cities such as Guangzhou and Xining with little surrounding agricultural production had lower $PM_{2.5}$ concentrations. In China's 12th Five Year Plan (2011–2015), nationwide controls on NO_x emissions will be implemented along with controls on SO_2 and primary particle emissions (Wang et al., 2014). In order to better improve the regional air quality for metropolitan areas; our results suggest that strict control measures on both NH_3 and NO_x would be beneficial in NC, at least in the suburban areas.

Rural sites in this study also had relatively high concentrations of all measured N_r species in air, altogether ranking in the order of NC > NE > NW > SE > SW (**Fig. 3f**). The higher concentrations in northern China are mainly due to the combined effect of high NH_3 emissions from N fertilized farmland (Zhang et al., 2008a) and urban air pollution (e.g. NO_2, HNO_3, pNH_4^+ and pNO_3^-) transported from population centers to the surrounding rural areas (Luo et al., 2013). The lower air concentrations of N_r species at background sites can be ascribed to the lack of both substantial agricultural and industrial emissions. Additionally, higher wind speeds occurred at some background areas (e.g. NC12, NC13 and NW4) (**Table S1**, Supplement), favoring the dispersion of atmospheric pollutants.

We found that regional variations in N_r concentrations in precipitation were not fully in accordance with ambient N_r concentrations (see Sect. 3.2) when assessed by land use types. It is commonly accepted that N concentrations in precipitation are affected by the amount of precipitation (Yu et al., 2011). Negative correlations between precipitation amount and monthly volume-weighted concentrations of NH_4^+-N and NO_3^--N were obtained by fitting exponential models in all six regions (**Fig. S4**, Supplement), indicating a dilution effect of rainwater on inorganic N concentration. The relationships were not significant (p>0.05) in NW and TP, which is probably caused by low precipitation amounts at or near the sampling sites (**Fig. S5**, Supplement). Nevertheless, dilution could explain some of the regional differences in precipitation N concentrations.

4.2 Dry and wet/bulk deposition of N_r species

A significant (p<0.001) positive correlation was observed between annual dry N deposition and total annual concentrations of atmospheric N_r species across all sites (**Fig. S6**, Supplement). Therefore, higher concentrations of N_r species at urban sites led to higher dry deposition rates compared with rural and background sites, mainly

删除的内容: Rural sites in this study also had relatively high concentrations of NO_2, HNO_3, pNH_4^+ and pNO_3^-, especially in northern China

删除的内容: This is

删除的内容: the VWM concentrations of NH_4^+-N and NO_3^--N were significantly higher (both p<0.05) in northern China than in southern China and TP (**Table 1**), although the differences were not significant (p>0.05) when comparing NE and NW with SW. This was due to multiple factors such as relative high N_r levels in northern China balanced by high rainfall in southern China (**Figs. S2** and **S6**, Supplement**)**. However,

删除的内容: S7

删除的内容: S8

删除的内容: In NC higher concentrations of N_r species led to higher dry deposition rates. In TP, a remote region of China, atmospheric N_r concentrations were lower than those in the other five regions, and thus dry deposition was also lower than in the other regions. Among land use types the highest total N deposition was observed at urban sites

attributable to elevated N_r emissions from urban sources (e.g., non-agricultural NH_3 emissions from landfills, wastewater treatments and NO_x emissions from traffic vehicles and power plants) and rapid development of intensive agricultural production in suburban areas surrounding cities; regardless of differences in dry deposition velocities of various N_r species in different land use types. At the national scale, dry N deposition rates contributed almost half 23-83%, averaging 52%) of the total inorganic N deposition, indicating the importance of dry deposition monitoring for comprehensive N deposition quantification.

In this study, regional variations of annual wet/bulk N deposition fluxes of NH_4^+-N, NO_3^--N and their sum showed different spatial patterns to those of corresponding annual VWM concentrations of them in precipitation (see Sect. 3.4). These findings, together with no significant differences (p>0.05) in total annual wet/bulk N deposition between NC and SE, reflect, not surprisingly, that regional wet/bulk N deposition is dependent not only on N_r concentrations in precipitation but also on annual rainfall amounts. As shown in Fig. 8, annual wet/bulk deposition fluxes of NH_4^+-N and NO_3^--N both showed significantly positive correlations with the corresponding annual VWM concentrations of inorganic N and annual precipitation amount, especially for NH_4^+-N, that more significant was found for precipitation amount than concentration. The measured wet/bulk N deposition rates (average 19.3 kg N ha^{-1} yr^{-1}) were almost twice the earlier average wet deposition value of 9.9 kg N ha^{-1} yr^{-1} for period of 1990-2003 in China (Lü and Tian, 2007). Our results show similar regional patterns and comparable magnitudes to those measured in the 2000s in China as reported by Jia et al. (2014) (~14 kg N ha^{-1} yr^{-1}, wet deposition) and Liu et al. (2013) (~21 kg N ha^{-1} yr^{-1}, bulk deposition).

The NH_4^+-N/NO_3^--N ratio in wet/bulk deposition can be used to indicate the relative contribution of N_r from agricultural and industrial activities to N deposition (Pan et al., 2012; Zhan et al., 2015; Zhu et al., 2015) because the major anthropogenic source of NH_4^+-N in precipitation is NH_3 volatilized from animal excrement and the application of nitrogenous fertilizers in agriculture, while anthropogenic sources of NO_3^--N in precipitation originate from NO_x emitted from fossil fuel combustion in transportation, power plant and factories (Cui et al., 2014). In this study the overall annual average ratio of NH_4^+-N/NO_3^--N in wet/bulk deposition was 1.3 ± 0.5 (standard deviation), with an increasing (but not significant) trend for urban (1.2 ± 0.6), rural (1.3 ± 0.4), and background (1.5 ± 0.4) sites (**Fig. 5b**). Our measured ratio was slightly lower than

删除的内容: (22
删除的内容: 82
删除的内容: 48
删除的内容: the
删除的内容: a
删除的内容: that
删除的内容: annual mean total N_r concentrations
删除的内容: 6
删除的内容: (Fig. 6a, b)
删除的内容: Fahey et al., 1999

765 average values of 1.6 in Europe (Holland et al., 2005) and 1.5 in the United States (Du
766 et al., 2014), and similar to an average value (1.2) reported elsewhere for 2013 in
767 China (Zhu et al., 2015). Based on these findings, we conclude that NH_4^+-N from
768 agricultural sources still dominates wet/bulk N deposition but the contribution has
769 decreased drastically between the 1980s and the 2000s (Liu et al., 2013). Reduced N
770 also contributed more than oxidized N to the total N deposition, and the ratio of
771 reduced to oxidized N deposition overall averaged 1.6 ± 0.7 in dry deposition and 1.4
772 ± 0.4 in the total deposition (**Fig. 5a, c**).
773 The overall mean annual deposition fluxes (wet/bulk plus dry) of NH_x and NO_y for
774 the period 2010-2014 was graded into five levels and plotted on maps showing the
775 spatial distribution of NH_3 and NO_x emissions (**Fig. 9a, b**). The anthropogenic
776 emission data of NH_3 and NO_x for the year 2010 in China were obtained from
777 the **GAINS (Greenhouse Gas and Air Pollution Interactions and Synergies)** model
778 (http://www.iiasa.ac.at/), and emission details for the 33 provinces of China are
779 summarized in **Table S5** of the Supplement. The spatial patterns of estimated NH_x
780 and NO_y deposition compare reasonably well with the regional patterns of NH_3 and
781 NO_x emissions, respectively, even though the emission data were estimated at the
782 province scale. With emission data, N deposition can be used to distinguish regional
783 differences in reactive N_r pollution. Across six regions, significantly positive
784 correlations were found between NH_3 emissions and NH_x deposition fluxes
785 (R^2=0.888, p<0.01) (**Fig. 9c**), and between NO_x emissions and NO_y deposition fluxes
786 (R^2=0.805, p<0.05) (**Fig. 9d**), implying that the N deposition fluxes to the six regions
787 are strongly dependent on the spatial pattern of anthropogenic N_r emissions among
788 the regions. The slopes of the relationships of NH_x vs NH_3, and NO_y vs NO_x were
789 0.51 and 0.48, which could be roughly interpreted that NH_x and NO_y deposition
790 fluxes represent about 51% NH_3 and 48% NO_x emissions, respectively.
791 For all Chinese regions except NC we cannot compare our data with other studies
792 because observations for different pollution climate sites in other regions are lacking.
793 For NC, the overall average total N deposition was 56.2 ± 14.8 kg N ha^{-1} yr^{-1}, 13-32%
794 lower than the previously estimated values in Northern China (Pan et al., 2012; Luo et
795 al., 2013). This difference may reflect differences in the numbers of sampling sites,
796 land use type and assumed dry deposition velocities. As expected, our estimated
797 deposition was substantially higher than the results of Lü and Tian (2007), who
798 suggested that the total N deposition ranged from 13 to 20 kg N ha^{-1} yr^{-1} in NC. This

删除的内容: There was no significant difference (p=0.385) between annual mean ratios of NH_4^+-N/NO_3^--N among northern China, southern China and TE

删除的内容: 1.7

删除的内容: 1.4

删除的内容: **4a** and **Fig. S5** in the online Supplement

删除的内容: **7a**

删除的内容: 883

删除的内容: **7c**

删除的内容: 796

删除的内容: **7d**

删除的内容: 50

删除的内容: 43

删除的内容: 50

删除的内容: 43

删除的内容: 53.0 ± 13.6

817 is attributed to their omission of many major species (e.g., gaseous NH_3, HNO_3 and
818 particulate N_r) from their data.
819 Compared to dry and wet N deposition fluxes estimated by CASTNET in the United
820 States, EMEP in Europe, and EANET sites in Japan, the average values of dry and
821 wet/bulk deposition in China are much higher (**Table 1**). In addition, on the basis of
822 2001 ensemble-mean modeling results from 21 global chemical transport models (Vet
823 et al., 2014), three regions of the globe where total deposition is very high: western
824 Europe (with levels from 20.0 to 28.1 kg N $ha^{-1}yr^{-1}$); South Asia (Pakistan, India and
825 Bangladesh) from 20.0 to 30.6 kg N $ha^{-1}yr^{-1}$ and East Asia from 20 to 38.6 kg N
826 $ha^{-1}yr^{-1}$ in eastern China (the global maximum). Extensive areas of high deposition
827 from 10 to 20 kg N $ha^{-1}yr^{-1}$ appear in the eastern U.S. and southeastern Canada as
828 well as most of central Europe. Small areas with total deposition of N from 10 to 20
829 kg N $ha^{-1}yr^{-1}$are present, and very large areas of the continents have deposition from
830 2 to 10 kg N $ha^{-1}yr^{-1}$. In contrast, the present study shows much higher total
831 deposition flux (39.9 kg N $ha^{-1}yr^{-1}$) at a national scale. In China, the consumption
832 rates of chemical fertilizer and fossil fuel have increased 2.0- and 3.2-fold,
833 respectively, between the 1980s and the 2000s (Liu et al., 2013). As a result, the
834 estimated total emission of NH_3 reached 9.8 Tg in 2006, contributing approximately
835 15% and 35% to the global and Asian NH_3 emissions (Huang et al., 2012), and NO_x
836 emissions from fossil fuel combustion increased from 1.1 Tg N in 1980 to about 6.0
837 Tg N in 2010 (Liu et al., 2013). The increasing NO_x and NH_3 emissions in China led
838 to higher atmospheric N deposition than those observed in other regions.
839 According to Endo et al. (2011), the low dry deposition fluxes in CASTNET, EMEP
840 and Japan's EANET network are due at least partly to low concentrations of N_r
841 compounds and/or the omission of dry deposition fluxes of major N_r species (e.g.,
842 NO_2 and NH_3) from the data. Meanwhile, the low wet deposition fluxes at these
843 networks are likely to be a result of the combined effects of low amounts of
844 precipitation and, especially, low atmospheric N_r concentrations. In addition,
845 emissions of nitrogen compounds in other parts of the world are declining. In the U.S.,
846 for example, NO_x emissions from the power sector and mobile sources were reduced
847 by half from 1990 to 2010 (Xing et al., 2013), which explained the declined N
848 deposition fluxes during period of 1990-2009 observed at 34 paired dry and wet
849 monitoring sites in the eastern US (Sickles II et al., 2015). In Europe, the total NO_x
850 and NH_3 emissions decreased by 31% and 29% from 1990 to 2009 (Torseth et al.,

删除的内容: 2

删除的内容: NO_x emissions from the electric power industry and from vehicles were reduced from1990 to 2007 (and continue to decline), which explained the declined N deposition fluxes observed at CASTNET (MACTEC, 2008)

2012), N deposition has decreased or stabilized in the United States and Europe since the late 1980s or early 1990s with the implementation of stricter legislation to reduce emissions (Goulding et al., 1998; Holland et al., 2005). However, wet deposition of ammonia, which is not regulated, has increased in recent years in the U.S. (Du et al., 2014).

删除的内容: In EMEP, the total NO_x emissions decreased from 2006 to 2007 in the 27 EMEP countries (Benedictow et al., 2009)

4.3 Implications of monitoring N_r concentration and deposition on regional N deposition simulation

Our results show that atmospheric concentrations and deposition of N_r in China were high in the 2000s, although the government has made considerable efforts to control environmental pollution by improving air quality in mega cities during and after the 2008 Beijing Summer Olympic Games (Wang et al., 2010; Chan and Yao, 2008). Ideally, the spatial distribution of monitoring sites should reflect the gradients in the concentrations and deposition fluxes of atmospheric N_r species. Given the fact that the arithmetic averages used in this study cannot give a completely accurate evaluation of N_r levels for the regions of China due to the limited numbers of monitoring sites and ecosystem types, it is important to develop and improve the quantitative methods for determining N deposition across China.

Numerical models are very useful tools to quantify atmospheric N deposition (including both spatial and temporal variations), but a challenge to the modeling approaches is that observations to validate the simulated concentrations and deposition fluxes are often lacking. In our study 43 monitoring sites were selected in a range of ecosystem types to provide more representative regional information on atmospheric N deposition in China. Although those measurements cannot define all aspects of N deposition across different regions, they add substantially to existing knowledge concerning the spatial patterns and magnitudes of atmospheric N deposition. The present measurements will be useful for better constraining emission inventories and evaluating simulations from atmospheric chemistry models. In future studies we will use models (e.g., FRAME, Dore et al., 2012) integrated with measurements from our monitoring network to fully address the spatial-temporal variations of atmospheric N deposition and its impacts on natural and semi-natural ecosystems at the regional/national level.

4.4 Uncertainty analysis of the N dry and wet deposition fluxes

The dry deposition fluxes were estimated by combining measured concentrations with modeled V_d. As summarized in Table S4, our estimates of dry deposition velocities

for different N_r species are generally consistent with the estimates in previous studies (e.g., Flechard et al., 2011; Pan et al., 2012). Some uncertainties may still exist in the inputs for dry deposition modeling. For example, underlying surface parameters (e.g., surface roughness length and land type) strongly affect dry deposition through their effect on both deposition velocity and the absorbability of the ground surface to each of the gaseous and particulate N_r species (Loubet et al., 2008). In addition, there is uncertainty in the deposition fluxes for both pNH_4^+ and pNO_3^- in our network, resulting from the difference between the cut-off sizes of particles in the samplers and that defined in the modeled V_d which were calculated for atmospheric $PM_{2.5}$ in GEOS-Chem model. For example, the cut-off sizes of the samples can collect also coarse NO_3^- particles (e.g. calcium nitrate) but should have little effect on NH_4^+ particles (mainly in the fine scale <1μm) (Tang et al., 2009), resulting in an underestimation of pNO_3^- deposition. Furthermore, NH_3 fluxes over vegetated land are bi-directional and the net direction of this flux is often uncertain. A so-called canopy compensation point was used in previous studies (Sutton et al., 1998) to determine the direction of the NH_3 flux. Since the principle of bi-directional NH_3 exchange was not considered in this study, NH_3 deposition may be overestimated at rural sites with relatively high canopy compensation points (e.g. up to 5 μg N m^{-3}) due to fertilized croplands or vegetation (Sutton et al., 1993). On the other hand, the total dry deposition flux in this study may be underestimated due to omission of the dry-deposited organic N species in our network and missing HNO_3 data at very few sites as noted earlier (see Sect. 2.2). The organic N species have been found as important contributors to the N dry deposition. For example, PAN accounted for 20% of the daytime, summertime NO_y ($NO + NO_2 + HNO_3 + NO_3^- + PAN$) dry deposition at a coniferous forest site (Turnipseed et al., 2006). However, the contribution of PAN and other known atmospheric organic nitrates to total N_r inputs must be minor on the annual time scale, as reported by Flechard et al. (2012). In previous work, dry deposition flux was inferred from atmospheric N_r concentrations and a literature-based annual mean deposition velocity (Shen et al., 2009), or reported by Luo et al. (2013) who did not consider the different dry deposition velocities of various N_r species among different land use types. Clearly, in this study we have greatly improved the estimation of dry deposition, but further work is still required to increase the reliability and accuracy of N dry deposition values.

Since wet/bulk deposition was measured directly, the reported fluxes are considered

删除的内容: Thus,

删除的内容: some

删除的内容: arise

删除的内容: Dry deposition velocities of N_r in this study were only modeled for 2012 (The production of GEOS-5 meteorological data ended in May 2013). We used monthly mean V_d values for 2012 for corresponding months in other years at each site. This may also lead to uncertainty in our dry deposition estimation while small differences in monthly dry deposition velocities of N_r between different years were reported at ten sites (~10%) in the northern China (Pan et al., 2012) and at a forest site (~11%) in southern China (Fan et al., 2009).

删除的内容: Although we have improved the estimation of dry deposition greatly compared with previous work (e.g., Shen et al., 2009; Luo et al., 2013), further work is still required to increase the reliability and accuracy of N dry deposition values

more accurate than dry deposition fluxes but still some uncertainties exist. On one hand, the estimated fluxes obtained from the open precipitation samplers contain contributions from wet plus unquantifiable dry deposition (including both gases and particles) and therefore likely overestimate actual wet deposition (Cape et al., 2009). For example, our previous research showed that annual unquantifiable dry deposition (the difference between bulk and wet deposition, approx. 6 kg N ha^{-1} on average) accounted for 20% of bulk N deposition based on observations at three rural sites on the North China Plain (Zhang et al., 2008b). This contribution increased to 39% in urban areas based on a recent measurement (Zhang et al., 2015). On the other hand, dissolved organic N compounds, which have been observed to contribute to be around 25-30% of the total dissolved nitrogen in wet deposition around the world (Jickells et al., 2013) and approximately 28% of the total atmosphere bulk N deposition in China (Zhang et al., 2012b), were not considered in the present study. Their exclusion here would contribute to an underestimation of the total wet N deposition.

Although the NNDMN is the only long-term national deposition network to monitor both N wet/bulk and dry deposition in China till now, large areas of the country or islands lack of sampling points may be missing hotspots or pristine sites of N deposition. The implementation of an adequate monitoring program is also difficult at present in some regions (e.g., northwest China and Tibetan Plateau). To address this issue, more new monitoring sites, covering regions with both extremely low and high N_r emissions, should be set up in the NNDMN in future work.

Conclusions

Our study represents the first effort to investigate inorganic dry and wet/bulk N deposition simultaneously, based on a nationwide monitoring network in China. We consider this unique dataset important not only for informing policy-makers about the abatement of pollutant emissions and ecosystem protection but also to validate model estimations of N deposition at the regional/national scale in China. The major results and conclusions are as follows.

1. Distinct spatial variability in annual mean concentrations of N_r species in air and precipitation was observed, with different regional variations based on land use type across the six regions. On a national basis, the order of total concentrations of N_r species, as well as each species, was urban > rural > background.

删除的内容: averaged total N_r concentrations following the order of NC > NW ≈ SW > SE > NE > TP

删除的内容: .

删除的内容: The

删除的内容: based on land use type

2. Large spatial variations were observed for both dry and wet/bulk N deposition. The spatial patterns of dry and wet/bulk deposition both followed urban > rural > background at the national scale. Dry N deposition correlated well with total concentrations of N_r in the air, but differences were found between patterns of wet/bulk N deposition and the N_r concentration in precipitation. This reflects the combining effect of both N_r concentrations and precipitation amounts on regional wet/bulk N deposition.

3. Spatial distribution of total annual N deposition fluxes across all sites compared well with the spatial pattern of nitrogen emissions at the regional level. When considering land use type, the total N deposition was highest at urban sites, followed by rural sites and background sites, mainly attributable to N_r emissions from urban sources and rapid development of intensive agricultural production in suburban areas.

4. Dry deposition fluxes of N_r species on average contributed 52% of the total N deposition (39.9 kg N ha^{-1} yr^{-1}) across all sites, indicating the importance of dry deposition monitoring for a complete N deposition assessment at the national scale.

5. Annual average ratios of reduced N/oxidized N in dry and wet/bulk deposition were respectively 1.6 and 1.3, and 1.4 for the total deposition. It shows that reduced N, mainly from agricultural sources, still dominates dry, wet/bulk, and total N deposition in China.

删除的内容: The spatial pattern of dry deposition followed NC > SW > SE > NE > NW > TP, whereas the pattern was NC > SE > SW > NE > TP > NW for wet N deposition.

删除的内容: the dependence of regional wet N deposition on both N_r concentration and precipitation amounts.

删除的内容: Total annual N regional deposition fluxes followed NC > SE > SW > NE > NW > TP, which

删除的内容: 48

删除的内容: 37.8

删除的内容: 1.7

Acknowledgments

This study was supported by the Chinese National Basic Research Program (2014CB954202), the China Funds for Distinguished Young Scholars of NSFC (40425007), and the National Natural Science Foundation of China (31121062, 41321064 and 41405144). The authors thank all technicians at monitoring sites in NNDMN.

References

Bey, I., Jacob, D. J., Yantosca, R. M., Logan, J. A., Field, B. D., Fiore, A. M., Li, Q., Liu, H., Mickley, L. J., and Schultz, M. G.: Global modeling of tropospheric chemistry with assimilated meteorology: Model description and evaluation, J. Geophys. Res., 106(D19), 23,073 –23,096, 2001.

Behera, S. N., Sharma, M., Aneja, V. P., and Balasubramanian, R.: Ammonia in the atmosphere: a review on emission sources, atmospheric chemistry and deposition on terrestrial bodies, Environ. Sci. Pollut. Res., 20, 8092–8131, doi:10.1007/s11356-013-2051-9, 2013.

Cape, J.N., Van Dijk, N., and Tang, Y.S.: Measurement of dry deposition to bulk collectors using a novel flushing sampler. J. Environ. Monit., 11, 353-358, doi: 10.1039/B813812E, 2009.

Chan, C.K. and Yao, X.H.: Air pollution in mega cities in China, Atmos. Environ., 42, 1–42, doi: 10.1016/j.atmosenv.2007.09.003, 2008.

Chen, D., Wang, Y. X., McElroy, M. B., He, K., Yantosca, R. M., and Le Sager, P.: Regional CO pollution in China simulated by high-resolution nested-grid GEOS-Chem model, Atmos. Chem. Phys., 11, 3825-3839, 2009.

Chen, X. Y. and Mulder, J.: Atmospheric deposition of nitrogen at five subtropical forested sites in South China, Sci. Total Environ., 378, 317–330, doi: 10.1016/j.scitotenv.2007.02.028, 2007.

Clark, C. M. and Tilman, D.: Loss of plant species after chronic low-level nitrogen deposition to prairie grasslands, Nature, 451, 712–715, doi:10.1038/nature06503, 2008.

Clarke, J. F., Edgerton, E. S., and Martin, B. E.: Dry deposition calculations for the Clean Air Status and Trends Network, Atmos. Environ., 31, 3667-3678, 1997.

CSY (China Statistical Yearbook), 2007-2014. Available at: http://www.stats.gov.cn.

Cui, J., Zhou, J., Peng, Y., He, Y. Q., Yang, H., Mao, J. D., Zhang, M. L., Wang, Y. H., and Wang, S. W.: Atmospheric wet deposition of nitrogen and sulfur in the agroecosystem in developing and developed areas of Southeastern China, Atmos. Environ., 89, 102–108, doi:10.1016/j.atmosenv.2014.02.007, 2014.

删除的内容: Benedictow, A., Fagerli, H., Gauss, M., Jan E., Tsyro, S., Nyıri, A., Simpson, D., ; Steensen, B. M., Klein, H., Valdebenito, A., Wind, P., Kirkevag, A., Griesfeller, J., Bartnicki, J., Olivie, D., Grini, A., Iversen, T., Semeena, V. S., Fagerli, H., Aas, W., Hjellbrekke, A. G., Mareckova, K., Wankmuller, R., Schneider, P., Solberg, S., Svendby, T., Liu, L., Posh, M., **Vieno, M., Reis, S.,** Kryza, M., Werner, M., and Walaszek, K.: Transboundary Acidification, Eutrophication and Ground Level Ozone in Europe in 2007. EMEP Report 1/2009. The Norwegian Meteorological Institute, Oslo, Norway, pp. 19–28, 2009.

Dentener, F., Drevet, J., Lamarque, J. F., Bey, L., Eickhout, B., Fiore, A. M. Hauglustaine, D., Horowitz, L. W., Krol, M., and Kulshrestha, U. C .: Nitrogen and sulfur deposition on regional and global scales: a multimodel evaluation, Global Biogeochemical Cy., 20, GB4003, doi: 10.1029/2005GB002672, 2006.

Dore, A.J., Kryza, M., Hall, J. Hallsworth, S., Keller, V., Vieno, M. and Sutton, M.A.: The influence of model grid resolution on estimation of national scale nitrogen deposition and exceedance of critical loads, Biogeosciences, 9, 1597-1609, 2012.

Du, E. Z., Vries, W. D., Galloway, J. N., Hu, X. Y., and Fang, J. Y.: Changes in wet nitrogen deposition in the United States between 1985 and 2012, Environ. Res. Lett., 9, 095004, doi:10.1088/1748-9326/9/9/095004, 2014.

EEA: Air Quality in Europe-2011 Report. Technical Report 12/2011. EEA, Kopenhagen, 2011.

Ellis, R. A., Jacob, D. J., Sulprizio, M. P., Zhang, L., Holmes, C. D., Schichtel, B. A., Blett, T., Porter, E., Pardo, L. H., and Lynch, J. A.: Present and future nitrogen deposition to national parks in the United States: critical load exceedances, Atmos. Chem. Phys., 13, 9083-9095, doi:10.5194/acp-13-9083-2013, 2013.

Endo, T., Yagoh, H., Sato, K., Matsuda, K., Hayashi, K., Noguchi, I., and Sawada, K.: Regional characteristics of dry deposition of sulfur and nitrogen compounds at EANET sites in Japan from 2003 to 2008, Atmos. Environ., 45, 1259–1267,doi:10.1016/j.atmosenv.2010.12.003, 2010.

Erisman, J. W., Vermeulen, A., Hensen, A., Flechard, C., Dammgen, U., Fowler, D., Sutton, M., Grunhage, L., and Tuovinen, J.P.: Monitoring and modelling of biosphere/atmosphere exchange of gases and aerosols in Europe, Environ. Pollut., 133, 403–413, doi:10.1016/j.envpol.2004.07.004, 2005.

Flechard, C. R., Nemitz, E., Smith, R. I., Fowler, D., Vermeulen, A. T., Bleeker, A., Erisman, J. W., Simpson, D., Zhang, L., Tang, Y. S., and Sutton, M. A.: Dry deposition of reactive nitrogen to European ecosystems: a comparison of inferential models across the NitroEurope network, Atmos. Chem. Phys., 11, 2703–2728,doi:10.5194/acp-11-2703-2011, 2011.

删除的内容:

Fahey, T. J., Williams, C. J., Rooney-Varga, J. N., Cleveland, C. C., Postek, K. M., Smith, S. D., and Bouldin, D. R.: Nitrogen deposition in and around an intensive agricultural district in central New York, J. Environ Qual., 28, 1585–1600, doi:10.2134/jeq1999.00472425002800050025x, 1999.

Fang, J. L., Hu, Z. Y., Wang, T. J., Zhou, J., Wu, C. Y. H., and Xia, X.: Atmospheric inorganic nitrogen deposition to a typical red soil forestland in southeastern China, Environ. Monit. Assess., 159, 241–253, doi:10.1007/s10661-008-0626-6, 2009.

1138 Fowler, D., Coyle, M., Skiba, U., Sutton, M. A., Cape, J. N., Reis, S., Sheppard, L. J.,
1139 Jenkins, A., Grizzetti, B., Galloway, J. N., Vitousek, P., Leach, A., Bouwman, A. F.,
1140 Butterbach-Bahl, K., Dentener, F., Stevenson, D., Amann, M., and Voss, M.: The
1141 global nitrogen cycle in the twenty-first century, Phil. Trans. R. Soc. B, 368,
1142 20130164, doi:10.1098/rstb.2013.0164, 2013.
1143 Galloway, J. N., Dentener, F. J., Capone, D. G., Boyer, E. W., Howarth, R. W.,
1144 Seitzinger, S. P., Asner, G. P., Cleveland, C. C., Green, P. A., Holland, E. A., Karl,
1145 D. M., Michaels, A. F., Porter, J. H., Townsend, A. R., and Vorosmarty, C. J.:
1146 Nitrogen cycles: past, present, and future, Biogeochem., 70, 153–226, 2004.
1147 Galloway, J. N., Townsend, A. R., Erisman, J. W., Bekunda, M., Cai, Z., Freney, J. R.,
1148 Martinelli, L. A., Seitzinger, S. P., and Sutton, M. A.: Transformation of the
1149 Nitrogen Cycle: Recent trends, questions, and potential solutions, Science, 320,
1150 889–892, 2008.
1151 Galloway, J. N., Leach, A. M., Bleeker, A., and Erisman, J. W.: A chronology of
1152 human understanding of the nitrogen cycle, Phil. Trans. R. Soc. B, 368, 20130120,
1153 doi:10.1098/rstb.2013.0120, 2013.
1154 Goulding, K. W. T., Bailey, N. J., Bradbury, N. J., Hargreaves, P., Howe, M., Murphy,
1155 D. V., Poulton, P. R., and Willison, T. W.: Nitrogen deposition and its contribution
1156 to nitrogen cycling and associated soil processes, New Phytol., 139, 49–58, 1998.
1157 Gu, B. J., Ge, Y., Ren, Y., Xu, B., Luo, W. D., Jiang, H., Gu, B. H., and Chang, J.:
1158 Atmospheric reactive nitrogen in China: Sources, recent trends, and damage costs,
1159 Environ. Sci. Technol., 46, 9240–9247, doi:10.1021/es301446g, 2012.
1160 Gu, B. J., Sutton, M. A., Chang, S. X., Ge, Y., and Jie, C.: Agricultural ammonia
1161 emissions contribute to China's urban air pollution, Front. Ecol. Environ., 12,
1162 265–266, doi:10.1890/14.WB.007, 2014.
1163 Holland, E. A., Braswell, B. H., Sulzman, J., and Lamarque, J. F.: Nitrogen deposition
1164 onto the United States and Western Europe: synthesis of observations and models,
1165 Ecol. Appl., 15, 38–57, 2005.
1166 Hu, H., Yang, Q., Lu, X., Wang, W., Wang, S., and Fan, M.: Air pollution and control
1167 in different areas of China. Crit. Rev. Environ. Sci. Technol., 40, 452–518,

doi:10.1080/10643380802451946, 2010.

Huang, X., Song, Y., Li, M. M., Li, J. F., Huo, Q., Cai, X. H., Zhu, T., Hu, M., and Zhang, H. S.: A high-resolution ammonia emission inventory in China, Global Biogeochem. Cy., 26, GB1030, doi:10.1029/2011GB004161, 2012.

Huang, Y. L., Lu, X. X., and Chen, K.: Wet atmospheric deposition of nitrogen: 20 years measurement in Shenzhen City, China, Environ. Monit. Assess., 185, 113–122, doi: 10.1007/s10661-012-2537-9, 2013.

Jia, Y. L., Yu, G. R., He, N. P., Zhan, X. Y., Fang, H. J., Sheng, W. P., Zuo, Y., Zhang, D. Y., and Wang, Q. F.: Spatial and decadal variations in inorganic nitrogen wet deposition in China induced by human activity. Sci. Rep., 4, 3763, doi: 10.1038/srep03763, 2014.

Jickells, T., Baker, A. R., Cape, J. N., Cornell, S.E., and Nemitz, E.: The cycling of organic nitrogen through the atmosphere. Philos. Trans. R. Soc. B 368, 20130115, doi:org/10.1098/rstb.2013.0115, 2013.

Li, Y. E. and Lin, E. D.: Emissions of N_2O, NH_3 and NO_x from fuel combustion, industrial processes and the agricultural sectors in China. Nutr. Cycl. Agroecosys., 57, 99–106, 2000.

Liu, X. J., Song, L., He, C. E., and Zhang, F. S.: Nitrogen deposition as an important nutrient from the environment and its impact on ecosystems in China, J. Arid Land, 2, 137–143, 2010.

Liu, X. J., Duan, L., Mo, J. M., Du, E., Shen, J. L., Lu, X. K., Zhang, Y., Zhou, X. B., He, C. E., and Zhang, F. S.: Nitrogen deposition and its ecological impact in China: An overview, Environ. Pollut., 159, 2251–2264, doi:10.1016/j.envpol.2010.08.002, 2011.

Liu, X. J., Zhang, Y., Han, W. X., Tang, A., Shen, J. L., Cui, Z. L., Vitousek, P., Erisman, J. W., Goulding, K., Christie, P., Fangmeier, A., and Zhang, F. S.: Enhanced nitrogen deposition over China, Nature, 494, 459–462, doi:10.1038/nature11917, 2013.

Liu, X. J., Xu, W., Pan, Y. P., and Du, E. Z.: Liu et al. suspect that Zhu et al. (2015) may have underestimated dissolved organic nitrogen (N) but overestimated total

particulate N in wet deposition in China, Sci. Total Environ., 520, 300–301, doi.org/10.1016/j.scitotenv.2015.03.004, 2015.

Loubet, B., Asman, W. A. H., Theobald, M. R., Hertel, O., Tang, S. Y., Robin, P., Hassouna, M., Dämmgen, U., Genermont, S., Cellier, P., and Sutton, M. A.: Ammonia deposition near hot spots: processes, models and monitoring methods. In: Sutton MA, Reis S, Baker SMH, editors. Atmospheric ammonia: detecting emission changes and environmental impacts. Netherlands: Springer; 205-251.,2008.

Lü, C. Q. and Tian, H. Q.: Spatial and temporal patterns of nitrogen deposition in China: Synthesis of observational data, J. Geophys. Res., 112, D22S05, doi:10.1029/2006JD007990, 2007.

Lü, C. Q. and Tian, H. Q.: Half-century nitrogen deposition increase across China: A gridded time-series data set for regional environmental assessments. Atmos. Environ., 97, 68-74, 2014.

Luo, X. S., Liu, P., Tang, A. H., Liu, J. Y., Zong, X. Y., Zhang, Q., Kou, C. L., Zhang, L. J., Fowler, D., Fangmeier, A., Christie, P., Zhang, F. S., and Liu, X. J.: An evaluation of atmospheric Nr pollution and deposition in North China after the Beijing Olympics, Atmos. Environ., 74, 209–216, doi:10.1016/j.atmosenv.2013.03.054, 2013.

Maston, P., Lohse, K. A., and Hall, S. J.: The globalization of nitrogen deposition: Consequences for terrestrial ecosystems, Ambio, 31, 113–119, 2002.

MEPC (Ministry of Environmental Protection of the People's Republic of China): China's environment and data center. www.zhb.gov.cn/. Viewed 23 April 2014, 2014

Pan, Y. P., Wang, Y. S., Tang, G. Q., and Wu, D.: Wet and dry deposition of atmospheric nitrogen at ten sites in Northern China. Atmos. Chem. Phys., 12, 6515-6535, doi:10.5194/acp-12-6515-2012, 2012.

Reche, C., Viana, M., Pandolfi, M., Alastuey, A., Moreno, T., Amato, F., Ripoll, A., and Querol, X.: Urban NH_3 levels and sources in a Mediterranean environment. Atmos. Environ., 57:153–164, doi:10.1016/j.atmosenv.2012.04.021, 2012.

删除的内容: MACTEC Engineering and Consulting, Inc. (MACTEC): Clean Air Status and Trends Network (CASTNET) 2007, Annual Report, U.S. Environmental Protection Agency, Washington, D.C, pp. 5–30, 2008.

1235 Richter, D. D., Burrows, J. P., N Nüß, H., Granier, C., and Niemeier, U.: Increase in
1236 tropospheric nitrogen dioxide over China observed from space, Nature 437,
1237 129–132, 2005.
1238 Seinfeld, J. and Pandis, S.: Atmospheric Chemistry and Physics: From Air Pollution
1239 to Climate Change, John Wiley and Sons, 2nd Edition, 1203 pp., 2006.
1240 Schwede, D., Zhang, L., Vet, R., and Lear, G.: An intercomparison of the deposition
1241 models used in the CASTNET and CAPMoN networks, Atmos. Environ., 45,
1242 1337–1346, doi:10.1016/j.atmosenv.2010.11.050, 2011.
1243 Shen, J. L., Tang, A. H., Liu, X. J., Fangmeier, A., Goulding, K. T. W., and Zhang, F.
1244 S.: High concentrations and dry deposition of reactive nitrogen species at two sites
1245 in the North China Plain, Environ. Pollut., 157, 3106–3113,
1246 doi:10.1016/j.envpol.2009.05.016, 2009.
1247 Simpson, D., Fagerli, H., Jonson, J.E., Tsyro, S., Wind, P., and Tuovinen, J. P.:
1248 Trans-boundary Acidification and Eutrophication and Ground Level Ozone in
1249 Europe: Unified EMEP Model Description, EMEP Status Report 1/2003 Part I,
1250 EMEP/MSC-W Report, The Norwegian Meteorological Institute, Oslo, Norway,
1251 2003.
1252 Skeffington, R. A. and Hill, T. J.: The effects of a changing pollution climate on
1253 throughfall deposition and cycling in a forested area in southern England, Sci. Total
1254 Environ., 434 , 28–38, doi:10.1016/j.scitotenv.2011.12.038, 2012.
1255 Sickles, J. E. and Shadwick, D. S.: Air quality and atmospheric deposition in the
1256 eastern US: 20 years of change, Atmos. Chem. Phys., 15, 173–197, doi:
1257 10.5194/acp-15-173-2015, 2015.
1258 Sutton, M.A., Pitcairn, C.E.R., and Fowler, D.: The exchange of ammonia between
1259 the atmosphere and plant communities. Adv. Ecol. Res., 24, 301-393,
1260 doi:10.1016/S0065-2504(08)60045-8, 1993.
1261 Sutton, M. A., Burkhardt, J. K., Guerin, D., Nemitz, E., and Fowler, D.: Development
1262 of resistance models to describe measurements of bi-directional ammonia
1263 surface-atmosphere exchange, Atmos. Environ., 32, 473–480,
1264 doi:10.1016/S1352-2310(97)00164-7,1998.

Sutton, M. A., Tang, Y. S., Miners, B., and Fowler, D.: A new diffusion denuder system for long-term, regional monitoring of atmospheric ammonia and ammonium, Water Air Soil Poll. Focus, 1, 145–156, 2001.

Tang, Y. S., Simmons, I., van Dijk, N., Di Marco, C., Nemitz, E., Dammgen, U., Gilke, K., Djuricic, V., Vidic, S., Gliha, Z.: European scale application of atmospheric reactive nitrogen measurements in a low-cost approach to infer dry deposition fluxes. Agr. Ecosyst. Environ., 133, 183–195, doi: 10.1016/j.agee.2009.04.027, 2009.

Torseth, K., Aas, W., Breivik, K., Fjaeraa, A. M., Fiebig, M., Hjellbrekke, A. G., Myhre, C. L., Solberg, S., Yttri, K. E.: Introduction to the European Monitoring and Evaluation Programme (EMEP) and observed atmospheric composition change during 1972–2009, Atmos. Chem. Phys., 12, 5447–5481, doi: 10.5194/acp-12-5447-2012, 2012.

Vitousek, P. M., Aber, J. D., Howarth, R. W., Likens, G. E., Matson, P. A., Schindler, D. W., Schlesinger, W. H., and Tilman, D. G.: Human alteration of the global nitrogen cycle: Sources and consequences, Ecol. Appl., 7, 737–750, 1997.

Vet, R., Artz, R. S., Carou, S., Shaw, M., Ro, C-U., Aas, W., Baker, A., and 14 authors: A global assessment of precipitation chemistry and deposition of sulfur, nitrogen, sea salt, base cations, organic acids, acidity and pH, and phosphorus, Atmos. Environ., 93, 3–100, doi:10.1016/j.atmosenv.2013.10.060, 2014.

Wang, S. X., Xing, J., Zhao, B., Jang, C., and Hao, J. M.: Effectiveness of national air pollution control policies on the air quality in metropolitan areas of China, J. Environ. Sci., 26, 13–22, doi: 10.1016/S1001-0742(13)60381-2, 2014.

Wang, T., Nie, W., Gao, J., Xue, L. K., Gao, X. M., Wang, X. F., Qiu, J., Poon, C. N., Meinardi, S., Blake, D., Wang, S. L., Ding, A. J., Chai, F. H., Zhang, Q. Z., and Wang, W. X.: Air quality during the 2008 Beijing Olympics: secondary pollutants and regional impact, Atmos. Chem. Phys., 16, 7603–7615, doi:10.5194/acp-10-7603-2010, 2010.

Wesely, M. L.: Parameterization of surface resistances to gaseous dry deposition in regional-scale numerical-models, Atmos. Environ., 23, 1293-1304, 1989.

Xing, J., Pleim, J., Mathur, R., Pouliot, G., Hogrefe, C., Gan, C. M., Wei, C.: Historical gaseous and primary aerosol emissions in the United States from 1990 to 2010, Atmos. Chem. Phys., 13, 7531–7549, doi: 10.5194/acp-13-7531-2013, 2013.

Yu, W. T., Jiang, C. M., Ma, Q., Xu, Y. G., Zou, H., and Zhang, S. C.: Observation of the nitrogen deposition in the lower Liaohe River Plain, Northeast China and assessing its ecological risk, Atmos. Res., 101, 460–468, doi:10.1016/j.atmosres.2011.04.011, 2011.

Zhan, X., Yu, G., He, N., Jia, B., Zhou, M., Wang, C., Zhang, J., Zhao, G., Wang, S., Liu, Y., and Yan, J.: Inorganic nitrogen wet deposition: Evidence from the North-South Transect of Eastern China, Environ. Pollut., 204, 1–8, doi: 10.1016/j.envpol.2015.03.016, 2015.

Zhang, F. S., Wang, J. Q., Zhang, W. F., Cui, Z. L., Ma, W. Q., Chen, X. P., and Jiang, R. F.: Nutrient use efficiency of major cereal crops in China and measures for improvement. Acta. Pedologia Sinica, 45, 915–924, 2008a (in Chinese with English abstract).

Zhang, G. Z., Pan, Y. P., Tian, S. L., Cheng, M. T., Xie, Y. Z., Wang, H., and Wang, Y. S.: Limitations of passive sampling technique of rainfall chemistry and wet deposition flux characterization. Res. Environ. Sci., 28, 684-690, doi:10. 13198/j.issn.1001-6929.2015.05.03, 2015.

Zhang, Y., Liu, X. J., Fangmeier, A., Goulding, K. T. W., and Zhang, F. S.: Nitrogen inputs and isotopes in precipitation in the North China Plain, Atmos. Environ., 42, 1436–1448, doi:10.1016/j.atmosenv.2007.11.002, 2008b.

Zhang, Y., Dore, A. J., Ma, L., Liu, X. J., Ma, W. Q., Cape, J. N., and Zhang, F. S.: Agricultural ammonia emissions inventory and spatial distribution in the North China Plain, Environ. Pollut., 158, 490–501, doi:10.1016/j.envpol.2009.08.033, 2010.

Zhang, Y., Song, L., Liu, X. J., Li, W. Q., Lü, S. H., Zheng, L. X., Bai, Z. C., Cui, G.Y., and Zhang, F. S.: Atmospheric organic nitrogen deposition in China. Atmos. Environ., 46, 195–204, doi:10.1016/j.atmosenv.2011.09.080, 2012a.

已下移 [1]: Zhang, Y., Liu, X. J., Fangmeier, A., Goulding, K. T. W., and Zhang, F. S.: Nitrogen inputs and isotopes in precipitation in the North China Plain, Atmos. Environ., 42, 1436–1448, doi:10.1016/j.atmosenv.2007.11.002, 2008b.

已移动(插入) [1]

已移动(插入) [2]

删除的内容: b

Zhang, L., Jacob, D. J., Knipping, E. M., Kumar, N., Munger, J. W., Carouge, C. C., van Donkelaar, A., Wang, Y. X., and Chen, D.: Nitrogen Deposition to the United States: Distribution, Sources, and Processes, Atmos. Chem. Phys., 12, 4539-4554, doi:10.5194/acp-12-4539-2012, 2012b.

Zhang, L. M., Gong, S. L., Padro, J., and Barrie, L.: A size-segregated particle dry deposition scheme for an atmospheric aerosol module, Atmos. Environ., 35 (3), 549-560, doi:10.1016/s1352-2310(00)00326-5, 2001.

Zhao, Y. H., Zhang, L., Pan, Y. P., Wang, Y. S., Paulot, F., and Henze, D. K.: Atmospheric nitrogen deposition to the northwestern Pacific: seasonal variation and source attribution, Atmos. Chem. Phys. Discuss., 15, 13657-13703, doi:10.5194/acpd-15-13657-2015, 2015.

Zhu, J. X., He, N. P., Wang, Q. F., Yan, G. F., Wen, D., Yu, G. R., and Jia, Y. L.: The composition, spatial patterns, and influencing factors of atmospheric wet nitrogen deposition in Chinese terrestrial ecosystems. Sci. Total Environ., 511, 777-785, doi:org/10.1016/j.scitotenv.2014.12.038, 2015.

删除的内容: 2012a

已上移 [2]: Zhang, Y., Song, L., Liu, X. J., Li, W. Q., Lü, S. H., Zheng, L. X., Bai, Z. C., Cui, G.Y., and Zhang, F. S.: Atmospheric organic nitrogen deposition in China. Atmos. Environ., 46, 195–204, doi:10.1016/j.atmosenv.2011.09.080, 2012b.

Figure captions

Fig. 1. Geographical distribution of the forty-three monitoring sites in China.

Fig. 2. Annual mean concentrations of N_r compounds in air (a) and volume-weighted concentrations of inorganic nitrogen species in precipitation (b) at all monitoring sites.

Fig. 3. Annual mean concentrations of (a) NH_3; (b) NO_2; (c) HNO_3; (d) pNH_4^+; (e) pNO_3^-; and (f) Total N_r: sum of all measured N_r in air and volume-weighted concentrations of NH_4^+ (g); NO_3^- (h) and Total inorganic N (TIN): sum of NH_4^+ and NO_3^- (i) in precipitation at different land use types in the six regions.

Fig. 4. Annual mean concentrations and deposition fluxes of N_r compounds at different land use types across China: concentrations in air (a); volume-weighted concentrations in precipitation (b); dry N deposition fluxes (c); wet/bulk N deposition fluxes (d). The number of sites with the same land use type can be found in Table S1 in the Supplement. Error bars are standard errors of means.

Fig. 5. Annual deposition flux of various N_r species at the forty-three selected sites in China: (a) dry deposition flux; (b) wet/bulk deposition flux; (c) total deposition flux. Yellow dots denote ratios of reduced N to oxidized N in dry deposition (a), NH_4^+-N to NO_3^--N in wet/bulk deposition (b) and/or reduced N to oxidized N in total deposition (c) at all sampling sites.

Fig. 6. Dry N deposition fluxes of (a) NH_3; (b) NO_2; (c) HNO_3; (d) pNH_4^+; (e) pNO_3^-; and (f) Total N_r: sum of all measured N_r in dry and wet/bulk N deposition fluxes of NH_4^+ (g); NO_3^- (h) and Total inorganic N (TIN): sum of NH_4^+ and NO_3^- (i) at different land use types in six regions. The number of sites with the same land use type can be found in Table S1 in the Supplement. Error bars are standard errors of means.

Fig. 7. Contribution of different pathways (dry-deposited N=gaseous N+ particulate N, wet/bulk-deposited N=precipitation N) to the estimated total N deposition in the six regions: (a) NC: north China; (b) NE: northeast China; (c) NW: northwest China; (d) SE: southeast China; (e) SW: southwest China; (f) TP: Tibetan Plateau.

Fig. 8. Correlations between annual wet/bulk NH_4^+-N deposition and annual volume-weighted concentration of NH_4^+-N (a) and annual precipitation (b); between

删除的内容: Atmospheric concentrations (a) and dry deposition fluxes (b) of N_r species at different land use types in the six regions of China. Error bars are standard errors of means. "N" in brackets denotes the number of sampling sites at each land use type.

删除的内容: Annual deposition flux of various N_r species at the forty-three selected sites in China: (a) dry deposition flux; (b) wet deposition flux Blank dots denote ratios of reduced N to oxidized N in dry deposition (a) and/or NH_4^+-N to NO_3^--N in wet deposition (b) at all sampling sites.

删除的内容: Contribution of different pathways (dry-deposited N=gaseous N+ particulate N, wet-deposited N=precipitation N) to the estimated total N deposition in the six regions: (a NC: north China; (b) NE: northeast China; (c) NW: northwest China; (d) SE: southeast China; (e) SW: southwest China; (f) TP: Tibetan Plateau.

删除的内容: Correlations between annual wet NH_4^+-N deposition and annual volume-weighted concentration of NH_4^+-N (a) and annual precipitation (b); between annual wet NO_3^--N deposition and annual volume-weighted concentration of NO_3^--N (c) and annual precipitation (d)

删除的内容: Spatial variation of atmospheric N deposition flux with emission distribution in China: (a) NH_3 emission *vs.* NH_x deposition; (b) NO_x emission vs. NO_y deposition; (c) relationship of NH_x deposition *vs.* NH_3 emission; (d) relationship of NO_y deposition *vs.* NO_x emission.

annual wet/bulk NO_3^--N deposition and annual volume-weighted concentration of NO_3^--N (c) and annual precipitation (d).

Fig. 9. Spatial variation of atmospheric N deposition flux with emission distribution in China: (a) NH_3 emission *vs.* NH_x deposition; (b) NO_x emission vs. NO_y deposition; (c) relationship of NH_x deposition *vs.* NH_3 emission; (d) relationship of NO_y deposition *vs.* NO_x emission.

1476

1477

Figure 1


Kazakhstan
Russia
Mongolia
India
Korea
Yellow Sea
East China Sea
South China Sea
Regions
North China
North East
North West
South East
South West
Tibetan Plateau
Land use types
Background Sites
Rural Sites
Urban Sites
0 560,000 1,120,000 1,680,000
Meters
N
70°0'0"E
80°0'0"E
90°0'0"E
100°0'0"E
110°0'0"E
120°0'0"E
130°0'0"E
140°0'0"E
50°0'0"N
40°0'0"N
30°0'0"N
20°0'0"N

Figure 2

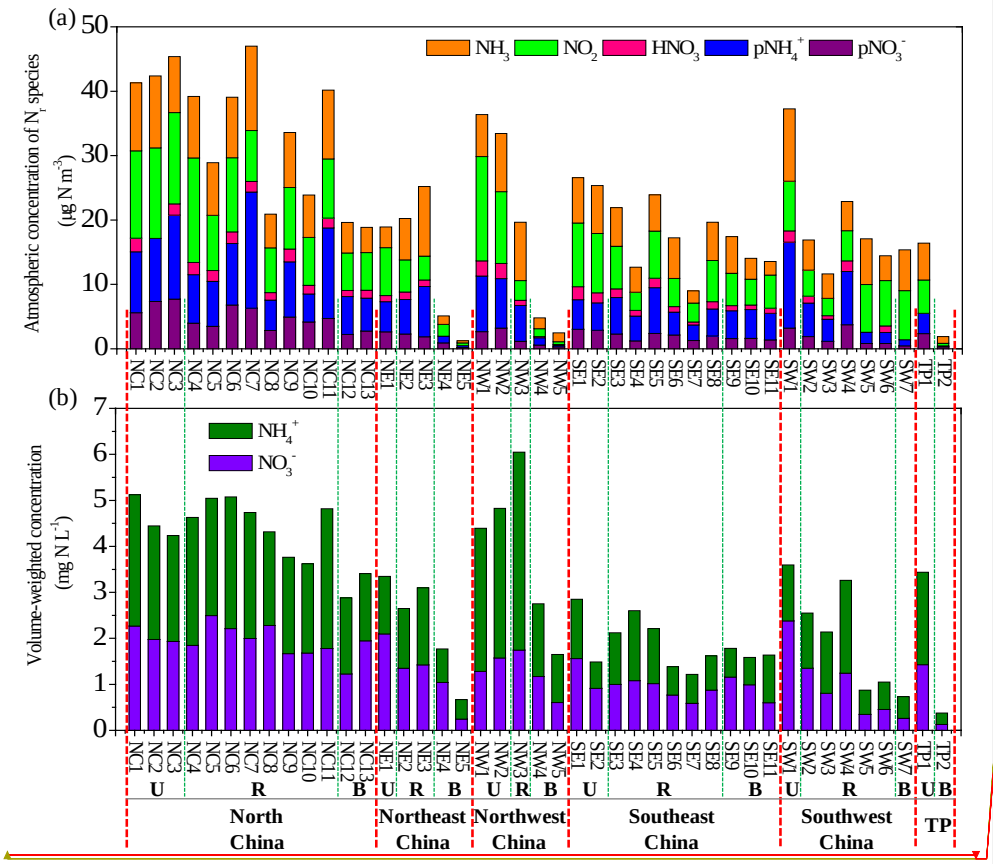

带格式的：字体：（默认）Times New Roman，（中文）+中文正文，小四

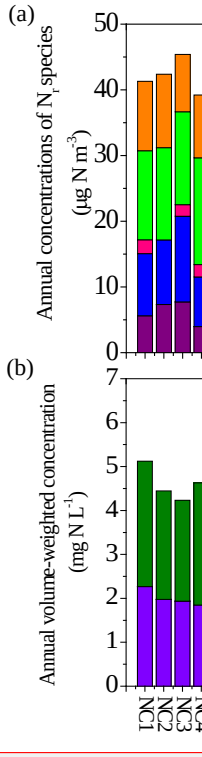

删除的内容：

Figure 3

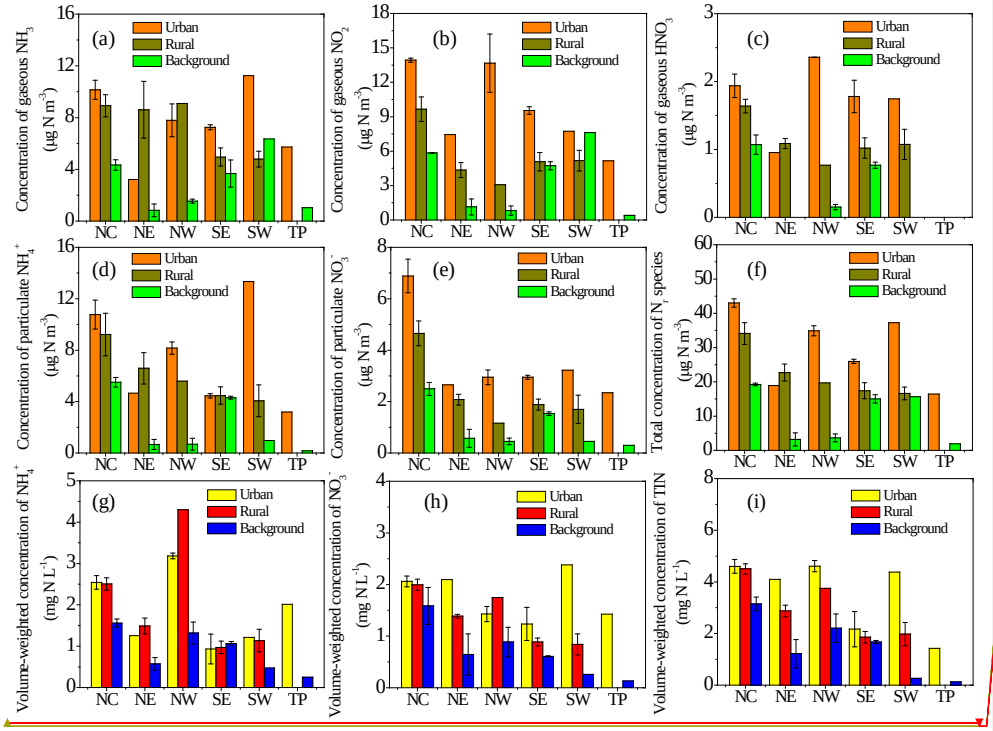

带格式的： 字体：（默认）Times New Roman，（中文）+中文正文，小四

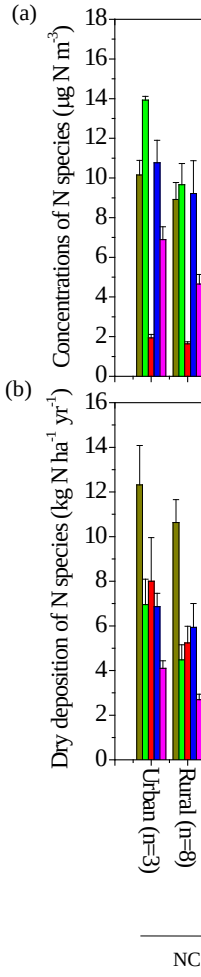

删除的内容：

Figure 4

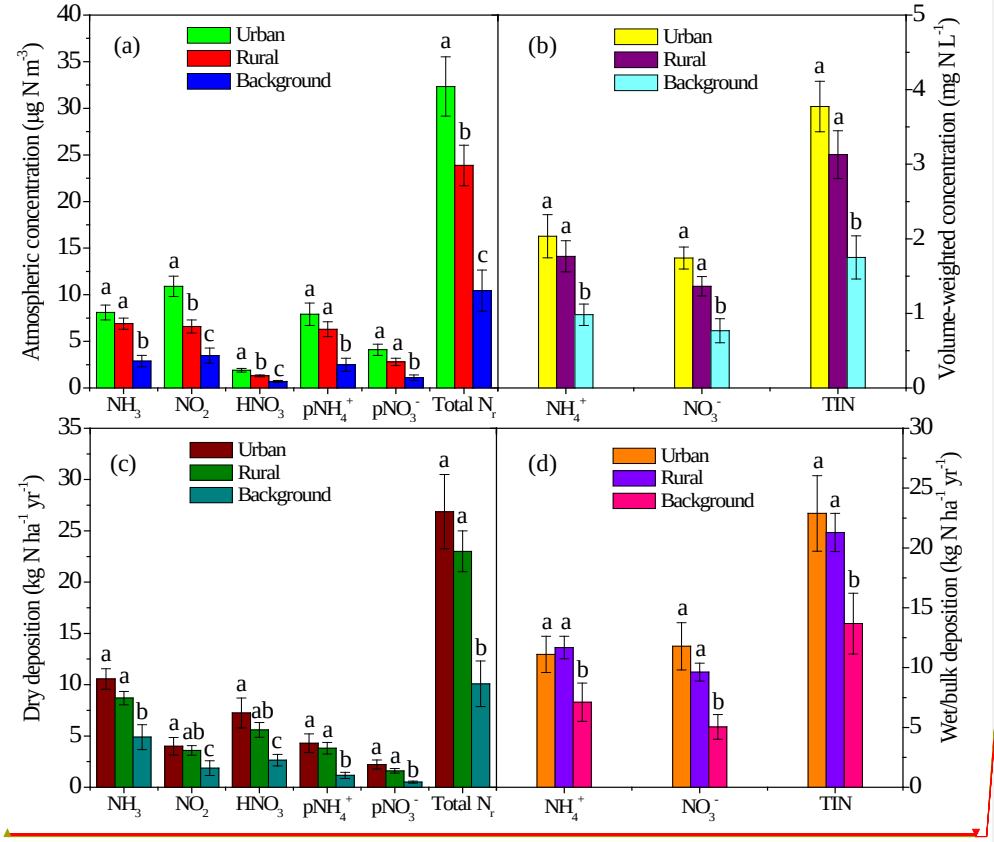

带格式的：字体：（默认）Times New Roman，（中文）+中文正文，小四，加粗

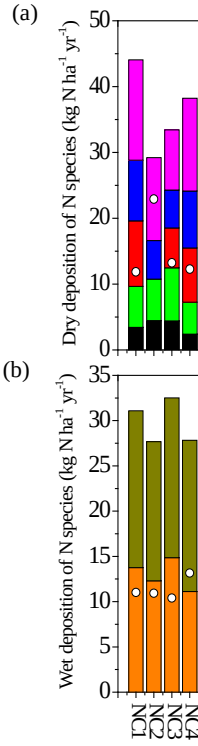

删除的内容：

1530 **Figure 5**

删除的内容: ▪

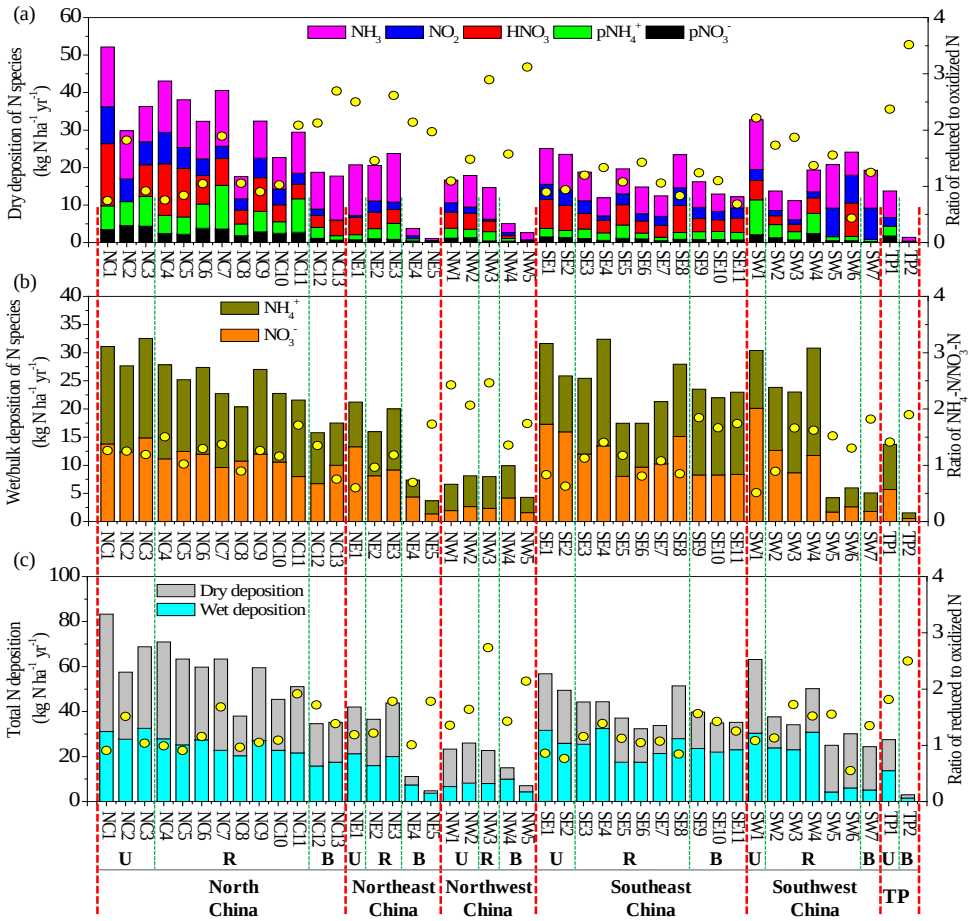

1531

1532

1533

1534

1535

1536

1537

1538

1539

1540

1541

1542

Figure 6

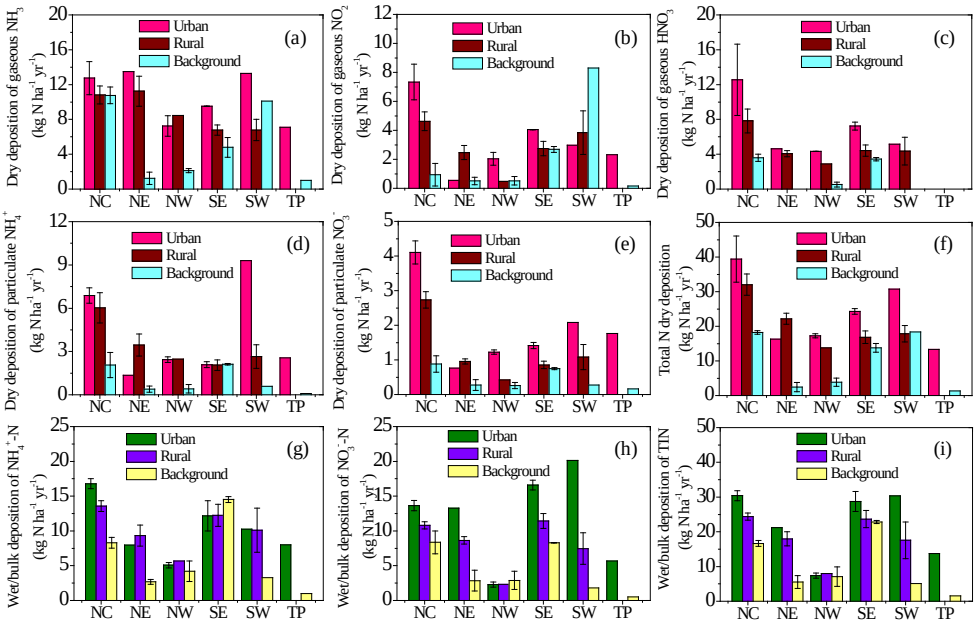
(a)
Dry deposition of gaseous NH_3 (kg N ha^{-1} yr^{-1})
(b)
Dry deposition of gaseous NO_2 (kg N ha^{-1} yr^{-1})
(c)
Dry deposition of gaseous HNO_3 (kg N ha^{-1} yr^{-1})
(d)
Dry deposition of particulate NH_4^+ (kg N ha^{-1} yr^{-1})
(e)
Dry deposition of particulate NO_3^- (kg N ha^{-1} yr^{-1})
(f)
Total N dry deposition (kg N ha^{-1} yr^{-1})
(g)
Wet/bulk deposition of NH_4^+-N (kg N ha^{-1} yr^{-1})
(h)
Wet/bulk deposition of NO_3^--N (kg N ha^{-1} yr^{-1})
(i)
Wet/bulk deposition of TIN (kg N ha^{-1} yr^{-1})
Urban
Rural
Background
NC
NE
NW
SE
SW
TP

Figure 7

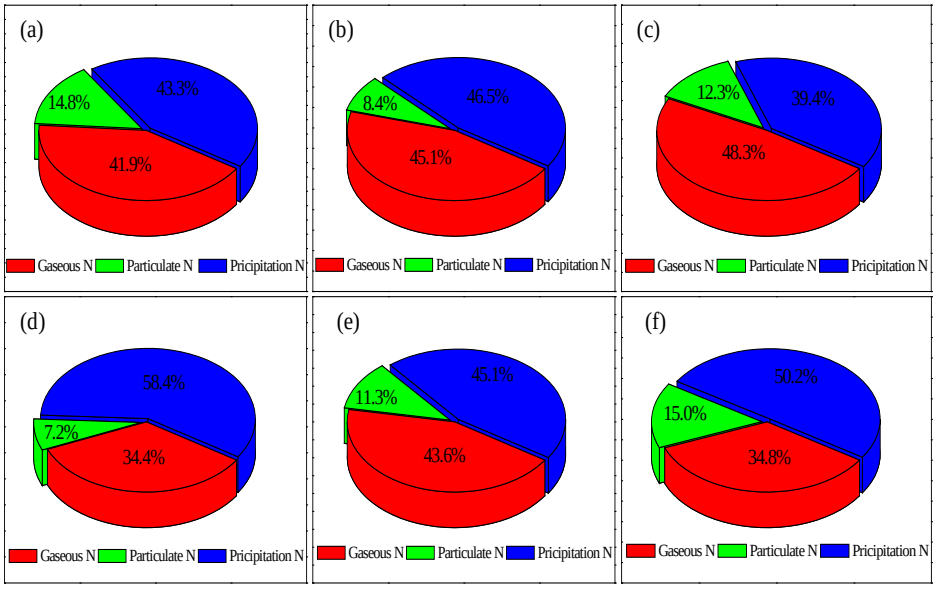

删除的内容: 5

带格式的: 字体: (默认) Times New Roman, (中文) +中文正文, 小四

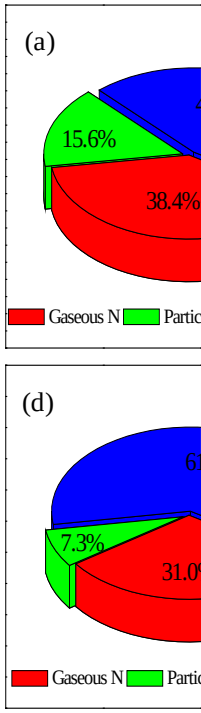

删除的内容:

带格式的: 字体: (默认) +西文正文, (中文) +中文正文

Figure 8

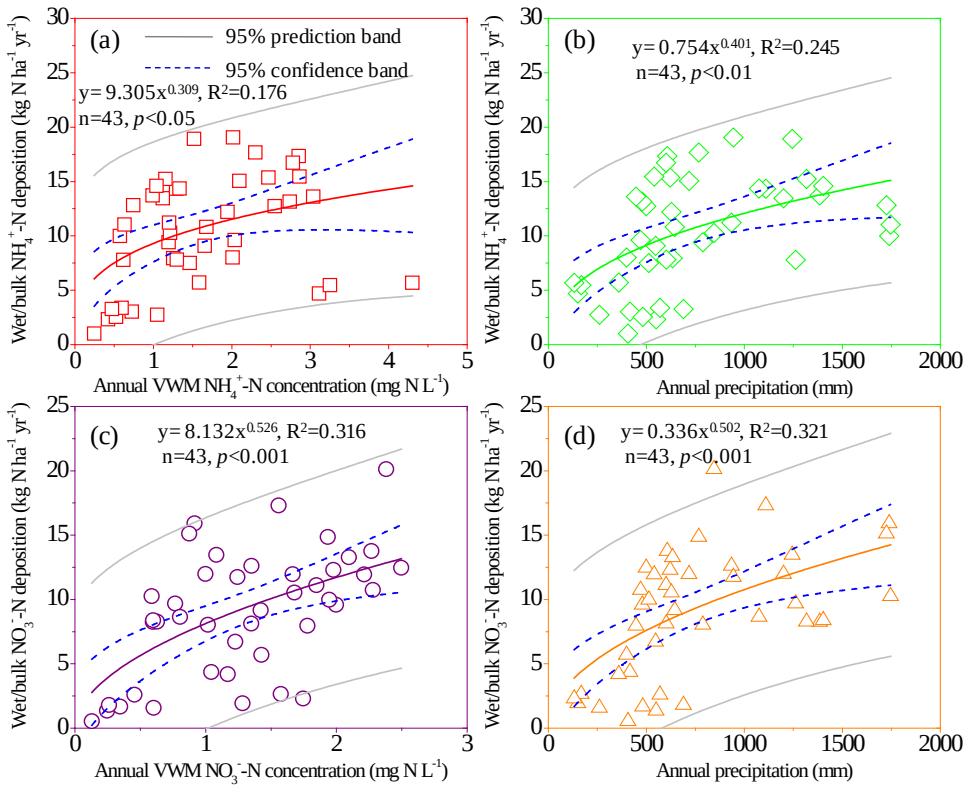

删除的内容: 6

带格式的: 字体: (默认) Times New Roman, (中文) +中文正文, 小四, 加粗

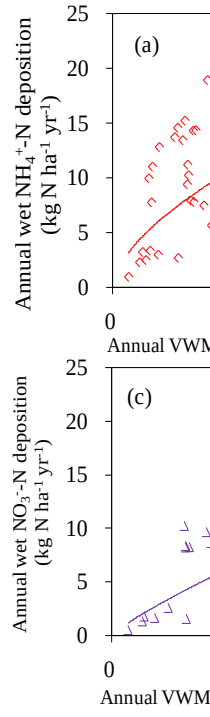

删除的内容:

带格式的: 字体: (默认) +西文正文, (中文) +中文正文

Figure 9

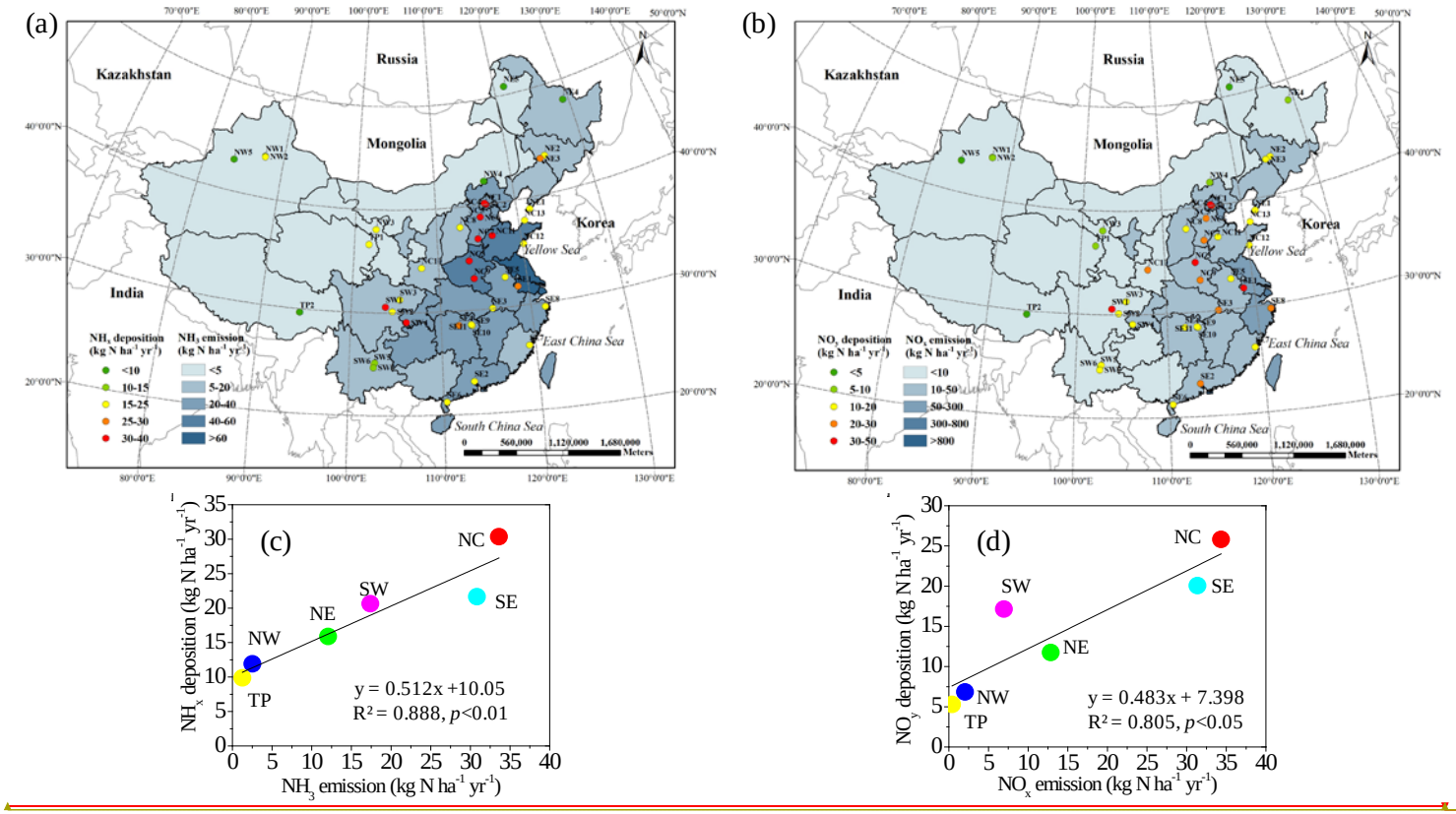

删除的内容: 7

带格式的: 字体: (默认) Times New Roman, (中文) +中文正文, 小四

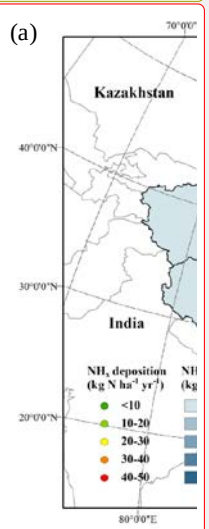

删除的内容:

带格式的: 字体: (默认) +西文正文, (中文) +中文正文

删除的内容: **Table 1.**Concentrations of various N_r species and the estimated N deposition fluxes in the six regions of China. Data in parentheses are standard errors.

Region

Table 1. Comparison of dry, wet (wet/bulk), and total deposition fluxes of N_r compounds between NNDMN in China and 3 networks in other countries.

Network		Japan EANET network[a]			CASTNET[b]			EMEP[c]			NADMM[d]		
Number of sites or grids		10sites			130sites			2447girds (0.5° × 0.5°)			33sites		
Observation period		Apr. 2003-Mar. 2008			Apr. 2006-Dec. 2013			Jan. 2003-Dec. 2007			Aug. 2006-Sep. 2014		
N deposition (kg N ha^{-1} yr^{-1})		Dry	Wet	Total	Dry	Wet	Total	Dry	Wet	Total	Dry	Wet/bulk	Total
	Average	3.9	6.6	10.6	3.1	1.3	4.4	3.9	4.8	8.7	18.7	18.2	36.9
	Median	4.1	5.9	11.2	3.0	0.7	4.1	3.7	4.7	8.5	18.7	21.3	36.5
	Max	7.0	15.8	18.2	9.7	10.3	19.6	15.8	16.9	28.0	43.1	32.4	70.9
	Min	1.0	2.1	3.0	0.03	0.1	0.3	0.1	0.6	0.7	1.1	1.5	2.9

[a]The Japan EANET data are sourced from Endo et al. (2011). Gaseous NO_2 was not included in estimates of dry N deposition.

[b] The CASNET data are available online (http://www.epa.gov/castnet/). Gaseous NH_3 was not included in estimates of dry N deposition.

[c]The EMEP data are sourced from Endo et al. (2011), in which the dry and wet deposition amounts at each grid covering 27 EMEP countries were estimated by the unified EMEP models (Simpson et al., 2003).

[d] Only including the rural and background sites in NNDMN.

删除的内容: 2

Sect. S1. Social-economical and geo-climatic conditions for six regions of China

In this study, we divided the research area into six typical regions: North China (NC), Northeast (NE), Northwest (NW), Southeast China (SE), Southwest China (SW) and Tibetan Plateau (TP). These regions reflect different social-economical and geo-climatic conditions across China (Liu et al., 2013). Basically, NC, SE and SW represent relatively developed regions, NE and NW represent less developed regions while TP represents the least developed region in China.

删除的内容: SC

Statistical data of the gross domestic product (GDP) for the six regions are sourced from the China Statistic Yearbook for the year 2013 (http://www.stats.gov.cn/tjsj/ndsj/2014/indexch.htm).

North China, an intensively managed agricultural region and economically developed area, comprises of Beijing, Tianjin, Hebei, Henan, Shandong, Shanxi and Shaanxi provinces, which is characterized by temperate monsoon climate. The region occupies 10% of the total area of China, and contributes 28% of the total national China GDP. Northeast China includes Liaoning, Jilin and Heilongjiang provinces and the northeast area of Inner Mongolia, and is characterized by a temperate monsoon climate. The region accounts for 6% of the China's total area, and contributes 9% of the total national GDP. Northwest China consists of the northwest region of Inner Mongolia, Xinjiang, Ningxia and Gansu provinces, characterizing by a temperate continental climate. The region occupies 35% of the total area of China, but only contributes 5% of China's GDP. Southeast China covers Shanghai, Jiangsu, Zhejiang, Anhui, Hubei, Hunan, Jiangxi, Fujian, Guangdong, Hong Kong, Macau, Taiwan and Hainan provinces: 13% of China's total area. The region contributes 46% of China's GDP and is characterized by a subtropical monsoon climate. Southwest China consists of Sichuan, Chongqing, Guizhou, Yunnan and Guangxi provinces, and is characterized subtropical and plateau monsoon climates. The region accounts for 14% of China's total area and contributes 12% of China's GDP. The Tibetan Plateau is a remote area of China that consists of Tibet and Qinghai provinces. The region is characterized by an alpine mountain climate. The region occupies 20% of the total area of China but only contributes 0.5% of China's GDP.

Section S2. Other information of the sampling sites

S2.1. Sampling sites in north China (NC)

Thirteen sampling sites, including 3 urban sites (NC1, NC2 and NC3), 8 rural sites (NC4, NC5, NC6, NC7, NC8, NC9, NC10, NC11) and 2background sites (NC12 and NC13), are located in north China.

NC1, located at the west campus of China Agricultural University (CAU, 40.02ºN, 116.28ºE), is near the fifth ring road in Beijing city. NC2, located at the campus of Beijing Normal University (39.96ºN, 116.37ºE), is near the third ring road in Beijing city. NC3 is located in the centre of Zhengzhou city, the capital of Henan province and Henan Academy of Agricultural Sciences (34.75ºN, 113.63ºE). These three urban sites (i.e. NC1, NC2, and NC3) are surrounded by complicated external environments, such as densely occupied residences, industry, small-scale urban agriculture, and roads. NC4is located at Dongbeiwang village (40.04ºN, 116.29ºE), Xibeiwang town, Haidian District, about 20 km the northwest of Beijing city. This site could be polluted by ammonia from agricultural fields and domestic animal farms and emissions from motor vehicles on an adjacent road (c. 0.2 km). NC5 is located at Shangzhuang Agricultural Experimental Station (40.11ºN, 116.20ºE) of CAU, in Shangzhuang town, about 33 km northwest of Beijing city. This site is surrounded by small villages and croplands. NC6 is located at the west campus of Hebei Agricultural University (38.85ºN, 115.48ºE) in Baoding city, Hebei province, about 8 km southwest of the downtown area. This site is surrounded by small villages and croplands, and is close to a main road (c. 0.5 km). NC7 is located at CAU's Quzhou experimental station (36.78ºN, 114.94ºE) in Quzhou town, Hebei province. NC7 is a typical rural agriculture dominated site with a recently constructed industrial district. This site is surrounded by croplands and small villages. A north-south main road is located 0.5 km west of the sampling site. NC8 is located at Yangqu dry farming water-saving demonstration base (38.05ºN, 112.89ºE), Shanxi Academy of Agricultural Sciences, in Hecun village, about 30 km northeast of Taiyuan city, Shanxi province. Hecun is a typical rural village with dryland farming. The sampling site is mainly polluted by ammonia from agricultural fields. NC9 is located at Zhumadian Agricultural Experiment Station (33.02ºN, 114.05ºE), Zhumadian Academy of Agricultural Sciences in Yicheng district of Zhumadian city, Henan province. This site is surrounded by croplands, small villages and small-scale livestock farming. NC10 is located at Wuquan Agricultural Experimental Base (34.31ºN, 108.01ºE), Northwest

删除的内容: *S1*

删除的内容: y

Agriculture & Forestry UniversityinYangling city, Shaanxi province. This site is about 8 km northwest of the downtown area, surrounding by croplands and small villages. NC11 is located at Yucheng Experimental Station (36.94ºN, 116.63ºE), Chinese Academy of Sciences, about 8 km southwest of Yucheng city, Shandong province. This site is surrounded by small villages and croplands. At all the above farmland sites, with the exception of NC8, the dominant cropping system is a winter wheat-summer maize rotation (two crops a year). Farmers usually apply nitrogen (N) fertilizers (mainly as urea and ammonium bicarbonate) in March-April, June-August and October to achieve high yields of maize and wheat. Typical application rates of N fertilizer are 500-600 kg N ha^{-1} yr^{-1} at most sites except NC9, where the rate is 100-150 kg N ha^{-1} yr^{-1}. At NC8 site, the dominant cropping system is spring maize (one crop a year). In addition there is small-scale vegetable production (e.g. brussels sprouts, beans and zucchini) throughout the year. Usually, N-fertilizers (compound fertilizer, urea and ammonium bicarbonate) are applied in March-May, with annual application rates of 150-300 kg N ha^{-1}.

NC12 is located at Lingshandao (LSD) island (35.77ºN, 120.18ºE, 514 m a.s.l.) in the Yellow Sea. LSD is the biggest island in north China, about 10 km southeast of Jiaonan city, Shandong province. NC13 is located at Changdao island (37.93ºN, 120.75ºE, 203 m a.s.l.), which is at the join of the Bohai Sea and the Yellow Sea, about 7 km north of Penglai city, Shandong province. There are almost no agricultural and/or industrial activities near these two coastal sampling sites.

S2.2. Sampling sites in northeast China (NE)

删除的内容: *S1*

Five sampling sites, including 1 urban site (NE1), 2 rural sites (NE2 and NE3), and 2 background sites (NE4, andNE5) are located in northeast China.

NE1 is located at Dalian Jiaotong University (38.92 ºN, 121.58ºE) which lies in the Shahekou district of Dalian city, Liaoning province. Dalian is a sea town (near the Bohai Sea) and is famous for business development. The sampling site is polluted by emissions from industry and transportation. NE2 is located at an experimental station ofthe Soil and Fertilizer Institute (43.53 º N, 124.83ºE), Jilin Academy of Agricultural Sciences, in Gongzhuling city, Jilin province. Arable land accounts for 81% of the total land area in Gongzhuling city, and the other 19% is used for residential, commercial buildings and roads. This site is surrounded by farmland and residences. NE3 is located in Sikeshu town (43.36 ºN, 124.17ºE), Lishu county. This site is about 21 km northwest of Siping city, Jilin province. At NE2 and NE3, the sampling sites

are both surrounded by agricultural fields with a spring maize (single harvest per year) cropping system. Compound fertilizers are the major N source for the crops, and these are usually applied once in April-May, with an annual application rate of 400 kg ha^{-1} yr^{-1} at NE1 and 250 kg $ha^{-1}yr^{-1}$at NE2. NE5 is located in a forested area in Wuying district (48.11 ºN, 129.25 ºE) of Yichun city, Heilongjiang province, about 50 km northeast of downtown. Forest coverage reaches 93% in Wuying district. NE6 (50.78ºN, 121.52ºE) is located in a forested region of Genhe city, Inner Mongolia, where forest cover reaches 92%. Genhe is at the north border of the Greater Hinggan Mountains, and its climate is cold temperate humid monsoon together with the characteristics of continental monsoon, which is similar to that of northeast China, i.e. temperate humid and semi-humid continental monsoon. Given this, NE5 is placed in northeast China in the present study. The forests in Wuyin and Genhe are both natural ecosystems and there are no agricultural and industrial activities near the sampling sites.

S2.3. Sampling sites in northwest China (NW)

删除的内容: *S1*

Five sampling sites, including 2 urban sites (NW1 and NW2), 1 rural sites (NW3) and 2 background sites (NW4 and NW5), are located in northwest China.

NW1 is located at Xinjiang Institute of Ecology and Geography (43.87ºN, 87.57ºE), Chinese Academy of Science, in the urban region of Urumqi city, Xinjiang province. This site may be polluted by emissions from motor vehicles and home heating in winter. NW2 is located at Xinjiang Academy of Agricultural Sciences, about 11 km away from NW1. This site has similar pollution sources as NW1.

NW3is located in Yongchang town (38.07ºN, 102.60 ºE), Wuwei city, Gansu province. The sampling site is surrounded by agricultural fields, small scale livestock housing and small villages. Maize is the major crop grown. Usually cropland receives chemical N fertilizers (urea, ammonium bicarbonate and compound fertilizers) in April, June and July, with an annual application rate of 350 kg N ha^{-1} yr^{-1}. NW5 is located at the meteorological observation site belonging to the Chinese Academy of Sciences, which is situated in temperate grassland in Duolun county (42.20ºN, 116.49ºE), Inner Mongolia. NW6is located at Bayinbuluke Grassland Ecosystem Research Station (42.88 ºN, 83.71ºE), Chinese Academy of Sciences, in the southern Tian Shan Mountains (3000-4500 m a.s.l.) of central Asia. Those two grassland sites (i.e. NW4 and NW5) are very unlikely to be subjected to influences from anthropogenic activities.

S2.4. Sampling sites in southeast China (SE)

删除的内容: *S1*

Eleven sampling sites, including 2 urban sites (SE1 and SE2), 6 rural sites (SE3, SE4, SE5, SE6, SE7 and SE8), and 3 background sites (SE9, SE10 and SE11), are located in southeast China.

SE1 is located in the southern urban area of Nanjing city (31.84ºN, 118.85ºE). The sampling site is surrounded by complicated external environments, such as housing, industry, small-scale urban agriculture, and is close to a highway (c. 0.5 km). SE2is located at Baiyun Experimental Station (23.20ºN, 113.31ºE), Guangdong Academy of Agricultural Sciences, in Guangzhou city, Guangdong province. This site is surrounded by densely occupied housing and traffic roads. SE3 is located at Wuxue Modern Agricultural Demonstration Base (30.01ºN, 115.79ºE) in Huaqiao town, about 28 km northeast of Wuxue city, Hubei province. The sampling site is surrounded by residential land and paddy fields, where the cropping system is double rice harvests per year. Compound fertilizer and urea are the major N nutrient sources for rice, and these are usually applied in May-July, at a rate of about 180 kg ha^{-1} yr^{-1}. SE4 is located in Santangjie town (28.61ºN, 111.97ºE), which is a remote rural site in Taojiang county, Hunan province. The sampling site is surrounded by mountains and paddy fields. The paddy fields are cultivated with a double rice rotation system, which receives compound fertilizer and urea twice per year (in May, June or July) at about 150 kg N ha^{-1} yr^{-1}. SE5is located at Anhui Tobacco Institute (32.88ºN, 117.56ºE), Anhui Academy of Agricultural Sciences in Fengyang county, Anhui province. The sampling site is surrounded by croplands and residences. In the croplands, the major annual cropping system is a winter wheat-summer maize rotation (two crops per year). Compound fertilizer and urea are the major N nutrient sources for the croplands, and these are usually applied in April, June and October, at a rate of 380-500 kg N ha^{-1} yr^{-1}. SE6 is located in Leizhou peninsula, Zhanjiang city (21.26ºN, 110.33ºE), Guangdong province. This area grows tropical fruit and farmers use urea at a rate of 400 kg N ha^{-1} yr^{-1} for fruit production. SE7 is located on a mountain in the remote rural region of Fuzhou city (26.17ºN, 119.36ºE), Fujian province. This site is surrounded by some agricultural land growing tobacco and paddy rice. Usually, about 200 kg N ha^{-1} yr^{-1} compound fertilizers are used as the major nitrogen source for the crops, applied in January-March, and July and August. SE8 is located in Chunhu town (29.61ºN 121.53ºE), Fenghua city, Zhejiang province. The sampling site is surrounded by a residential area, a very small amount of agricultural land and mountains. SE9, located

in Huinong village (28.52ºN, 113.41ºE), Hunan province, is a rural background site. In a 2-km radius around the sampling site, there is forest and a reservoir, which contribute little to anthropogenic NH_3 and NO_x emissions. SE10, a rural background site is located in Feiyue village (28.56ºN, 113.34ºE), Hunan province. There were no typical emission sources around the site in a 2 km radius except forest and a residential area. SE11 is located at the centre of a 3 km^2 forest in Xishan village (28.61ºN, 113.31ºE), Hunan province. The forest has an average elevation of 250 m and is composed of masson pine, fir and shrubs. For convenience of access (e.g., the accessibility to road and the availability of main power), N deposition monitoring was conducted in the valley between two small hills in the forest. The valley is 100 m wide and 2000 m long in the main wind direction. The sampling site was selected in the centre of the valley, without human activity and anthropogenic emission sources of NH_3 and NO_x. The nearest N_r emission sources are more than 2 km away from the monitoring site, and consist of some small paddy fields distributed at the edge of the forest, accounting for no more than 5% of the total forest area.

S2.5. Sampling sites in southwest China (SW)

删除的内容: *S1*

Seven sampling sites, including 1 urban site (SW1), 5 rural sites (SW2, SW3, SW4, SW5 and SW6) and 1 background site (SW7), are located in southwest China.

删除的内容: 2

SW1is located in a residential area (30.55ºN, 103.84ºE) which lies in the Wenjiang district of Chengdu city, Sichuan province. The sampling site is surrounded densely occupied housing, roads and small-scale urban agriculture. SW2 is located at Xiangshui village (30.13ºN, 104.63ºE), Ziyang city, Sichuan province. This site is surrounded by paddy fields with a single rice cropping system (single harvest per year) and mountains. N fertilizers (urea and compound fertilizer) are applied mainly in June and July, at a rate of 270 kg N ha^{-1} yr^{-1}. SW3 is located at the Purple Soil Ecological Experiment Station (31.28ºN, 105.47ºE), Chinese Academy of Sciences, in Yanting county, Sichuan province. Agriculture is the dominant source of N at this site. In the agricultural fields, rice-wheat and maize-oilseed rape (canola) are the major double cropping systems for the paddy and upland fields in conventional farming practice, respectively. Ammonium bicarbonate is the major N nutrient sources for the croplands, usually applied at about 300 kg N ha^{-1} yr^{-1} for summer and winter crops together. SW4is located in Huangzhuang village (29.06ºN, 106.18ºE) in Jiangjin district of Chongqing, a city characterized by heavy industry production. The sampling site is surrounded by paddy fields and dry farmland with sorghum or oilseed rape. Farmers

apply N fertilizers mainly in April-July, October and November. Paddy fields at this site usually receive compound fertilizers including 180 kg N ha^{-1} yr^{-1}, whereas the dryland areas planted with sorghum usually receive ammonium phosphate and ammonium bicarbonate (altogether adding about 200 kg N ha^{-1} yr^{-1}), and the drylands used for oilseed rape production usually receive compound fertilizers at 135 kg N ha^{-1} yr^{-1}. SW5 is located in the suburbs of Kunming, a city characterized by flower and vegetable production, and about 500 m away from the Dian Lake (24.97ºN, 102.67ºE). This site is surrounded by agricultural fields and small villages, and is near a road (c. 0.2 km) with few vehicles. Leek is the most important cash crop in the region, and N fertilizer (urea) is usually applied every two months, at a rate of 300-400 kg N ha^{-1} yr^{-1}. SW6, located at the campus of Yunnan Agricultural University (25.13ºN, 102.75ºE), is in the northern rural area of Kunming city. This site is surrounded by housing, commercial buildings and roads without large agricultural sources. SW7 is a typical rural background site located in Kunyang town (24.67ºN, 102.61ºE), and is surrounded by small agricultural land (c. 62 ha), phosphate fertilizer plants and mountains.

S2.6. Sampling sites in the Tibetan plateau (TP)

删除的内容: *S1*

Two sampling sites, including 1 urban site (TP1) and 1background site (TP2), are located in the Tibetan plateau.

TP1, located at a meteorological station belonging to Xining Weather Bureau, is in the northern suburbs of Xining city, Qinghai province. Surrounding this site are schools, housing and commercial buildings. TP2 is located at an ecological experimental station belonging to the Agricultural and Animal Husbandry College of Tibet University, which lies in the wide valley area of the middle and lower reaches of the Niyang River in Linzhi county, Tibet province. TP2 (Linzhi site) is relatively undisturbed remote site, surrounded by grassland free from human activity.

Sect. S3. Information on measuring methods, sample replications and collection

S3.1. Description of the DELTA system and the ALPHA and Gradko passive samplers

The DELTA system comprises a denuder filter sampling train, a low-volume pump (D210, TCP Micropumps Ltd., UK) and a high sensitivity dry gas meter (SK25, Kimmon Manufacturing Co., Ltd., Japan). Briefly, the sampling train consists of two potassium carbonate plus glycerol (1 % (m/v) K_2CO_3 + 1 % (m/v) glycerol in methanol) coated denuders in series for the simultaneous collection of HNO_3,

followed by two citric acid (5% (m/v) citric acid in methanol) coated denuders for NH_3 and finally by a filter-pack assembly with a first K_2CO_3/glycerol impregnated filter to capture particle phase anions (NO_3^-, SO_4^{2-}, Cl^-) and cations (NH_4^+, Na^+, Mg^{2+}, Ca^{2+}), and a second filter coated with citric acid to collect any volatilized particulate NH_4^+. The empirically determined effective size cut-off for particle sampling is of the order of 4.5 µm (E. Nemitz, personal communication). The air was drawn through the sampling train at a rate of 0.2-0.4 L min^{-1} and directly into the first denuder with no inlet line to avoid sampling losses. The total sampled air volume of the DELTA system was recorded by the gas meter which was checked every month for data reading, performance and maintenance.

The ALPHA passive sampler, described in detail by Puchalski et al. (2011) is made up of a 26 mm long, 27 mm outer diameter polyethylene tube with one open end. The open end contains a 5 µm PTFE membrane allowing gaseous NH_3 to diffuse through, which is then absorbed onto a citric acid-coated collection filter located at the other end of the diffusion path. The Gradko passive sampler consists of a 71.0 mm long × 11.0 mm internal diameter acrylic tube with coloured and white thermoplastic rubber caps.NO_2 is absorbed into a 20% triethanolamine/deionised-water solution coated onto two stainless steel wire meshes within the coloured cap. Both types of passive samplers at each site were installed at 2 m height above the ground and deployed as three replicates for monthly sampling. For the ALPHA passive sampler, the NH_3 concentration was calculated by considering a temperature dependent diffusion coefficient (Puchalski et al., 2011; Xu et al., 2014), while a constant gas diffusion coefficient based on an assumption of 25 °C was used for the calculation of NO_2 concentration, in accordance with the Gradko introduction manual and previous studies (Luo et al., 2013; Shen et al., 2013).

The DELTA sampling trains and all the passive samplers were prepared and measured in the laboratory at China Agricultural University (CAU), Beijing. The prepared samplers were sealed in individual airtight storage bags and shipped in cool boxes, sent out to the monitoring sites for monthly field exposure, then sent back in the same bags and boxes to the laboratory for extraction and analysis. All the samplers were exposed to ambient air for one month at each site and thus provided monthly mean ambient N_r concentrations. Laboratory and field (travel) blanks were prepared and transported together with the field-exposed samples. Three laboratory blanks were prepared for each batch of field exposed samples and represent extracts from samples

prepared in the laboratory. Three field blanks were prepared for each batch of field exposed samples and represent extracts from unexposed samplers that were transported to and from the monitoring sites with the field exposed samplers.

S3.2. Description of particulate sampler

For pNH_4^+ and pNO_3^- sampling, particulate samplers equipped with solar panels were used to collect 7-10 days of PM_{10} samples per month. The average of these 7-10 samples is assumed to represent the monthly average concentration. The sampler was placed about 2 m above the ground and ran for 24h to obtain a particulate matter sample on 47 mm quartz filters (Whatman, Maidstone, UK). Each filter was equilibrated for 24-h in a room at 40 % relative humidity and 25 ℃ and then weighed on an electronic balance (Satorius, GÖTTINGEN, Germany, precision: 10 μg) before and after sampling. After collection, the loaded quartz filters were sealed in aluminum foil and stored in on-site refrigerators at about 3 °C until analysis in the coordinating laboratories of local universities or institutes. Field blank measurements were made each month at the corresponding sites.

References

Liu, X. J., Zhang, Y., Han, W. X.,Tang, A. H., Shen, J. L., Cui, Z. L., Vitousek, P. M., Erisman, J. W., Goulding, K., Christie, P., Fangmeier, A., and Zhang, F. S.: Enhanced nitrogen deposition over China, Nature, 494, 459-462, doi:10.1038/nature11917, 2013.

Luo, X. S., Liu, P., Tang, A. H., Liu, J. Y., Zong, X. Y., Zhang, Q., Kou, C. L., Zhang, L. J., Fowler, D., Fangmeier, A., Christie, P., Zhang, F. S., and Liu, X. J.: An evaluation of atmospheric N_r pollution and deposition in North China after the Beijing Olympics, Atmos. Environ., 74, 209–216, doi:10.1016/j.atmosenv.2013.03.054, 2013.

Puchalski, M. A., Sather, M. E., Walker, J. T., Lehmann, C. M. B., Gay, D. A., Mathew, J., and Robarge, W. P.: Passive ammonia monitoring in the United States: Comparing three different sampling devices, J. Environ. Monit., 13, 3156–3167, doi: 10.1039/c1em10553a, 2011.

Shen, J. L., Li, Y., Liu, X.J., Luo, X. S., Tang, A. H., Zhang, Y. Z., and Wu, J. S.: Atmospheric dry and wet nitrogen deposition on three contrasting land use types of an agricultural catchment in subtropical central China, Atmos. Environ., 67, 415–424, doi:10.1016/j.atmosenv.2012.10.068, 2013.

Xu, W., Zheng, K., Liu, X.J., Meng, L.M., Huaitalla, R.M., Shen, J.L., Hartang, E., Gallmann, E., Roelcke, M., and Zhang, F.S.: Atmospheric NH_3 dynamics at a typical pig farm in China and their implications. Atmos. Pollut. Res., 5, 455–463, doi:10.5094/APR.2014.053, 2014.

Sect. S4. Validation of ALPHA passive sampler

The ALPHA passive samplers were used to monitor atmospheric concentrations of NH_3 at seven sites (NC2, NE4, NE5, SW5, SW7, TP1 and TP2) of the network at which the DELTA systems could not be used due to absence of an external power supply. To ensure that differences across sites are due to the pollution climate rather than an artifact caused by methodological choices, we performed simultaneous and continuous 1-month measurements of NH_3 concentrations by using ALPHA passive samplers and the active DELTA denuders at three urban (NC1, NC3 and NE1) and three rural (NC8, SE3 and SE7) sites from Nov. 2013 to Oct. 2014.

Monthly mean concentrations of NH_3 provided by ALPHA passive samplers and the DELTA denuders were reasonably comparable at all site (**Fig S1a-f**), with overall averaged values of 6.7 ± 5.0 (standard deviation) and 7.0 ± 5.1 μg N m^{-3}, respectively. In addition, the correlation between the two methodologies was highly significant (R^2=0.919, p<0.001). Thus any differences in the data can be ascribed to the pollution climate.

Sect. S5. Introduction to the calculation of V_d for all N_r species as well as the estimation of dry deposition

The model calculation of dry deposition of N_r species follows a standard big-leaf resistance-in-series model as described by Wesely (1989) for gases and Zhang et al. (2001) for aerosol. V_d is calculated as the function $V_d=(R_a+R_b+R_c)^{-1}$ determined by local meteorological condition and surface type as described in Zhang et al. (2012). Here R_a is the aerodynamic resistance to turbulent transfer from the lowest model layer (70 m above the surface) to the roughness height, R_b is the boundary layer resistance to molecular diffusion, and R_c is the canopy or surface uptake resistance. In the present study we have run the model calculation of dry deposition velocities for the whole of 2012 and archived the hourly values for both gases and aerosols over the model domain. Then, the monthly V_d at each site was averaged based on the hourly dataset for further estimation of dry deposition flux of each N_r species during the

删除的内容: Parameterization of dry deposition of gases and aerosols follows a standard big-leaf resistance-in-series model (Wesely, 1989).

observation, which was statistically summarized according to land use type and is presented in **Table S3**. Annual mean dry deposition velocities of N_r species for six land use types in this study, averaged from monthly mean values, were fit well into range of annual values calculated and used for similar land use types in other studies (**Table S4** of Supplement).

删除的内容: S2

删除的内容: S3

References

Wesely, M. L.: Parameterization of surface resistance to gaseous dry deposition in regional-scale numerical models. Atmos. Environ., 23, 1293-1304, 1989.

Zhang, L., Jacob, D. J., Knipping, E. M., Kumar, N., Munger, J. W., Carouge, C. C., van Donkelaar, A., Wang, Y. X., and Chen, D.: Nitrogen Deposition to the United States: Distribution, Sources, and Processes, Atmos. Chem. Phys., 12, 4539-4554, doi:10.5194/acp-12-4539-2012, 2012.

Zhang, L. M., Gong, S. L., Padro, J., and Barrie, L.: A size-segregated particle dry deposition scheme for an atmospheric aerosol module, Atmos. Environ., 35 (3), 549-560, doi:10.1016/s1352-2310(00)00326-5, 2001.

Figure captions

Fig. S1. Comparison between simultaneous measurements of NH_3 concentrations by ALPHA passive samplers and the DELTA systems at six sampling sites in the network (a. NC1, b. NC3, c. NE1, d. NC8, e. SE3, f. SE7, g. ALPHA_NH_3 vs. DELTA_NH_3 across all sites). Site names for codes can be found in Table S1.

Fig. S2. Monthly mean atmospheric concentrations of N_r species (a. NH_3, b. NO_2, c. HNO_3, d. pNH_4^+ and e. pNO_3^-) at the forty-three monitoring sites in China. The boundary of the box indicates the 25^{th} and 75^{th} percentile. The black lines and red squares within the box mark the median and the mean, respectively. Whiskers above and below the box indicate the maximum and minimum values. Site names for codes can be found in Table S1.

Fig. S3. Monthly volume-weighted N_r concentrations in precipitation at the forty-three monitoring sites in China (a. NH_4^+-N, b. NO_3^--N). The black lines within the box denote the median. The blue circles denote the volume-weighted mean concentrations of N_r species in rainwater, calculating from the water amount and deposition fluxes of all precipitation events at each site during the sampling period. Whiskers above and below the box indicates the maximum and minimum values. Site names for codes can be found in Table S1.

Fig. S4. Relationships between monthly precipitation and volume-weighted concentrations of NH_4^+ and NO_3^- in precipitation at the sampling sites in the six regions. NC, NE, NW, SE, SW, and TP are the region codes and denote North China, Northeast China, Northwest China, Southeast China, Southwest China, and the Tibetan Plateau, respectively.

Fig. S5. Annual mean precipitation amounts at the forty-three sites in China. Site names for codes can be found in Table S1.

Fig. S6. Relationship between total annual dry N deposition fluxes and total annual atmospheric N_r concentrations across all forty-three sites. The plots with same color denote the same land use type.

删除的内容: **Fig. S3.** Annual mean concentrations of atmospheric N_r species above the different land use types. Error bars are standard errors of means. Values without the same letters are significantly different at $p < 0.05$. The number of sites with the same land use type can be found in Table S1.

删除的内容: S4

已移动(插入) [1]

删除的内容: 7

删除的内容:

删除的内容: **Fig. S5.** Annual total dry and wet deposition rates of N_r at the forty-three monitoring sites in China. Site names for codes can be found in Table S1.

删除的内容: S6

已上移 [1]: **Fig. S7.** Relationships between monthly precipitation and volume-weighted concentrations of NH_4^+ and NO_3^- in precipitation at the sampling sites in the six regions. NC, NE, NW, SE, SW, and TP are the region codes and denote North China, Northeast China, Northwest China, Southeast China, Southwest China, and the Tibetan Plateau, respectively.

删除的内容: 8

删除的内容: Site names for codes can be found in Table S1

Fig. S1

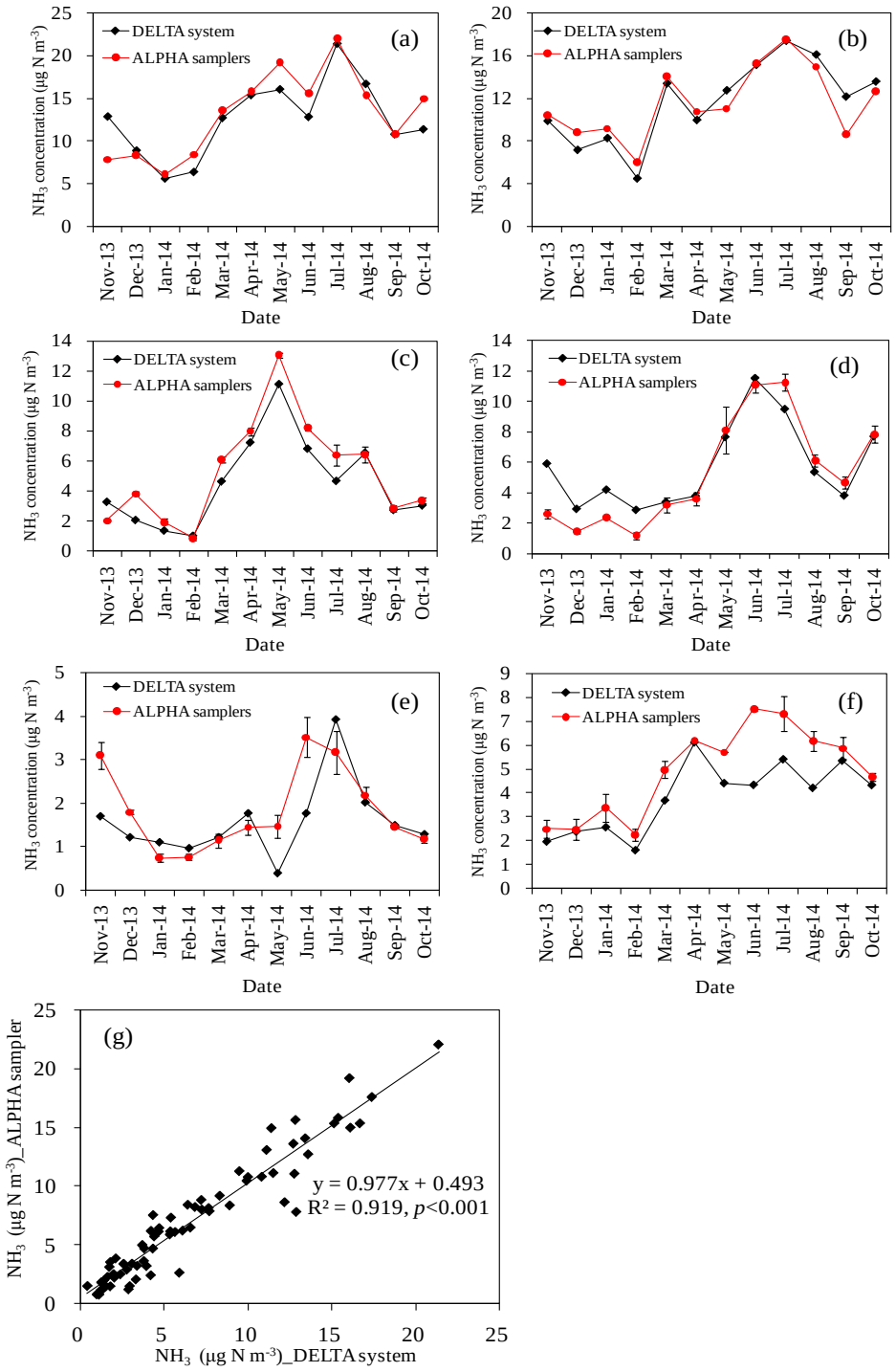
(a)
(b)
(c)
(d)
(e)
(f)
DELTA system
ALPHA samplers
NH3 concentration (µg N m-3)
Date
Nov-13
Dec-13
Jan-14
Feb-14
Mar-14
Apr-14
May-14
Jun-14
Jul-14
Aug-14
Sep-14
Oct-14
(g)
y = 0.977x + 0.493
R² = 0.919, p<0.001
NH3 (µg N m-3)_ALPHA sampler
NH3 (µg N m-3)_DELTA system

460 **Fig. S2**

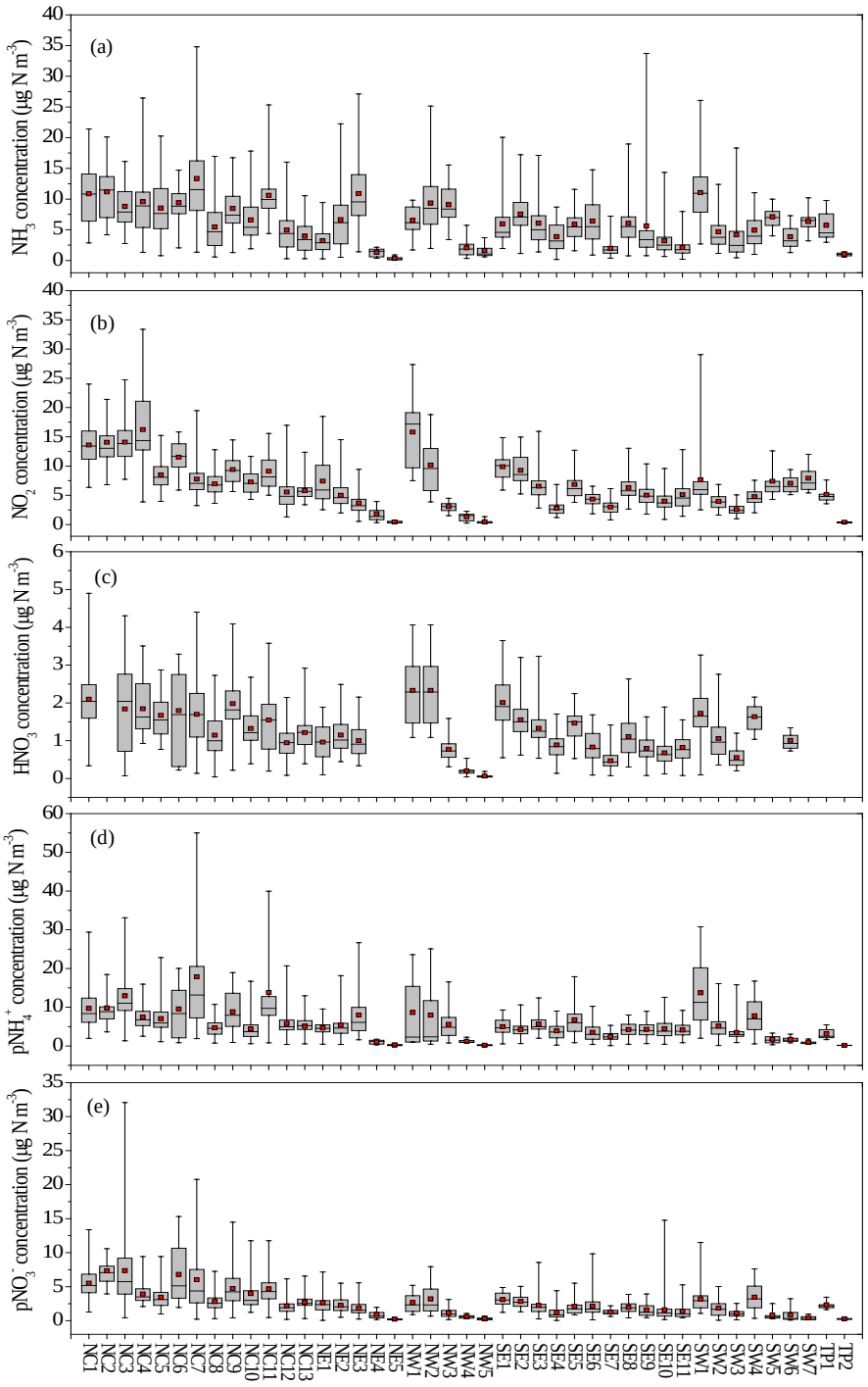

461

462

463

464

删除的内容: ▪

Fig. S3

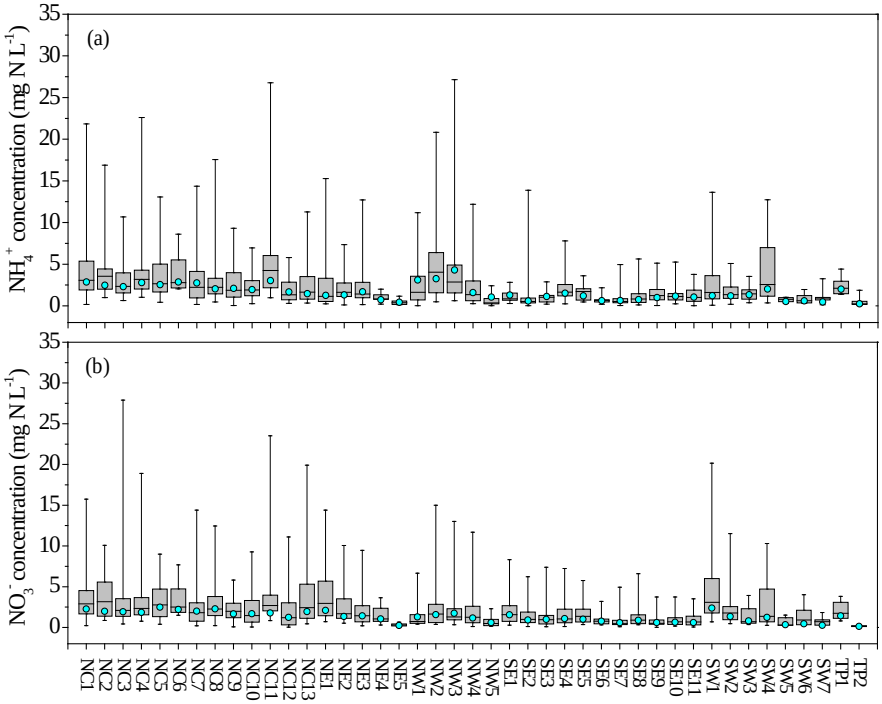

删除的内容: Fig. S3

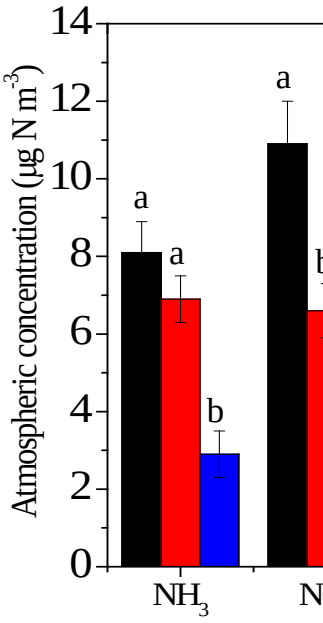

带格式的: 字体: Times New Roman, 小四

删除的内容: S4

505

506

删除的内容:

Fig. S5

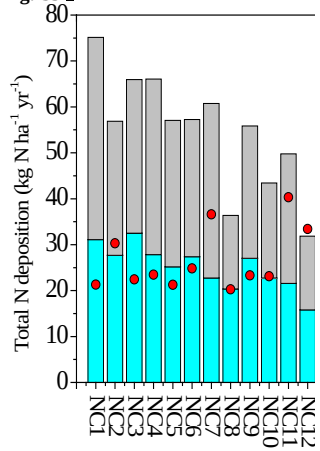

Fig. S4

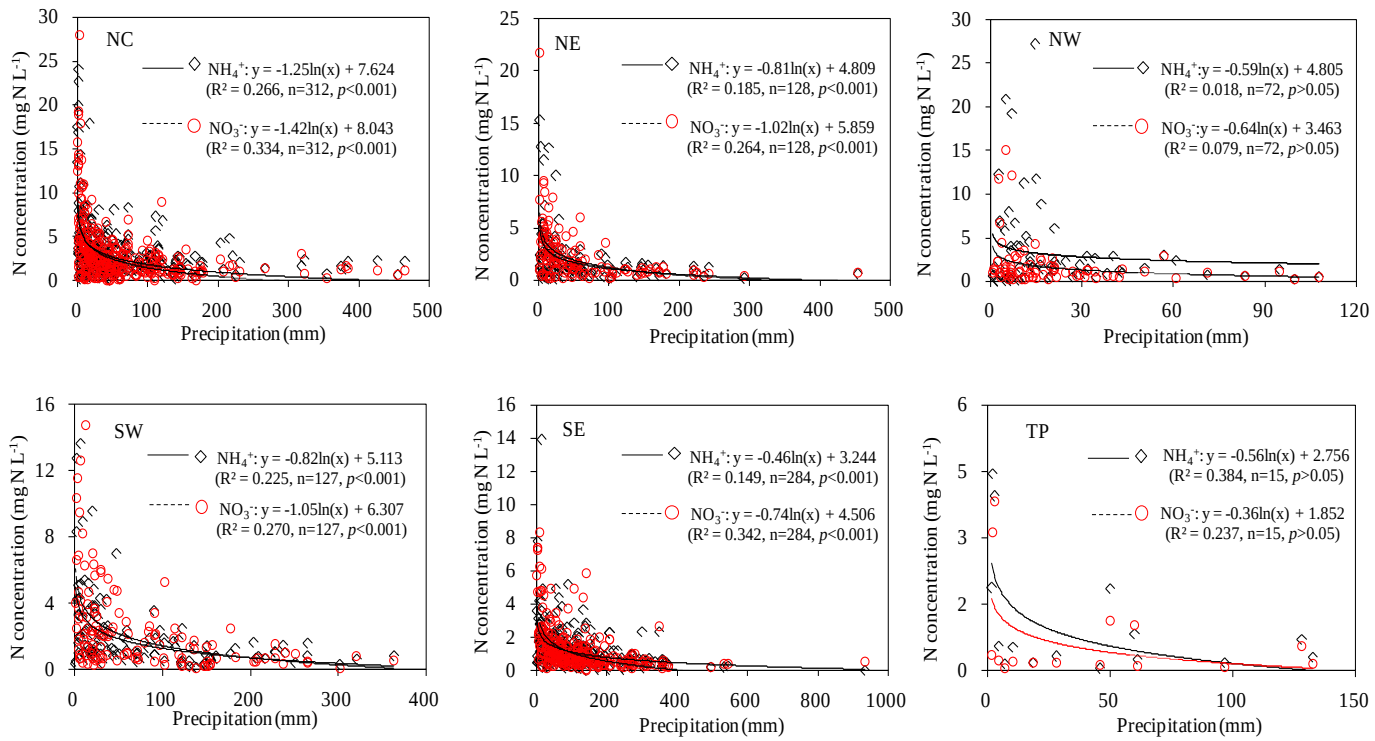

带格式的：字体：Times New Roman，小四

Fig. S5

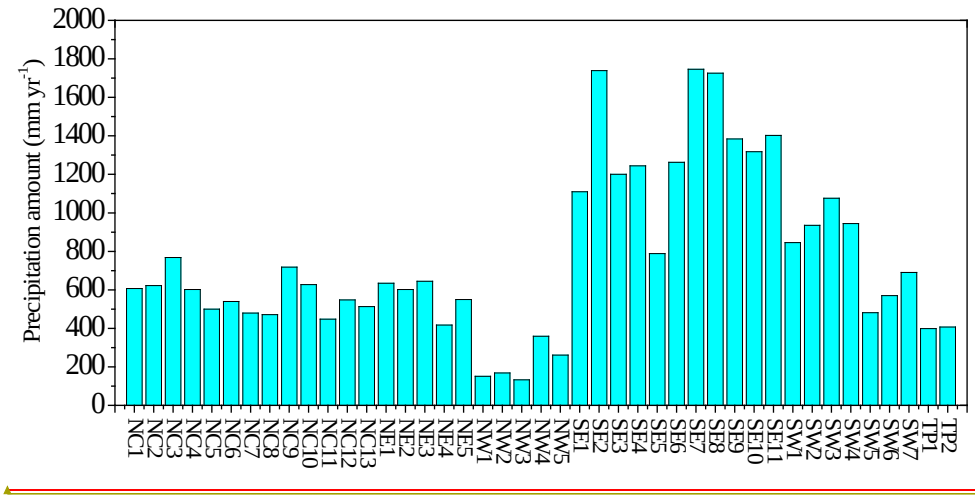

带格式的：字体：Times New Roman，小四

Fig. S6

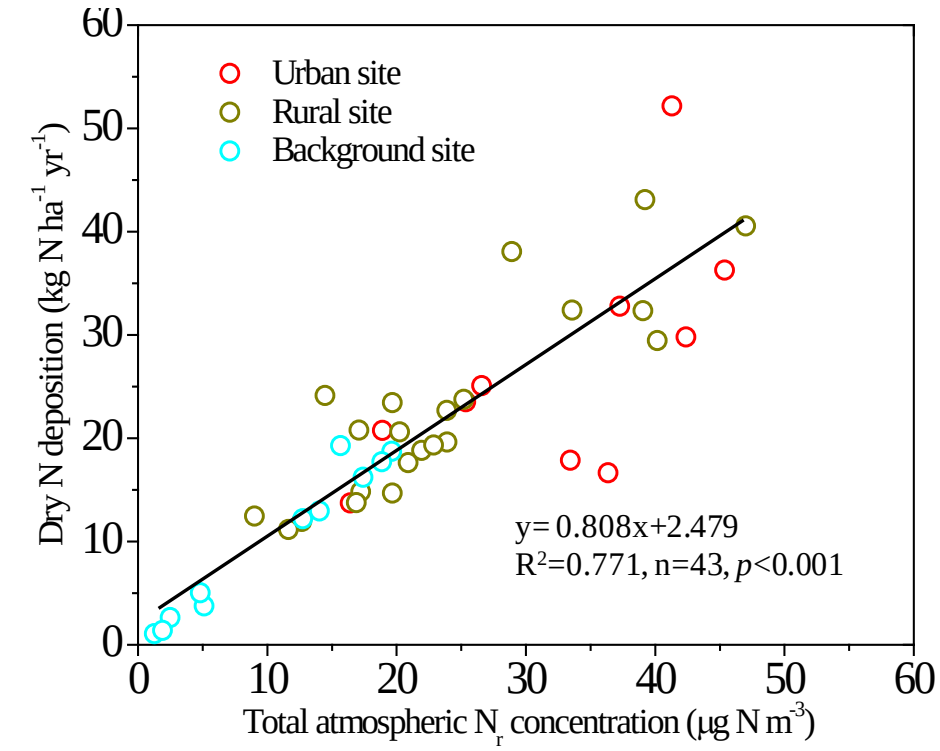

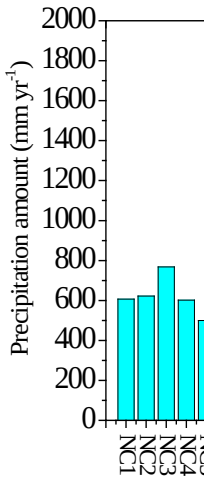

删除的内容:

带格式的: 字体: Times New Roman, 小四

Table S1. Descriptions of the forty-tree sampling sites in the Nationwide Nitrogen Deposition Monitoring Network (NNDMN)[a]

Site Code	Site Name	Region	Coordinate	Meteorological parameters[b]				Population density (persons km^{-2})	Land use type
				Wind speed (m s^{-1})	Rainfall (mm)	Temp. (°C)	RH (%)		
NC1	China Agric. University	NC	116.28 º E, 40.02 º N	2.5	556	12.4	56	7616	Urban
NC2	BeijingNormal University	NC	116.37 º E, 39.96 º N	2.5	556	12.4	56	7616	Urban
NC3	Zhengzhou	NC	113.63 º E, 34.75 º N	2.5	641	14.6	65	17069	Urban
NC4	Dongbeiwang	NC	116.29 º E, 40.04 º N	2.5	556	12.4	56	587	Rural
NC5	Shangzhuang	NC	116.20 º E, 40.11 º N	2.5	556	12.4	56	327	Rural
NC6	Baoding	NC	115.48 º E, 38.85 º N	2.0	519	12.9	61	3029	Rural
NC7	Quzhou	NC	114.94 º E, 36.78 º N	1.8	517	13.9	61	606	Rural
NC8	Yangqu	NC	112.89 º E, 38.05 º N	2.1	443	10.1	59	58	Rural
NC9	Zhumadian	NC	114.05 º E, 33.02 º N	2.3	958	15.0	72	815	Rural
NC10	Yangling	NC	108.01 º E, 34.31 º N	1.6	599	13.3	71	1763	Rural
NC11	Yucheng	NC	116.63 º E, 36.94 º N	2.5	567	13.1	64	495	Rural
NC12	Lingshandao	NC	120.18 º E, 35.77 º N	4.9	712	12.7	71	482	Background
NC13	Changdao	NC	120.75 º E, 37.93 º N	5.5	562	12.2	68	786	Background
NE1	Dalian	NE	121.58 º E, 38.92 º N	4.6	623	10.8	65	14280	Urban
NE2	Gongzhuling	NE	124.83 º E, 43.53 º N	3.8	573	5.7	63	271	Rural
NE3	Lishu	NE	124.17 º E, 43.36 º N	2.8	611	6.7	64	221	Rural
NE4	Wuyin	NE	129.25 º E, 48.11 º N	2.1	628	1.1	69	33	Background
NE5	Genhe	NE	121.52 º E, 50.78 º N	2.2	518	-6.2	67	5	Background
NW1	Shengdisuo	NW	87.57 º E, 43.87 º N	2.5	265	7.2	57	5122	Urban

删除的内容: Fig. S7 ...

带格式的: 字体: Times New Roman, 小四

带格式的: 字体: Times New Roman, 小四

NW2	Tufeisuo	NW	87.58 º E, 43.82 º N	2.5	265	7.2	57	236	Urban
NW3	Wuwei	NW	102.60 º E, 38.07 º N	1.8	170	8.2	52	58	Rural
NW4	Duolun	NW	116.49 º E, 42.20 º N	3.4	374	2.4	60	5	Background
NW5	Bayinbuluke	NW	83.71 º E, 42.88 º N	2.7	272	-4.3	70	26	Background
SE1	Nanjing	SE	118.85 º E, 31.84 º N	2.5	1062	15.7	75	729	Urban
SE2	Baiyun	SE	113.27 º E, 23.16 º N	1.8	1748	22.1	77	322	Urban
SE3	Wuxue	SE	115.79 º E, 30.01 º N	2.0	1418	17.3	77	469	Rural
SE4	Taojiang	SE	111.97 º E, 28.61 º N	1.8	1332	17.1	78	372	Rural
SE5	Fengyang	SE	117.56 º E, 32.88 º N	2.6	935	15.4	73	331	Rural
SE6	Zhanjiang	SE	110.33 º E, 21.26 º N	2.9	1678	23.2	82	639	Rural
SE7	Fuzhou	SE	119.36 º E, 26.17 º N	2.6	1374	20	75	97	Rural
SE8	Fenghua	SE	121.53 º E, 29.61 º N	2.4	1408	16.8	79	413	Rural
SE9	Feiyue	SE	113.34 º E, 28.56 º N	1.3	1502	16.9	81	228	Background
SE10	Huinong	SE	113.41 º E, 28.52 º N	1.3	1502	16.9	81	313	Background
SE11	Xishan	SE	113.31 º E, 28.61 º N	1.3	1502	16.9	81	313	Background
SW1	Wenjiang	SW	103.84 º E, 30.55 º N	1.4	939	18.6	80	1650	Urban
SW2	Ziyang	SW	104.63 º E, 30.13 º N	1.1	945	17.3	80	555	Rural
SW3	Yanting	SW	105.47 º E, 31.28 º N	1.2	879	16.4	77	253	Rural
SW4	Jiangjin	SW	106.18 º E, 29.06 º N	1.3	855	16.4	77	383	Rural
SW5	Dianchi	SW	102.67 º E, 24.97 º N	2.1	991	15.1	72	858	Rural
SW6	Yunnan Agric. University	SW	102.75 º E, 25.13 º N	2.1	991	15.1	72	2384	Rural
SW7	Kunyang	SW	102.61 º E, 24.67 º N	2.3	903	16.3	75	204	Background
TP1	Xining	TP	101.79 º E, 36.62 º N	1.5	387	6	56	2167	Urban
TP2	Linzhi	TP	94.36 º E, 29.65 º N	1.7	673	8.9	63	5	Background

[a]See Sect. S2 in the online supplement for the details of all the sampling sites in the network.

[b]There were no mean annual meteorological data for the forty-three monitoring sites; the surface climate parameters presented (1961-2012) were obtained from the nearest meteorological observation stations available on the China Meteorological Data Sharing Services website (http://cdc.gov.cn/).

[c] The population density was estimated by dividing population by area of the town/district/county where the monitoring site is located. Population data were sourced from the sixth census of China in 2010 and can be accessed online (http://www.stats.gov.cn).

590

591

592 **Table S2.** Monitoring periods for atmospheric N deposition and types of underlying surface at the forty-three sites in China.

Site Code	Site Name	Monitoring period		Underlying surface
		Dry deposition	Wet deposition	
NC1	China Agric. University	Apr. 2010-Sep. 2014	Apr. 2010-Sep. 2014	Vegetations
NC2	Beijing Normal University	Oct. 2013-Sep. 2014	Jan. 2012-Sep. 2014	Roof
NC3	Zhengzhou	May. 2010-Sep.2014	Jan. 2010-Dec. 2011	Vegetations
NC4	Dongbeiwang	Aug. 2006-Sep. 2008	Aug. 2006-Sep. 2008	Vegetations
NC5	Shangzhuang	Apr. 2010-Sep. 2014	Apr. 2010-Sep. 2014	Vegetations
NC6	Baoding	Jan. 2011-Dec. 2011	Jan. 2011-Dec. 2011	Vegetations
NC7	Quzhou	Apr. 2010-Sep. 2014	Apr. 2010-Sep. 2014	Vegetations
NC8	Yangqu	Apr. 2010-Sep. 2014	Apr. 2010-Sep. 2014	Vegetations
NC9	Zhumadian	Apr. 2010-Sep. 2014	Jan. 2011-Sep. 2014	Vegetations
NC10	Yangling	Apr. 2010-Sep. 2014	Apr. 2010-Sep. 2014	Vegetations
NC11	Yucheng	Sep. 2012-Sep. 2014	Jan. 2013-Sep. 2014	Vegetations
NC12	Lingshandao	Feb. 2011-Sep. 2014	Feb. 2011-Sep. 2014	Vegetations
NC13	Changdao	Sep. 2010-Sep. 2014	Sep. 2010-Sep. 2014	Vegetations
NE1	Dalian	Sep. 2010-Sep. 2014	Sep. 2010-Sep. 2014	Vegetations
NE2	Gongzhuling	Jul. 2010-Sep. 2014	Jul. 2010-Sep.2014	Vegetations
NE3	Lishu	Jul. 2010-Sep. 2014	Jul. 2010-Sep.2014	Vegetations
NE4	Wuyin	Oct. 2010-Sep. 2011	Oct. 2010-Sep. 2011	Vegetations
NE5	Genhe	Oct. 2010-Sep. 2011	Oct. 2010-Sep. 2011	Vegetations

NW1	Shengdisuo	Sep. 2009-Dec. 2011	Sep. 2009-Aug. 2010	Vegetations
NW2	Tufeisuo	Sep. 2009-Dec. 2011	Sep. 2009-Aug. 2010	Vegetations
NW3	Wuwei	Oct. 2010-Sep. 2014	Oct. 2010-Sep. 2014	Vegetations
NW4	Duolun	Jul. 2013-Sep. 2014	Jan. 2010-Sep. 2014	Grass
NW5	Bayinbuluke	May.2010-Aug. 2011	Nov. 2010-Jun. 2012	Grass
SE1	Nanjing	Sep. 2010-Feb. 2012	Sep. 2010-Feb. 2012	Vegetations
SE2	Baiyun	May. 2010-Sep. 2014	May. 2010-Sep. 2014	Roof
SE3	Wuxue	Aug. 2011-Sep. 2014	Aug. 2011-Sep. 2014	Roof
SE4	Taojiang	Oct. 2010-Sep. 2014	Jan. 2011-Sep. 2014	Roof
SE5	Fengyang	Feb. 2013-Sep. 2014	Oct. 2013-Sep. 2014	Vegetations
SE6	Zhanjiang	Aug. 2010-Sep. 2014	Jan. 2013-Sep. 2014	Vegetations
SE7	Fuzhou	Apr. 2010-Sep. 2014	Apr. 2010-Sep. 2014	Vegetations
SE8	Fenghua	Aug. 2010-Sep. 2014	Jan. 2011-Sep. 2014	Vegetations
SE9	Feiyue	Sep. 2010-Sep. 2014	Sep. 2010-Sep. 2014	Vegetations
SE10	Huinong	Sep. 2010-Sep. 2014	Sep. 2010-Sep. 2014	Vegetations
SE11	Xishan	Sep. 2010-Sep. 2014	Sep. 2010-Sep. 2014	Vegetations
SW1	Wenjiang	Oct. 2010-Sep. 2014	Jan. 2011-Sep. 2014	Vegetations
SW2	Ziyang	Jul. 2010-Sep. 2014	Jan. 2011-Sep. 2014	Vegetations
SW3	Yanting	May. 2011-Oct. 2013	May. 2011-Dec. 2012	Vegetations
SW4	Jiangjin	Jan. 2013-Sep. 2014	Jan. 2013-Sep. 2014	Vegetations
SW5	Dianchi	Apr. 2009-Mar. 2010	Apr. 2009-Mar. 2010	Vegetations
SW6	Yunnan Agric. University	Apr. 2009-Mar. 2010	Apr. 2010-Mar. 2010	Vegetations
SW7	Kunyang	Apr. 2009-Mar. 2010	Apr. 2009-Mar. 2010	Vegetations

TP1	Xining	Dec. 2013-Nov. 2014	Dec. 2013-Nov. 2014	Vegetations
TP2	Linzhi	Jan. 2009-Dec. 2009	Jan. 2009-Dec. 2009	Vegetations

Table S3. Statistics of monthly mean dry deposition velocities of N_r species for the three land use types, basing on the modeled hourly values at the forty-three sites from January 2010 to May 2013[a].

Land use type		Monthly mean deposition velocities (cm s^{-1})				
		NH_3	NO_2	HNO_3	pNH_4^+	pNO_3^-
Urban	N	410	410	410	410	410
	Min	0.30	0.01	0.12	0.06	0.06
	Max	1.63	0.44	5.78	0.35	0.35
	Mean	0.45	0.12	1.22	0.17	0.17
	Median	0.34	0.10	1.15	0.17	0.17
	SD	0.29	0.10	1.00	0.07	0.07
Rural	N	902	902	902	902	902
	Min	0.09	0.01	0.05	0.07	0.07
	Max	1.10	0.46	5.78	0.37	0.37
	Mean	0.40	0.17	1.49	0.18	0.18
	Median	0.35	0.16	1.49	0.18	0.18
	SD	0.16	0.12	1.10	0.06	0.06
Background	N	451	451	451	451	451
	Min	0.20	0.01	0.06	0.05	0.05
	Max	1.48	0.57	8.88	0.31	0.31
	Mean	0.47	0.17	1.78	0.16	0.16
	Median	0.43	0.13	1.48	0.16	0.16
	SD	0.22	0.15	1.66	0.06	0.06

[a] The forty-three sites consist of 10 urban, 22 rural and 11 background sites. Among the forty-three monitoring sites, 20 farmland, 5 coastal, 6 forest and 2 grassland sites were included in the rural and background sites.

删除的内容: six

删除的内容: for the whole 2012

删除的内容: Land use type

Table S4. Comparison of annual deposition velocities of nitrogen compounds on different land use types in this study with literature.

Land use type	Country	Deposition velocity (cm s^{-1})					References
		NH_3	NO_2	HNO_3	pNH_4^+	pNO_3^-	
Farmland	China	0.40 (0.06)	0.18 (0.08)	1.52 (0.72)	0.19 (0.03)	0.19 (0.03)	This study
		0.26	0.12	0.81	0.16	0.16	Zhu et al. (2010)
		0.74	0.59	2	0.24	0.24	Shen et al. (2009)
		0.13	0.23	—	—	—	Yang et al. (2010)
		0.18	0.10	0.76	—	0.25	Zhang et al. (2004)
		0.71	0.05	—	—	—	Pan et al. (2012)
	West Africa	0.23-0.42	0.20-0.35	0.63-0.73	—	—	Delon et al. (2012)
	Britain	—	0.16	2.06	0.10	0.26	Marner and Harrison. (2004)
	Europe	0.35-0.75	0.05-0.20	0.8-1.0	0.11-0.20	0.10-0.25	Flechard et al. (2011)
Urban	China	0.45 (0.27)	0.12 (0.06)	1.25 (0.57)	0.17 (0.04)	0.17 (0.04)	This study
		0.78	0.06	—	—	—	Pan et al. (2012)
		0.28	0.07	1.77	0.44	0.44	Li et al. (2013)
		0.50	0.60	1.1	0.24	0.24	Luo et al. (2013)
	Greece	0.81	0.26	2.4	0.1	0.2	Anatolaki et al. (2007)
	Britain	—	0.08	7.27	1.02	1.78	Marner and Harrison. (2004)
Coastal	China	0.65 (0.26)	0.16 (0.11)	1.56 (0.54)	0.13 (0.03)	0.13 (0.03)	This study
		—	—	—	0.6	1.15	Zhang et al. (2007)
		0.63	0.00534	0.63	—	—	Zhang et al. (2010)
		0.55	0.01	0.84	0.27	0.27	Zhang et al. (2004)
		—	—	—	0.019	0.088	Qi et al. (2013)

删除的内容: 39
删除的内容: 17
删除的内容: 07
删除的内容: 03
删除的内容: 44
删除的内容: 18
删除的内容: 02
删除的内容: 18
删除的内容: 02
删除的内容: 41
删除的内容: 18
删除的内容: 0.88
删除的内容: 31
删除的内容: 54
删除的内容: 17
删除的内容: 15
删除的内容: 10
删除的内容: 08
删除的内容: 29
删除的内容: 12
删除的内容: 12

Table S4 (*continued*)

Land use type	Country	Deposition velocity (cm s^{-1})					References
		NH_3	NO_2	HNO_3	pNH_4^+	pNO_3^-	
Forest	China	0.41 (0.05)	0.19 (0.05)	2.23 (1.28)	0.16 (0.01)	0.16 (0.01)	This study
		0.1	0.05	—	—	—	Pan et al. (2012)
		0.20	0.09-0.11	2.43-2.46	0.27-0.33	0.27-0.33	Zhang et al. (2004)
	Belgium	1.1-2.9	0.25	—	—	—	Staelen et al. (2012)
	Switzerland	2.2-3.0	0.3-0.4	1.5	0.2-0.4	0.2-0.4	Schmitt et al. (2005)
	Britain	—	0.26	7.27	1.02	1.78	Marner and Harrison. (2004)
	Europe	0.75-2.4	0.06-0.28	2.3-4.4	0.2-2.0	0.2-2.5	Flechard et al. (2011)
Grassland	China	0.378 (0.002)	0.15 (0.01)	1.09 (0.26)	0.194 (0.002)	0.194 (0.002)	This study
		0.23	0.13	1.16	0.28	0.28	Zhang et al. (2004)
		1.1	0.25	—	—	—	Staelen et al. (2012)
	Britain	—	0.16	1.39	0.06	0.15	Marner and Harrison. (2004)
	Europe	0.45-1.1	0.05-0.25	1.1-1.2	0.12-0.14	0.11-0.19	Flechard et al. (2011)
All land uses	The United States	0.65	0.36	2.70	0.15	0.15	Zhang et al. (2012)

Values in the parentheses are standard deviations of annual mean deposition velocities at sampling sites with the same land use type.

References

Anatolaki, Ch. and Tsitouridou, R.: Atmospheric deposition of nitrogen, sulfur and chloride in Thessaloniki, Greece, Atmos. Res., 85, 413–428, doi:10.1016/j.atmosres.2007.02.010, 2007.

Delon, C., Galy-Lacaux, C., Adon, M.,Liousse, C., Serca, D., Diop, B., and Akpo, A.:. Nitrogen compounds emission and deposition in West

带格式表格

删除的内容: 39

删除的内容: 18

删除的内容: 04

删除的内容: 1.31

删除的内容: 0.49

删除的内容: 15

删除的内容: 15

删除的内容: 01

删除的内容: 0.80

删除的内容: 17

删除的内容: 186

删除的内容: 005

删除的内容: 186

删除的内容: 005

665 African ecosystems: comparison between wet and dry savanna, Biogeosciences., 9, 385–402, doi:10.5194/bg-9-385-2012, 2012.
666 Flechard, C. R., Nemitz, E., Smith, R. I., Fowler, D., Vermeulen, A.T., Bleeker, A., Erisman, J. W., Simpson, D., Zhang, L., Tang, Y. S., and
667 Sutton, M. A.: Dry deposition of reactive nitrogen to European ecosystems: a comparison of inferential models across the NitroEurope
668 network, Atmos. Chem. Phys., 11, 2703–2728,doi:10.5194/acp-11-2703-2011, 2011.
669 Li, K. H., Liu, X. J., Song, W., Chang, Y. H., Hu, Y. K., and Tian, C. Y.: Atmospheric Nitrogen Deposition at Two Sites in an Arid Environment
670 of Central Asia, PloS ONE, 8, e67018, doi: 10.1371/journal .pone.0067018, 2013.
671 Luo, X. S., Liu, P., Tang, A. H., Liu, J. Y., Zong, X. Y., Zhang, Q., Kou, C. L., Zhang, L. J., Fowler, D., Fangmeier, A., Christie, P., Zhang, F. S.,
672 and Liu, X. J.: An evaluation of atmospheric N_r pollution and deposition in North China after the Beijing Olympics, Atmos. Environ., 74,
673 209–216, doi:10.1016/j.atmosenv.2013.03.054, 2013.
674 Marner, B. B. and Harrison, R. M.: A spatially refined monitoring based study of atmospheric nitrogen deposition, Atmos. Environ.,38,
675 5045–5056, doi:10.1016/j.atmosenv.2004.06.016, 2004.
676 Pan, Y. P., Wang, Y. S., Tang, G. Q., and Wu, D.: Wet and dry deposition of atmospheric nitrogen at ten sites in Northern China, Atmos. Chem.
677 Phys., 12, 6515–6535, doi:10.5194/acp-12-6515-2012, 2012.
678 Qi, J. H., Shi, J. H., and Gao, H. W.: Atmospheric dry and wet deposition of nitrogen species and its implication for primary productivity in
679 coastal region of the Yellow Sea, China, Atmos. Environ., 81, 600–608, doi:10.1016/j.atmosenv.2013.08.022, 2013.
680 Schmitt, M., Thöni, L., Waldner, P., and Thimonier, A.: Total deposition of nitrogen on Swiss long-term forest ecosystem research (LWF) plots:
681 comparison of the throughfall and the inferential method, Atmos. Environ., 39, 1079–1091, doi:10.1016/j.atmosenv.2004.09.075, 2005.
682 Shen, J. L., Tang, A. H., Liu, X. J., Fangmeier, A., Goulding, K. T. W., and Zhang, F. S.: High concentrations and dry deposition of reactive
683 nitrogen species at two sites inthe North China Plain, Environ. Pollut., 157, 3106–3113,doi:10.1016/j.envpol.2009.05.016, 2009.
684 Staelens, J., Wuyts, K., Adriaenssens, S.,Avermaet, P. V., Buysse, H., den Bril, B. V., Roeken, E., Ottoy, J. P., Verheyen, K., Thas, O., and

Deschepper, E.: Trends in atmospheric nitrogen and sulphur deposition in northern Belgium, Atmos. Environ., 49, 186–196, doi: 10.1016/j.atmosenv.2011.11.065, 2012.

Yang, R., Hayashi, K., Zhu, B., Li, F., and Yan, X.: Atmospheric NH_3 and NO_2 concentration and nitrogen deposition in an agricultural catchment of Eastern China, Sci. Total. Environ., 408, 4624–4632, doi:10.1016/j.scitotenv.2010.06.006, 2010.

Zhang, L., Jacob, D. J., Knipping, E.M., Kumar, N., Munger, J. W., Carouge, C. C., van Donkelaar, A., Wang, Y. X., and Chen, D.: Nitrogen deposition to the United States: distribution, sources, and processes, Atmos. Chem. Phys., 12, 4539–4554, doi:10.5194/acp-12-4539-2012, 2012.

Zhang, G., Zhang, J., and Liu, S. M.: Characterization of nutrients in the atmospheric wet and dry deposition observed at the two monitoring sites over Yellow Sea and East China Sea, J. Atmos. Chem., 57, 41–57, doi:10.1007/s10874-007-9060-3, 2007.

Zhang, Y., Wang, T. J., Hu, Z. Y., and Xu, C. K.: Temporal variety and spatial distribution of dry deposition velocities of typical air pollutants over different landuse types, Climatic Environ. Res., 9, 591–604, 2004 (in Chinese with English abstract).

Zhang, Y., Yu, Q., Ma, W. C., and Chen, L. M.: Atmospheric deposition of inorganic nitrogen to the eastern China seas and its implications to marine biogeochemistry, J. Geophys. Res., 115, 1-10, doi:10.1029/2009JD012814, 2010.

Table S5. Emission inventory of NH_3 and NO_x for thirty-three provinces as well as the six regions of China in 2010 (kt)

Region	Site	Area ($\times 10^3 km^2$)	NH_3 (kt)	NO_x(kt)
North China	Beijing	16.4	61.5	389.2
	Tianjin	11.9	48.4	731.3
	Hebei	188.8	904.1	1685.2
	Shandong	187.1	1027.2	1941.8
	Shanxi	156.7	322.5	779.7
	Henan	167.0	1165.4	1140.0
	Shaanxi	205.8	281.5	452.1
	Total	933.8	3810.5	7120.2
Northeast China	Liaoning	148.0	340.4	1021.6
	Jilin	190.2	329.4	474.5
	Heilongjiang	437.0	465.9	716.5
	Total	612.1	1135.8	2212.6

Northwest China	Xinjiang	1660	374.2	308.9
	Inner Mongolia	1183	380.2	660.0
	Ningxia	66.4	73.9	177.0
	Gansu	453.7	199.0	374.4
	Total	3363.1	1027.2	1520.3
Southeast China	Shanghai	6.3	55.0	1091.2
	Jiangsu	102.6	806.3	1557.0
	Zhejiang	101.8	346.6	1199.8
	Anhui	140.3	631.9	768.1
	Hubei	185.9	668.2	783.5
	Hunan	211.8	742.6	566.2
	Jiangxi	166.9	461.3	439.7
	Fujian	124.0	288.9	439.4
	Guangdong	179.8	618.1	1382.1
	Hong Kong & Macau	1.1	6.7	251.2
	Taiwan	36.2	120.0	431.9
	Hainan	35.4	92.0	89.7
	Total	1254.8	4838.8	8962.7

Southwest China	Sichuan	485.0	925.4	650.1
	Chongqing	82.4	254.3	296.4
	Guizhou	176.2	465.5	312.9
	Yunan	390.0	700.0	453.1
	Guangxi	236.7	547.8	399.5
	Total	1370.3	2893.1	2112.0
Tibetan plateau	Tibet	1200.0	172.2	85.2
	Qinghai	722.3	121.6	85.0
	Total	1922.3	293.8	170.2

The emission data of NO_x and NH_3 for the year 2010 are from the **GAINS (Greenhouse Gas and Air Pollution Interactions and Synergies)** Model (available online: http://www.iiasa.ac.at/)